Parkinson's Disease

Animal Models of Parkinson's Disease 2012

Guest Editors: Yuzuru Imai, Katerina Venderova, and Kah-Leong Lim

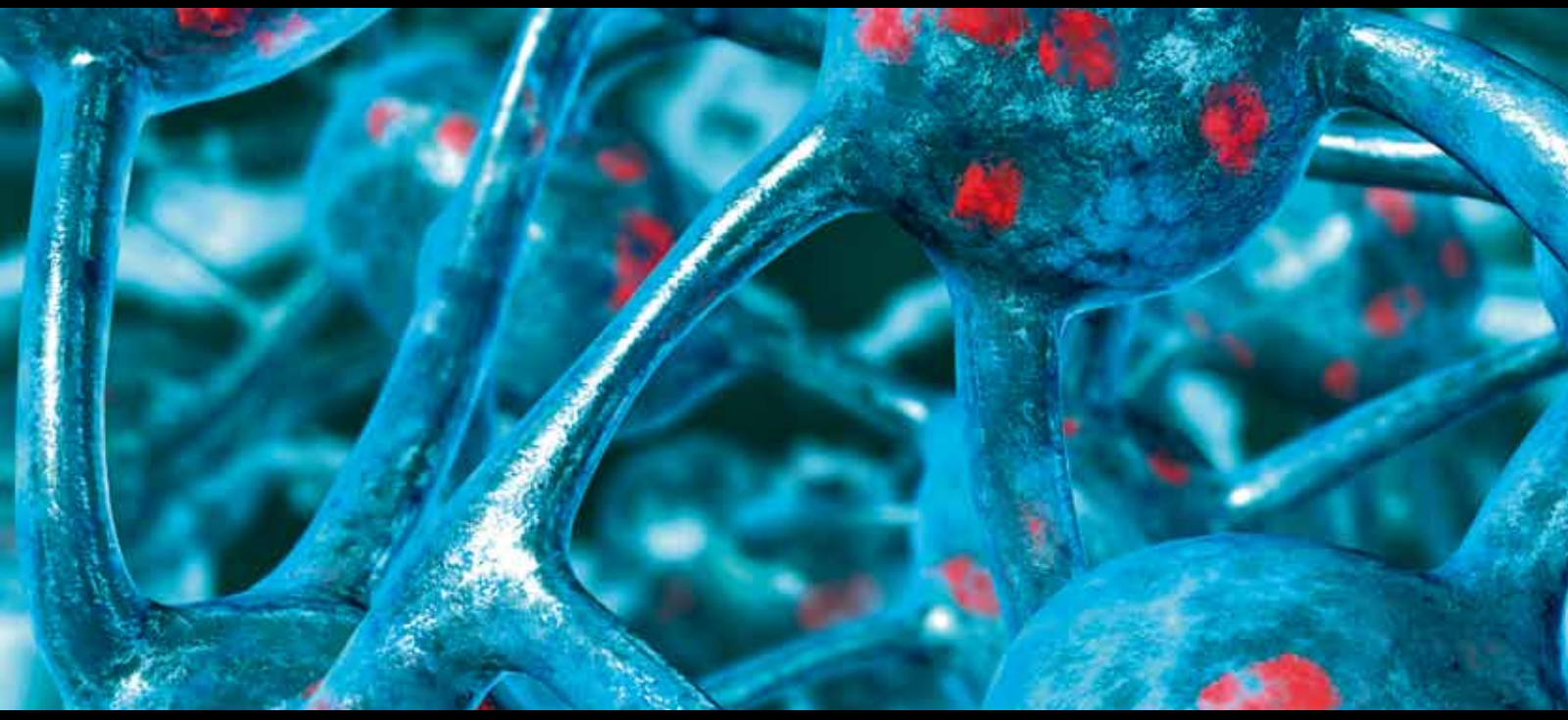

Animal Models of Parkinson's Disease 2012

Animal Models of Parkinson's Disease 2012

Guest Editors: Yuzuru Imai, Katerina Venderova,
and Kah-Leong Lim

Editorial Board

Contents

Hindawi Publishing Corporation
Parkinson's Disease
Volume 2012, Article ID 729428, 2 pages
doi:10.1155/2012/729428

Editorial

Animal Models of Parkinson's Disease 2012

Yuzuru Imai,[1] Katerina Venderova,[2] and Kah-Leong Lim[3]

[1] *Department of Neuroscience for Neurodegenerative Disorders, Juntendo University Graduate School of Medicine, Tokyo 113-8421, Japan*
[2] *Department of Physiology and Pharmacology, Thomas J. Long School of Pharmacy and Health Sciences, University of the Pacific, Stockton, CA 95211, USA*
[3] *Department of Physiology, National University of Singapore, Block MD9, 2 Medical Drive, Singapore 117597*

Correspondence should be addressed to Yuzuru Imai, yzimai@juntendo.ac.jp

Received 26 August 2012; Accepted 26 August 2012

Parkinson's disease (PD) is a prevalent movement disorder, which is characterized by age-dependent degeneration of dopaminergic neurons in the midbrain. Recent advances in PD study have suggested that multiple nervous systems are affected as well as the nigrostriatal system, involving decline of cognitive function, sleep disturbance, mood change, and dysfunction of the autonomic nervous system. Multifactorial causes of PD are hypothesized. Neurotoxins including artificial compounds, pesticides, heavy metals as well as dopamine itself have been proposed to be environmental risk factors of PD. Recent genome-wide genetic and mutational studies have revealed various genetic risk factors and SNPs while microglial activation in the affected regions have emerged to be involved in the disease development as a local microenvironmental factor. One of the pathological hallmarks of PD is the appearance of ubiquitin-positive cytoplasmic inclusions called Lewy bodies (LBs) in the affected regions. A presynaptic protein α-synuclein, which is the first identified monogenic PD gene product, is a major component of LBs. Understanding of the neuropathological mechanism underlying the formation of LBs is a key aspect of PD study. Newly identified monogenic PD gene products, leucine-rich repeat kinase 2 (LRRK2), ATPase type 13A2, and Vps35 are implicated in vesicle transport, endosomal—autophagic and lysosomal pathways. Dysregulation of these gene products might be involved in abnormal protein turnover associated with the LB formation.

Dysfunction of mitochondrial pathway and oxidative stress are also a focus based on the findings that PD-related neurotoxins such as 1-methyl-4-phenyl-1,2,3,6-tetrahydropyridine (MPTP), 6-hydroxydopamine (6-OHDA), and rotenone could interfere with mitochondrial functions and that monogenic PD gene products DJ-1, PINK1, and Parkin are involved in mitochondrial maintenance and redox regulation.

Autologous cell transplantation is fast becoming a reality now that technology for induced pluripotent stem (iPS) and induced dopaminergic (iDA) cells from fibroblasts achieves improvement on a daily basis [1]. At the same time, the methodology of gene therapy is also enhanced with the use of new DNA delivery tools. A wide variety of PD animal models contribute to the understanding of neuropathological mechanisms described above and the development of therapeutic approaches as an alternative to humans, although none of them have fully recapitulated the symptoms and pathology of PD so far.

This special issue is composed of an excellent review and 4 distinguished original articles that summarize the most recent progresses and ideas obtained from animal models in the specific fields, while reporting a new sensitive assay for PD models and a potential therapeutic approach.

The review paper briefly outlines newly developed rat models for *α-synuclein-* or *LRRK2*-linked PD. Aggregation of α-synuclein, which is accelerated by pathogenic mutations and phosphorylation at Ser129, is believed to lead to LB formation. Rat models introduced with these forms of α-synuclein have revealed *in vivo* effects of the aggregation-prone α-synuclein. Genome-wide association studies of sporadic PD have identified *LRRK2* and *α-synuclein* as risk loci, suggesting that these two genes are closely involved in the fundamental neuropathology of PD [2, 3]. Rat models for LRRK2 are also discussed as tools for potential therapeutic research.

Neurotoxicity of glutamate, which is the major excitatory neurotransmitter of neurons, is known to occur after brain injury and spinal cord injury. G. Bustos et al. have reported that activation of NMDA receptor upon glutamate release evokes BDNF expression in the early presymptomatic response of the *substantia nigra* in PD [4]. A current study by E. Riquelme et al. addresses the possibility of trkB involvement in this pathway.

Near-infrared light (NIr) treatment has a neuroprotective effect on dopaminergic neurons in the *substantia nigra* exposed to MPTP, presumably through the regulation of the mitochondrial activity and redox status [5, 6]. V. E. Shaw et al. examine an effect of NIr treatment on the subthalamic region in MPTP-treated mice, by estimating abnormally activated Fos-positive cells.

Drosophila melanogaster is a useful model system for human disease study as ~75% of disease-associated genes are conserved between humans and *Drosophila*. Although the orthologue of α-synuclein gene is not found in the *Drosophila* genome, transgenic expression of α-synuclein causes progressive motor defects, which is usually evaluated by climbing ability in a test for negative geotaxis [7]. R. Shaltiel-Karyo et al. report here that defects in courtship-associated behavior is detectable at a much earlier stage of the α-synuclein model fly. Their assay could be an alternative to detect impairment of the coordinated motor activity in PD model files.

Minocycline (MC), which has anti-inflammatory and anti-oxidative properties, is a promising drug for neurodegenerative disease; however this drug has deleterious effects on some neurodegenerative models [8, 9]. To understand and control the diverse actions of MC, A. A. Inamdar et al. find that genetic factors modulate the effects of MC using a *Drosophila* model, a powerful tool to elucidate the interactions between drugs and genes.

Yuzuru Imai
Katerina Venderova
Kah-Leong Lim

References

[1] M. Caiazzo, M. T. Dell'Anno, E. Dvoretskova et al., "Direct generation of functional dopaminergic neurons from mouse and human fibroblasts," *Nature*, vol. 476, no. 7359, pp. 224–227, 2011.

[2] W. Satake, Y. Nakabayashi, I. Mizuta et al., "Genome-wide association study identifies common variants at four loci as genetic risk factors for Parkinson's disease," *Nature Genetics*, vol. 41, no. 12, pp. 1303–1307, 2009.

[3] J. Simon-Sanchez, C. Schulte, J. M. Bras, M. Sharma, J. R. Gibbs et al., "Genome-wide association study reveals genetic risk underlying Parkinson's disease," *Nature Genetics*, vol. 41, pp. 1308–1312, 2009.

[4] G. Bustos, J. Abarca, V. Bustos et al., "NMDA receptors mediate an early up-regulation of brain-derived neurotrophic factor expression in substantia nigra in a rat model of presymptomatic Parkinson's disease," *Journal of Neuroscience Research*, vol. 87, no. 10, pp. 2308–2318, 2009.

[5] R. Ying, H. L. Liang, H. T. Whelan, J. T. Eells, and M. T. Wong-Riley, "Pretreatment with near-infrared light via light-emitting diode provides added benefit against rotenone- and MPP^+-induced neurotoxicity," *Brain Research*, vol. 1243, pp. 167–173, 2008.

[6] V. E. Shaw, S. Spana, K. Ashkan et al., "Neuroprotection of midbrain dopaminergic cells in MPTP-treated mice after near-infrared light treatment," *Journal of Comparative Neurology*, vol. 518, no. 1, pp. 25–40, 2010.

[7] M. B. Feany and W. W. Bender, "A Drosophila model of Parkinson's disease," *Nature*, vol. 404, no. 6776, pp. 394–398, 2000.

[8] S. Zhu, I. G. Stavrovskaya, M. Drozda et al., "Minocycline inhibits cytochrome c release and delays progression of amyotrophic lateral sclerosis in mice," *Nature*, vol. 417, no. 6884, pp. 74–78, 2002.

[9] Y. Du, Z. Ma, S. Lin et al., "Minocycline prevents nigrostriatal dopaminergic neurodegeneration in the MPTP model of Parkinson's disease," *Proceedings of the National Academy of Sciences of the United States of America*, vol. 98, no. 25, pp. 14669–14674, 2001.

Hindawi Publishing Corporation
Parkinson's Disease
Volume 2012, Article ID 938528, 16 pages
doi:10.1155/2012/938528

Research Article

The Protective Effect of Minocycline in a Paraquat-Induced Parkinson's Disease Model in *Drosophila* is Modified in Altered Genetic Backgrounds

Arati A. Inamdar,[1,2] Anathbandhu Chaudhuri,[1,3] and Janis O'Donnell[1]

[1] *Department of Biological Sciences, University of Alabama, Tuscaloosa, AL 35487-0344, USA*
[2] *Department of Plant Biology and Pathology, Rutgers University-The State University of New Jersey, Room 291D, Foran Hall, 59 Dudley Road, New Brunswick, NJ 08901, USA*
[3] *Department of Pharmacology and Experimental Neuroscience, University of Nebraska Medical Center, Omaha, NE 68198-5800, USA*

Correspondence should be addressed to Arati A. Inamdar, inamdar@rci.rutgers.edu

Received 10 January 2012; Accepted 4 June 2012

Academic Editor: Katerina Venderova

Epidemiological studies link the herbicide paraquat to increased incidence of Parkinson's disease (PD). We previously reported that *Drosophila* exposed to paraquat recapitulate PD symptoms, including region-specific degeneration of dopaminergic neurons. Minocycline, a tetracycline derivative, exerts ameliorative effects in neurodegenerative disease models, including *Drosophila*. We investigated whether our environmental toxin-based PD model could contribute to an understanding of cellular and genetic mechanisms of minocycline action and whether we could assess potential interference with these drug effects in altered genetic backgrounds. Cofeeding of minocycline with paraquat prolonged survival, rescued mobility defects, blocked generation of reactive oxygen species, and extended dopaminergic neuron survival, as has been reported previously for a genetic model of PD in *Drosophila*. We then extended this study to identify potential interactions of minocycline with genes regulating dopamine homeostasis that might modify protection against paraquat and found that deficits in GTP cyclohydrolase adversely affect minocycline rescue. We further performed genetic studies to identify signaling pathways that are necessary for minocycline protection against paraquat toxicity and found that mutations in the *Drosophila* genes that encode c-Jun N-terminal kinase (JNK) and Akt/Protein kinase B block minocycline rescue.

1. Introduction

The pathogenic mechanisms of PD, whether triggered by mutations or aberrant copy number of a PD-associated gene or by environmental sources, are associated with increased oxidative stress within dopaminergic neurons, exacerbated by the highly reactive nature of dopamine itself [1–3]. Chronic neuronal dysfunction overstimulates the normally protective neuroinflammatory response further amplifies oxidative conditions, accelerating disease progression [4, 5]. Therefore, compounds with antioxidant and anti-inflammatory capabilities are of great interest for their potential therapeutic benefits in chronic neurodegenerative diseases including PD. Minocycline (MC), a second generation tetracycline drug known to be clinically safe [6], has shown promising ameliorative effects in animal models for chronic neurodegenerative diseases, including neurotoxin-induced PD models [7–9]. MC appears to have anti-inflammatory properties that mediate neuroprotection in PD animal models [10] as well as antioxidant properties [11]. Despite numerous reports of beneficial effects, however, other studies find deleterious consequences for MC treatment in some models of neurodegenerative disease and neuronal injury [12, 13] and damage to isolated mitochondria in micromolar concentrations [14]. Moreover, no single mode of action nor direct target of this antibiotic has been identified, which may partially account for the diversity of reported effects [15]. Genetic background is another

feature that may contribute to these seemingly contradictory responses, as genetic variation amongst individuals is known to modify the functional activity of drugs [16]. Such gene-drug interactions are cumbersome to investigate in humans or even in vertebrate model organisms. Invertebrate genetic models offer a simplified means of investigating three-way interactions between genes relevant to disease susceptibility and progression, environmental conditions, and therapeutic agents.

The genetic model organism, *Drosophila melanogaster*, is increasingly recognized as a useful model for neurodegenerative diseases due to its relative simplicity, ease of manipulation, high degree of conservation of neural mechanisms and signaling pathways, and availability of powerful genetic and molecular reagents for investigations of disease mechanisms [17, 18]. Thus, this model system should facilitate dissection of relevant response pathways during disease progression and identification of those alter responses to drugs such as MC.

The effects of MC have been investigated mainly in mammalian models, although it has been shown that MC enhances survival of paraquat- (PQ-) fed *Drosophila* [19] and delays dopamine loss in a *DJ-1* genetic PD model in *Drosophila* [20]. We have developed a *Drosophila* model based upon ingestion of PQ, which recapitulates characteristic symptoms of PD with degeneration of dopaminergic neurons and accompanying neurological symptoms, including resting tremors and postural instability. Moreover, we demonstrated that mutations directly altering the regulation of DA homeostasis dramatically alter susceptibility to PQ [21, 22]. Thus, this model offers the ability to simultaneously modify genetic background and environmental toxins.

In this paper, we confirm the results of previous studies [19, 20] utilizing this environmental toxin model to demonstrate that MC prolongs survival of PQ-exposed adult *Drosophila* and that it diminishes PQ-induced mobility defects, blocks associated changes in the DA homeostasis pathway, diminishes levels of reactive oxygen species (ROS), and prolongs DA neuron survival, as reported in the *Drosophila* DJ-1 model [20]. Moreover, we demonstrate that MC dose can dramatically alter the outcome of survival studies. We then extend the analysis of MC action by demonstrating that mutations in genes altering DA homeostasis and PQ susceptibility can affect the ameliorative action of MC. We further employ this system to identify signaling pathways that can modify PQ-induced toxicity and the protective effects of MC in this *in vivo Drosophila* model. Using loss of function mutants and overexpression transgenic lines, we found that JNK and Akt1 play an important role in protecting DA neurons against PQ toxicity and reductions in expression of these kinases diminishes the ability of MC to protect against PQ.

2. Materials and Methods

Drosophila Strains and Culture Maintenance. Two strains were utilized as wild type control lines in all experiments testing mutant strains: Canton S, a wild type strain, and $y\ w^{1118}$, a yellow-body, white-eye strain that is otherwise wild type. For all experiments employing Gal4 expression to drive UAS-transgenes, TH-Gal4/+, and UAS-transgene/+ were utilized as controls. Mutant strains obtained from the Bloomington *Drosophila* Stock Center were as follows: *rolled* (rl^1), a weak loss-of-function allele of the gene encoding ERK, bsk^1/CyO and bsk^2/CyO and $Df(2L)J27,\ bsk^{[J27]}/CyO$, $P\{ry[+t7.2] = sevRas1.V12\}FK1$ loss-of-function alleles of the gene encoding JNK, $ry^{506}\ P\{PZ\}Akt1^{04226}/TM3$, $ry^{RK}\ Sb^1\ Ser^1$ and $y^1\ w^{67c23}$; $P\{w^{+mC}y^{+mDint2} = EPgy2\}Akt1^{EY10012}/TM3$, $Sb^1\ Ser^1$ carrying loss-of-function alleles of *Akt/PKB*, a loss-of-function allele for the gene encoding reaper, *reaper*, $y^1\ w^{67c23}$; $P\{SUPor\text{-}P\}KG07184\ ry^{506}$, and a null mutant allele of *Nedd2-like caspase* (*Nc/Dronc*), $y^1\ w^*$; $Nc^{51}/TM3$, Sb^1. Transgenic strains employed for wild type expression of kinases were JNK (*bsk*), $y^1\ w^{1118}$; $P\{UAS\text{-}bsk.A\text{-}Y\}1$ and *Akt1*, $y^1\ w^{1118}$; $P\{UAS\text{-}Akt1\}/CyO$.

The transgenic strain *UAS-2X eGFP* (Chromosome II) was obtained from the Bloomington *Drosophila* Stock Center and a *TH-Gal4* strain [23] was obtained from Jay Hirsh (University of Virginia). Loss-of-function *Catsup* alleles are described in Stathakis et al. [24], $pale^2/TM3$, *Sb* is a loss-of-function mutation in the gene encoding TH [25]. The loss of function Pu^{Z22} is described in Mackay et al. [26]. All mutants and transgenic strains were mated to the appropriate wild type strain, and all assays were performed on mutants heterozygous for the wild type genes. All stocks were maintained at 25°C.

2.1. Feeding Experiments. Separated male and female flies, 48–96 hr after-eclosion, were fed on filter paper saturated with one of the following solutions: 5% sucrose, 5% sucrose with 1 or 10 mM paraquat, minocycline HCl at varying concentrations, 10 mM PQ with 1 mM MC, and 1 mM PQ with 200 μM NG-nitro-L-arginine methylester (L-NAME). Feedings were continued as indicated in Section 3. All chemicals were obtained from Sigma (St. Louis, MO).

2.2. Locomotion Assay. The mobility of adult male and female flies from each treatment group was assessed using a negative geotaxis climbing assay. A single fly was placed in an empty plastic vial, tapped to the bottom, and the time required to climb 5 cm was recorded three times sequentially with 10 min rest periods between each measurement. Each replication value recorded was an average of the three trials; each assay was conducted on 10 flies per test group.

2.3. HPLC Analysis. Monoamine and pteridine levels were determined using an ESA CoulArray Model 5600A high performance liquid chromatography system. Fifty adult heads were extracted in 60 μL 0.1 M perchloric acid, followed by centrifugation. Ten μL aliquots of each extract were injected. Analyses were conducted on three replicas of each test set. Amines and pteridines were separated on a Phenomenex Synergi 4 μm Hydro-RP column (4.5 × 150 mm) according to the method of McClung and Hirsh [27]. Separations were performed with isocratic flow at 1 mL/min. Amines

were detected with the ESA CoulArray electrochemical analytical cell, Model 5011 (channel 1 at −50 mV, channel 2 at 300 mV). Pteridines were detected with a Linear Model LC305 fluorescence detector (excitation wavelength 360 nm and emission wavelength 456 nm). Analysis was performed using ESA CoulArray software.

2.4. GTPCH Assay. GTPCH activity was assayed as previously described [21]. Briefly, extracts were prepared from 30 heads of 3–5 days old adult males in 100 μL 50 mM Tris, 2.5 mM EDTA, and pH 8.0. Extracts were centrifuged at 10,000 rpm for 10 min and the protein concentrations of supernatants were determined using the BioRad Protein Assay Reagent. GTP was added to extract corresponding to 45 μg of protein to a final concentration of 0.2 mM in a final volume of 70 μL. The mixture was incubated for 1 hr at 37°C to convert GTP to dihydroneopterin triphosphate (dNP3), followed by its oxidation in 30 μL of 1% iodine and 2% potassium iodide in 1 M HCl and dephosphorylation with 2 units of alkaline phosphatase (Roche). Neopterin peaks were detected by fluorescence at excitation wavelength of 353 nm and emission wavelength of 438 nm.

2.5. Confocal Microscopy. Whole mounts of dissected brains from *TH-Gal4*; *UAS-eGFP*, *TH-Gal4*; *UAS-eGFP/UAS-bsk^{WT}*, and *TH-Gal4*; *UAS-eGFP/UAS-Akt^{WT}* adults fed with sucrose alone, with paraquat, or with paraquat and minocycline together were examined for dopaminergic neuron morphology and number, detected by visualizing GFP-expressing neurons. Each brain was scanned to include 15–18 sections for optimum visualization of DA neurons. The Z-sections were then utilized to get the average of all sections using a Leica TCS SP2 AOBS confocal microscope except for confocal images in Figure 8, which were captured using Zeiss LSM 710 Confocal Microscopy.

2.6. Catalase Assay. Crude enzyme extracts from adult flies fed PQ and MC as described above were prepared from ten heads from each treatment group in 150 μL 0.1 M sodium-potassium phosphate buffer containing 0.1 M Triton X-100 (pH 7.0), and activity assays were conducted following the method of [28]. The reaction of head extract with H_2O_2 was determined at absorbance wavelength 230 nm and calculated using a molar extinction coefficient for H_2O_2 of 62.4. One unit of catalase activity was defined as 1 μmole of H_2O_2 decomposed per min. All values represent the average of 6–8 replications from independently prepared extracts.

2.7. Lipid Peroxidation Assay. Head extracts from fifty heads were prepared in 100 μL of 0.1 M phosphate buffer from female flies at 2–4 days after eclosion fed as described above for 24 hr. Two mL of reagent TCA-TBA (thiobarbituric acid)-HCl was added to 1 mL of head extract and heated for 15 min in a boiling water bath to allow malondialdehyde, the product of the lipid peroxidase reaction, to develop a red chromophore, detected spectrophotometrically at 535 nm, as described by [29].

2.8. Griess Assay for NOS Activity. Head extracts from fifty heads were prepared in 100 μL of 0.1 M phosphate buffer with 1 M KCl (pH 7.4). Following centrifugation to remove debris, the supernatants were mixed with freshly prepared Modified Griess reagent (Sigma) in a volume ratio of 1 : 1. After a 15 min incubation period at room temperature in dark, nitrite levels were measured spectrophotometrically at 595 nm, with concentrations of nitrite calculated against a silver nitrite-derived standard curve and data was presented as a concentration of nitrite generated by extracts of 50 fly heads.

2.9. Statistical Analysis. One-way ANOVA with Dunnett's post-test or by two-tailed Student's *t*-test were used to analyze the data using GraphPad Prism (San Diego, CA). The figure legends describe the analyses of the data.

3. Results

3.1. Effect of Minocycline on Paraquat-Induced Truncation of Life-Span. Because MC toxicity has been reported in some mammalian disease models, we first tested a range of MC concentrations from 100 μM to 50 mM on non-PQ-treated flies to assess potential deleterious effects. We found that ingestion of 5 mM MC or greater affected viability, while lower concentrations caused no observable toxicity (Figure 1(a)). The results of this test for adult males are shown in Figure 1(a); females gave comparable results (data not shown). All subsequent experiments utilized MC concentrations of 1 mM or less to avoid drug-related toxicity.

We then asked whether concentrations of antibiotic at 1 mM or lower could rescue the toxic effects of 10 mM PQ (Figure 1(b)). When exposed to PQ alone, the average survival duration of adult males was approximately three days. Cofeeding of MC at concentrations of 500 μM and below did not improve survival duration; however, co-feeding of 1 mM MC with PQ extended the average survival duration an additional 48 hr, from three to five days (Figures 1(b) and 1(c)). Unless otherwise noted, all subsequent experiments were performed using 10 mM PQ and 1 mM MC. We then tested the efficacy of MC under three different regimens, comparing PQ and MC co-feeding, prefeeding MC for 2 days prior to PQ exposure, and prefeeding PQ for 2 days prior to exposure to MC alone. We found that neither prefeeding nor posttreatment of MC were able to modify the survival duration of PQ-exposed flies (data not shown). However, extending the MC pre-feeding period to 5 days resulted in extension of life span to almost the same degree as the co-feeding regimen (Figure 1(c)).

3.2. MC Protects against PQ-Induced Mobility Defects. We employed a climbing assay, which is a sensitive indicator of the onset of dopaminergic neuron-linked movement dysfunction, to assess whether MC could rescue the mobility deficits induced by PQ, similar to those observed by Faust et al. [20], in a *Drosophila DJ-1* genetic model of PD and in several mammalian models [30, 31]. Within 24 hr of the initiation of PQ feeding in the absence of MC,

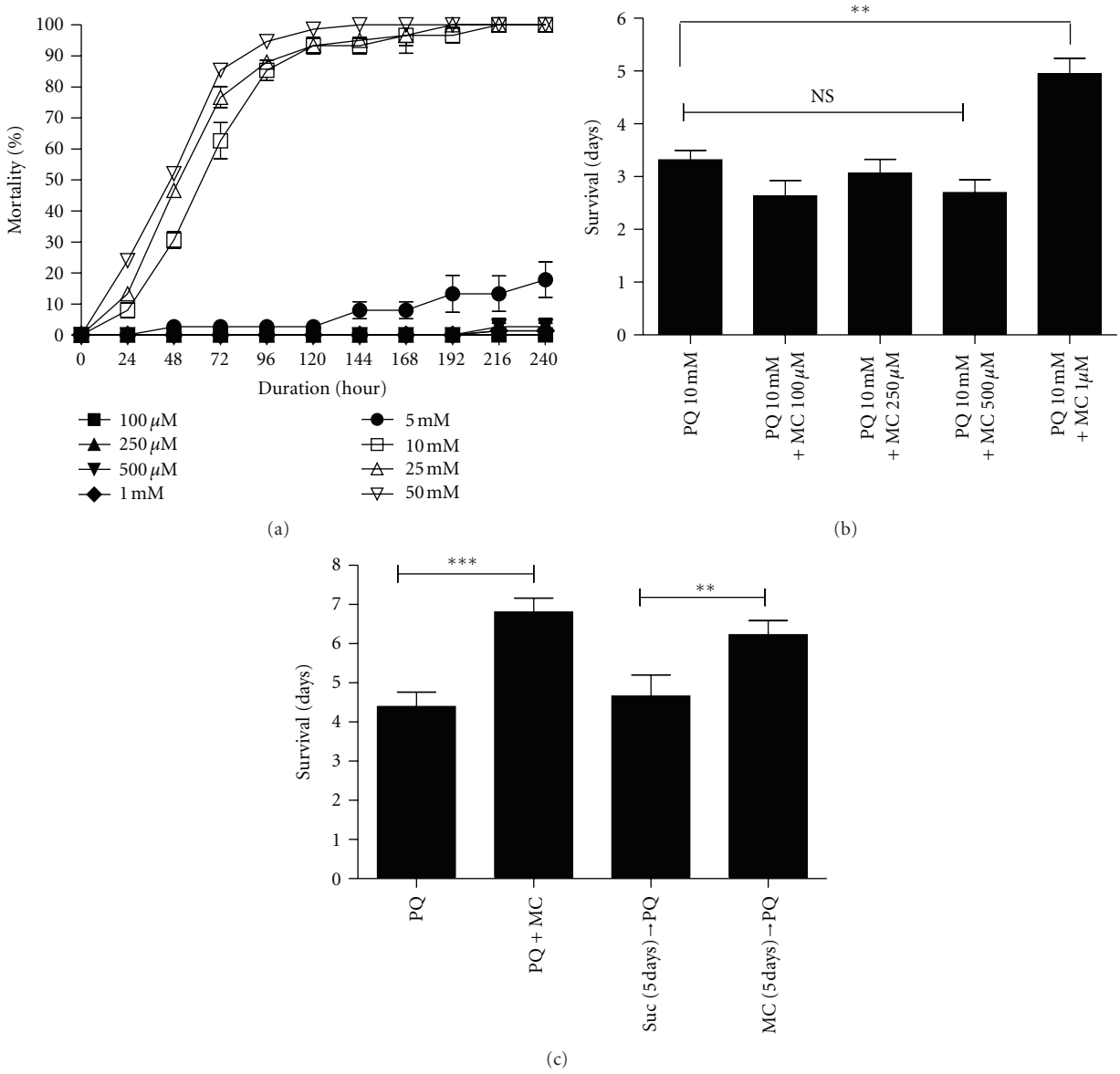

Figure 1: Effect of MC in absence and presence of 10 mM PQ on survival of adult male flies. (a) Effect of increasing concentrations of MC (100 μM–50 mM) on survival of adult male flies. Data were collected every 24 hrs for each group until 100% mortality was noted with 50 mM MC. (b) Effect of different doses of MC co-fed with 10 mM PQ on the life span of wild type adult males. Co-feeding of 1 mM MC with 10 mM PQ significantly extends the survival duration compared with PQ alone. ** represents the difference between PQ-fed flies and those fed PQ with 1 mM MC at $P < 0.005$. NS = nonsignificant. Error bars indicate the standard error of the mean. Each data point was derived at least 10 replications of 15 flies each. (c) Wild type flies at 48 hrs after eclosion were fed PQ and/or MC using different regimens as shown in the graph. The MC co-feeding group was compared to the PQ alone group and the MC prefeeding group was compared with the same aged group prefed 5% sucrose. Both co-feeding and prefeeding regimens improved the survival duration compared to PQ alone. ** = $P < 0.005$ and *** = $P < 0.001$ and represent the significant difference between PQ and prefeeding and co-feeding groups. Error bars represent SEM, and n = 50–60 flies for all groups in (a), (b), and (c).

tremors and bradykinesia were apparent. At 48 hr, these flies were unable to climb and exhibited a strong bradykinesia-like behavior. In contrast, when PQ was cofed with MC, no movement defects were apparent, and mobility was comparable to the negative geotaxis activity of control and minocycline-only flies (Figure 2).

3.3. MC Delays PQ-Induced Loss of Dopaminergic Neurons. We previously established that the onset of movement dysfunction upon PQ ingestion coincides with the loss of region-specific subsets of dopaminergic neurons in the adult brain [21]. In light of the ability of MC to ameliorate PQ-induced tremors and mobility deficits, we next asked

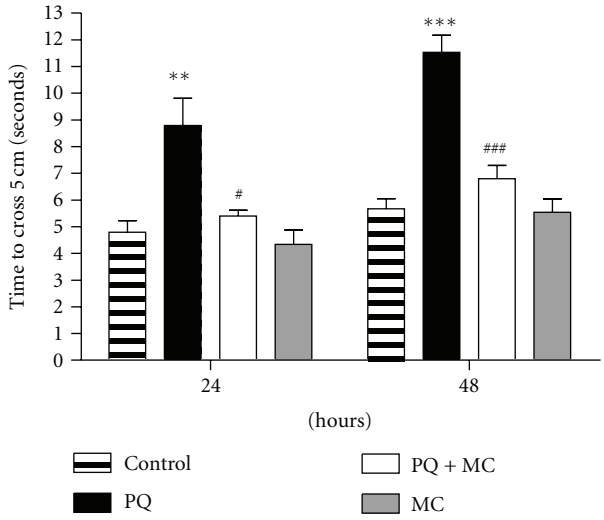

Figure 2: MC protects against PQ-induced mobility defects. The time required for adult male flies to climb 5 cm, after 24 and 48 hr of exposure to 10 mM PQ or 10 mM PQ with 1 mM MC flies was assayed. The ingestion of 1 mM MC alone has no effect on mobility, while ingestion of PQ alone adversely affects mobility. PQ and MC co-feeding results in mobility performance near control levels. The * and # indicate the significance of differences between control and PQ-fed flies and between PQ only and co-fed flies, respectively. ***/### indicate $P < 0.001$,** indicates $P < 0.005$, and # = $P < 0.05$. Error bars represent standard error of the mean. Each data point represents at least 15 replications of 10 flies each.

whether this effect is mediated through protection of at-risk dopaminergic neurons. Dopaminergic neurons were detected by the TH promoter-directed expression of GFP in the transgenic strain, *TH-Gal4; UAS-eGFP*. We compared dopaminergic neuron morphology and numbers in brains at 24 and 48 hr after the initiation of feeding 5% sucrose only, PQ only, MC only, or PQ with MC (Figure 3). Figure 3(a) displays characteristic results in dopaminergic neuron cluster PPM2 after 24 hr of treatment. The number and morphology of these neurons after the MC-only treatment were indistinguishable from neurons in control brains. As we had observed previously, using both the GFP reporter and immunolocalization of TH to identify dopaminergic neurons [21], these neurons display characteristic patterns of morphological changes and neuronal sensitivity after PQ exposure (Figure 3(a)), whereas neurons in animals exposed to MC with PQ retained near normal morphology and neuron number (Figures 3(a), 3(b), and 3(c)). Upon treatment with PQ only (Figure 3(a)) for 24 hrs, we observed that the PAL subgroup in the anterior region and the PPL1, PPM2, and PPM3 subgroups in the posterior brain exhibited statistically significant neuron loss relative to controls (Figure 3(b)). In the animals that were co-fed PQ and MC, there was no neuron loss in the PPM1 or PPL2 subgroups at 24 hr, and neuron numbers and morphology in other clusters were almost identical to those in control brains (Figures 3(a) and 3(b)). After 48 hrs of PQ feeding, previously affected clusters continued to deteriorate, while neurodegeneration was noted in the previously unaffected PPM1 and PPL2 clusters, while improved survival of all dopaminergic neuron groups was noted in the PQ and MC co-fed flies (Figure 3(c)). Therefore, we conclude that the extension of life span observed when flies were fed MC along with PQ and delay of the onset of movement deficits correlate with protection against PQ-induced neurodegeneration.

3.4. MC Blocks Changes in DA Pathway Components Indicative of PQ-Induced Oxidative Stress. The production of DA is rate-limited by two enzymes: tyrosine hydroxylase (TH), which converts tyrosine to L-DOPA, and GTP cyclohydrolase (GTPCH), which is rate-limiting for the production of tetrahydrobiopterin (BH_4), a cofactor for and regulator of TH catalysis. We previously observed that sensitivity to PQ is at least partially defined by the activity of the BH_4 and DA biosynthesis pathways [21]. We found that following PQ ingestion, but prior to loss of dopaminergic neurons, there is a transient stimulation of DA pathway activity, followed by a decrease in BH_4 and DA levels and a corresponding increase in oxidative products, biopterin and DOPAC, respectively. The observed protection by minocycline against the effects of PQ might be mediated through interactions with the DA homeostasis machinery, either modulating DA synthesis or transport or through its ability to act as a scavenger of ROS [11], delaying the PQ-induced oxidative depletion of DA and subsequent oxidative damage. Ingestion of MC alone for 24 hr has no significant effect on the production of pathway metabolites or on GTPCH activity (Figure 4), ruling out the possibility that MC modulates DA homeostasis. PQ induced dynamic changes of enzyme activity, pathway products, and oxidative products. After 24 hr of PQ exposure, L-DOPA pools are significantly elevated, indicating an increase in TH activity; however, DA was depleted and the DA metabolite, DOPAC (3,4-dihydroxyphenylacetic acid) was elevated, as expected in an oxidative environment (Figures 4(a) and 4(b)). Similarly, GTPCH activity increased (Figure 4(c)), while BH_4 pools are diminished and the oxidized product biopterin increased with PQ exposure (Figure 4(a)). In contrast, when MC was co-fed with PQ for 24 hr, the effect of PQ on each of these components was significantly less severe, consistent with the reported antioxidant property of MC.

3.5. MC Reduces PQ-Generated Reactive Oxygen Species. The ability of MC to block the PQ-induced changes in the DA and BH_4 biosynthesis pathways indicative of oxidative stress led us to hypothesize that MC was serving principally as a scavenger of PQ-generated ROS in *Drosophila*. We employed two assays for oxidative stress, lipid peroxidation [29], and induction of catalase activity [28, 32]. PQ ingestion results in a two-fold elevation of lipid peroxidation within the first 24 hr (Figure 5(a)). Co-feeding of MC with PQ almost completely blocks this indicator of lipid damage. Elevated catalase activities were detected in the heads of both PQ and PQ plus MC groups (Figure 5(b)); however, the catalase activity in flies that had ingested MCwith PQ was significantly lower than those exposed to PQ only.

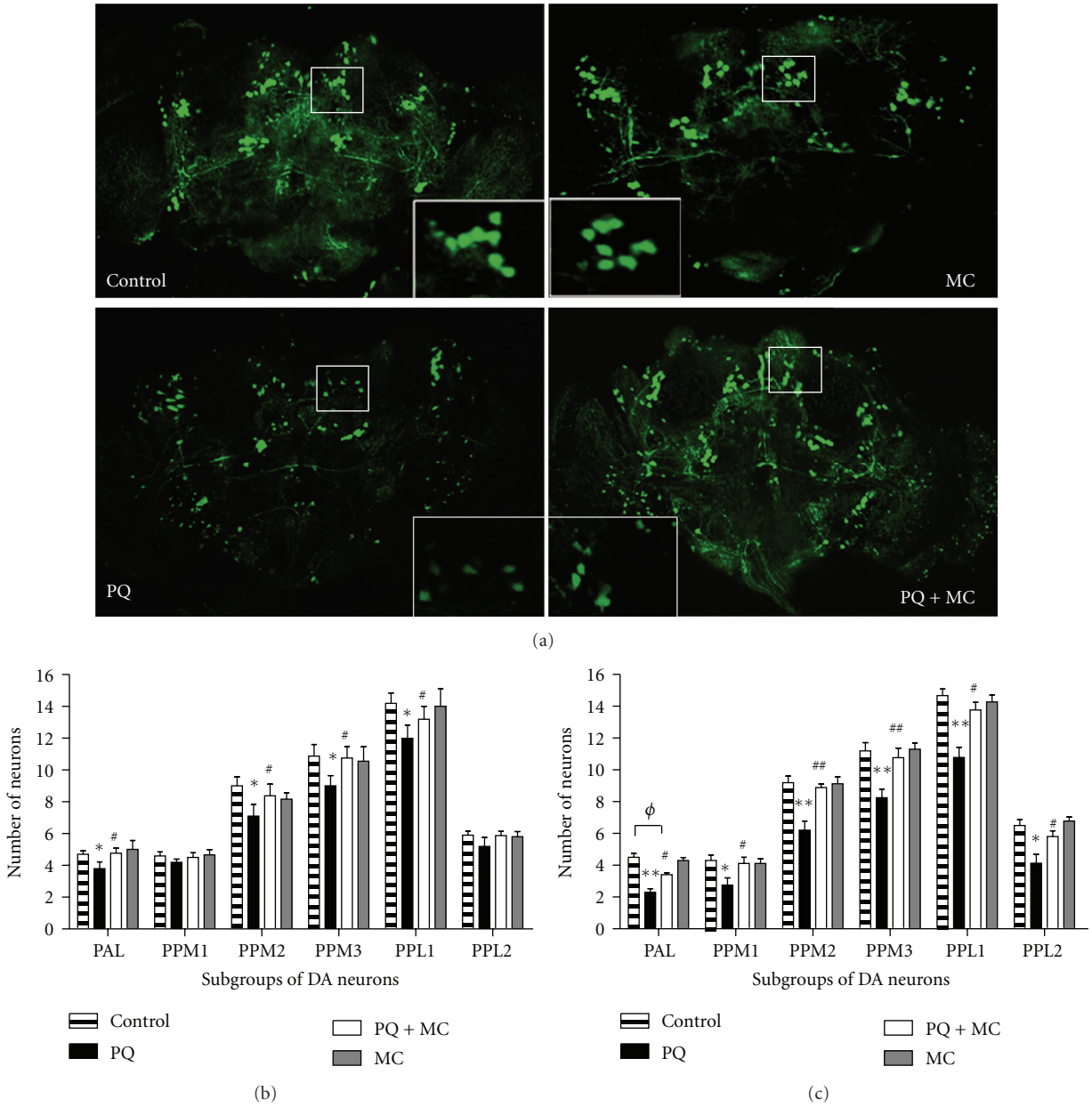

Figure 3: MC confers protection to dopaminergic neurons. (a) The effect of a 24 hr exposure of adult males to sucrose (Control), 1 mM MC alone (MC), 10 mM PQ alone (PQ), and 10 mM PQ with 1 mM MC (PQ + MC) on the dopaminergic neurons of *TH-GAL4; UAS-eGFP* adult brains. The inset in each image demonstrates the change in the morphology and number of the PPM2 subgroup of neurons. The exposure to MC alone (MC) and sucrose (control) does not alter the number or morphology of the dopaminergic neurons. The addition of MC to PQ delays neuron loss and onset of abnormal neuron morphology relative to PQ only. Scale bar for whole brain images = 100 μm. (b) and (c) MC delays PQ-induced selective loss of dopaminergic neurons. The average number of neurons per subset was determined 24 hr (b) and 48 hr (c) after the initiation of feeding and shows that MC delays, but does not prevent, PQ-mediated neuronal loss in different dopaminergic neurons. Each subset of dopaminergic neurons was scored separately in 15–25 brains. The significance of the difference in each neuron cluster between the PQ-treated and control groups and between the PQ-treated and co-fed groups is indicated as * and $^{\#}$, respectively, where $^{*} = P < 0.05$, $^{**} = P < 0.005$, $^{\#} = P < 0.05$, and $^{\#\#} = P < 0.005$. $^{\phi}$ represents the significant difference between control and PQ with MC co-fed brains where $^{\phi} = P < 0.05$. Error bars represent standard error of the mean.

These results strongly suggest that MC has a strong capacity to suppress ROS generated by PQ.

3.6. MC Cannot Rescue Pu (GTP Cyclohydrolase) Mutants. Mutations in the rate-limiting genes for BH_4 and DA synthesis, *Punch* (*Pu*; GTPCH) [33] and *pale* (*ple*; TH) [25], respectively, result in decreased DA pools in adult heads and increased sensitivity to PQ [21]. Conversely, loss-of-function alleles of *Catecholamines up* (*Catsup*), a negative regulator of TH and GTPCH, have elevated BH_4 and DA pools and

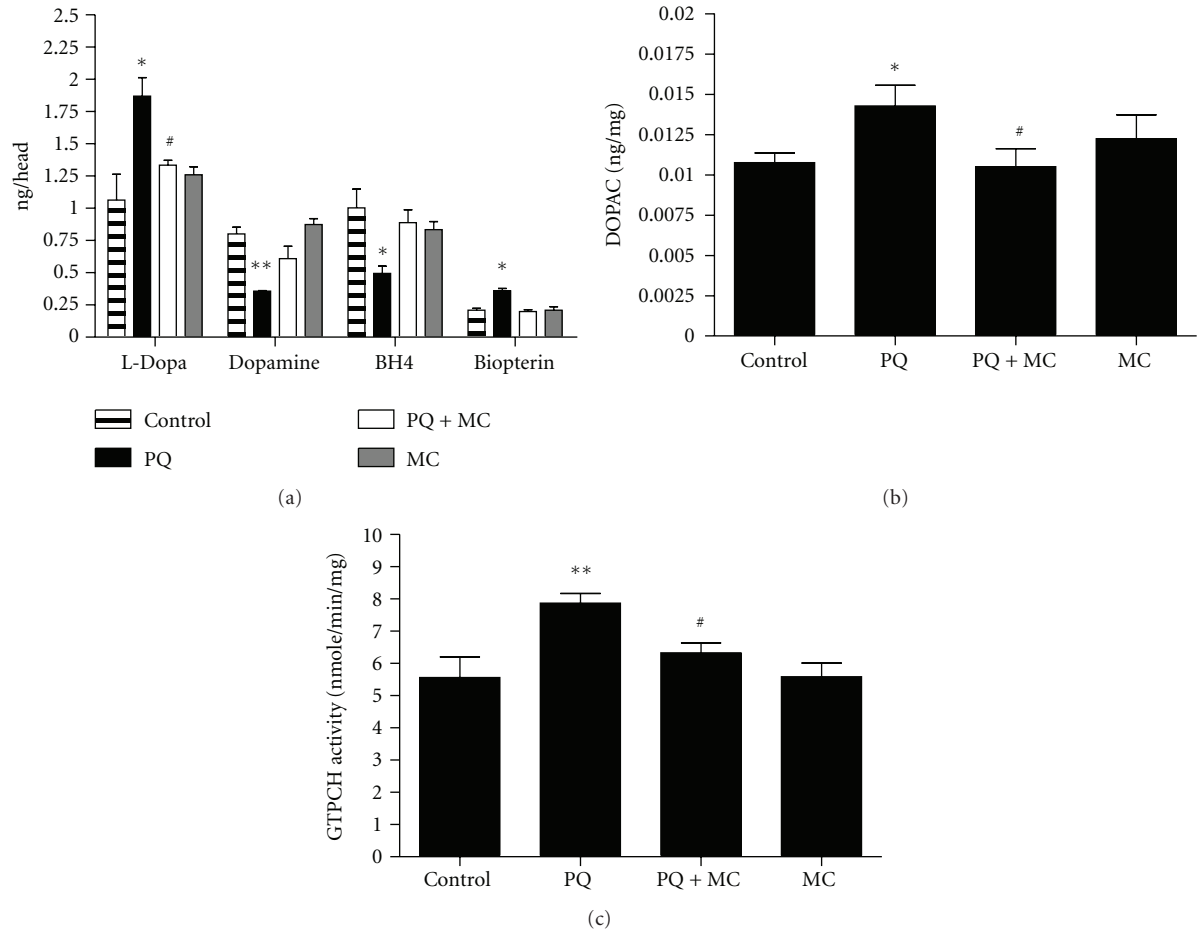

Figure 4: MC blocks the changes induced by PQ in the DA and BH_4 biosynthesis pathways. (a) Changes in the DA and BH_4 metabolites in adult males exposed to 10 mM PQ or 10 mM PQ with 1 mM MC for 24 hrs. The increase in L-DOPA levels, indicative of PQ-stimulated TH activity, is reduced by MC. (b) The DA metabolite, DOPAC, is elevated by PQ exposure and is significantly decreased by the co-feeding of MC to male adults for 24 hr. (c) The compensatory increase in GTPCH activity in PQ-fed adult males is reduced in PQ-MC co-fed males at 24 hr of ingestion. The significance of differences in each subset between the PQ-treated and control groups, and PQ-treated and co-fed groups is indicated as * and $^{\#}$, respectively, where * and $^{\#} = P < 0.05$ and ** and $^{\#\#} = P < 0.005$. Error bars represent the standard error of the mean. Each data point represents at least 10 replications of 15 flies each.

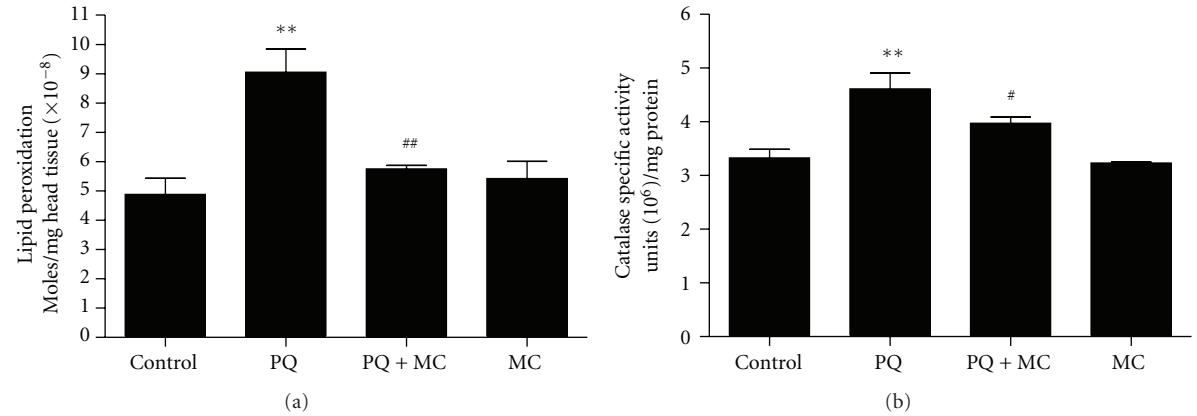

Figure 5: MC reduces PQ-generated reactive oxygen species. (a) The level of lipid peroxidation product was determined in head extracts of males that had ingested PQ or PQ with MC for 24 hr. MC significantly decreases the amount of lipid peroxidation induced by PQ. (b) MC reduces the specific activity of catalase after 24 hr of ingestion in co-fed male flies. The significance of differences between the PQ-treated and control groups and between the PQ-treated and co-fed groups was indicated as * and $^{\#}$, respectively, where * and $^{\#} = P < 0.05$. Error bars represent standard error of the mean. The experiments were done as 5–8 replicas of 10 head extracts.

a strong resistance to PQ [22, 24]. While we continue exploring the mechanistic basis for the differential sensitivity to PQ, these mutant strains provided the opportunity to begin defining genetic components that might have roles in modulating the protective effects of MC. We found that *Catsup* heterozygotes survive PQ 24 hrs longer, on average, than wild type adults, while *Pu* and *ple* heterozygotes die 48 hrs or more before wild type flies (Figure 6(a)). MC extended the survival of wild type flies and the *Catsup* and *ple* mutants, by approximately 2 days for each strain. Therefore, we detected no DA-specific interactions with MC in these mutants.

Strikingly, however, MC was unable to improve the survival of *Pu* mutants under these conditions. One possibility is that the heterozygous *Pu* mutants might provide a sensitized background which reveals an otherwise undetectable deleterious effect of 1 mM MC. However, in other studies, we found that ingestion of MC at concentrations up to 5 mM by *Pu* mutants had no discernable effect on survival (Ajjuri and O'Donnell, in preparation). Alternatively, oxidative damage in *Pu* mutants, perhaps related to a *Pu* function other than regulation of DA synthesis, might progress too rapidly for MC to impart its protective effect. One such candidate is nitric oxide synthase (NOS), which requires BH_4 as a cofactor. It is well known that limiting BH_4, which should be a consequence of loss-of-function mutations in *Pu*, results in the catalytic uncoupling of NOS, dramatically enhancing oxidative stress through production of elevated peroxides and peroxynitrites [34, 35]. Since *Pu* mutants have reduced levels of BH_4 [33], we hypothesized that the failure of MC protection in *Pu* mutants is linked to catastrophic oxidative damage stemming from induction of NOS by PQ and its subsequent uncoupling. If this hypothesis is correct, then inhibition of NOS catalytic activity should limit the production of ROS and RNS and, thereby, improve survival of the *Pu* mutant flies. As expected, heterozygous *Pu* mutants have lower NOS activity than wild type flies. Ongoing experiments to date have revealed no detectable effects of MC alone on NOS activity (unpublished data). PQ ingestion resulted in elevated NO production, as determined by the Griess assay, in both wild type and *Pu* mutant heads (Figure 6(b)). MC reduced nitrite levels in wild type flies, suggesting its ability to reduce the inflammatory response in flies as in mammals. However, MC was ineffective in reducing nitrite levels in *Pu* mutants, exposed to 10 mM PQ (Figure 6(b)). We then fed 1 mM PQ, to slow the rate of accumulation of oxidative damage, in an effort to further dissect events contributing to neurodegeneration. We observed that NOS inhibitor L-NAME reduced nitrite levels in both wild type and *Pu* mutants (Figure 6(c)). Moreover, ingestion of L-NAME was able to prolong survival of the *Pu* mutant strain as well as wild type flies exposed to 1 mM PQ (Figure 6(d)). In contrast, even at this 10-fold lower concentration of PQ, MC was still unable to improve the survival of *Pu* mutants. These results suggest that the failure of MC to rescue *Pu* mutants was due to its inability to limit NOS activity and therefore reduce oxidative damage when BH_4 production is compromised.

3.7. Loss of Function Mutants of the Genes Encoding JNK and Akt Are Sensitive to 1 mM PQ but Involvement of Reaper, Caspase, and Rolled in PQ-Induced Toxicity Was Not Detected. Signal transduction pathways associated with oxidative stress, inflammatory, and apoptotic responses are likely targets of minocycline action [15]. However, it also is known that dopaminergic signaling and homeostasis, highly conserved processes in flies and mammals, are highly responsive to environmental stressors across species lines [36, 37]. This feature of dopaminergic function is highlighted by our findings that PQ induces early changes in DA metabolism and that mutations in genes altering DA homeostasis strongly affect the sensitivity of *Drosophila* to PQ [21, 22]. The roles of such signal transduction pathways are likely to be highly complex, as discrepancies in evidence for participation of particular kinases in responses to oxidative damage and subsequent neurodegeneration emphasize [38, 39]. As a foundation towards employing our whole organism disease model to better understand the interface between regulation of signal transduction and dopamine homeostasis in dopaminergic neurodegeneration, we next turned our attention to MC effects under conditions in which specific signaling pathways previously implicated in neurodegeneration mechanisms are genetically modified.

The mitogen-activated protein kinase (MAPKs) subfamilies, extracellular signal regulated kinases (ERK), c-Jun N-terminal kinases (SAPK/JNK), and p38 kinases, are known to be activated by a wide range of stimuli including inflammatory cytokines and diverse environmental stressors and to mediate a variety of downstream effects likely to be integral to protection against neurodegenerative mechanisms [40, 41]. In mammalian models for neuronal injury and neurodegenerative diseases, pharmacological approaches have provided evidence that p38 and JNK are mainly implicated in neuronal death processes, while ERK may promote cellular recovery/survival from neuronal death implicated in these conditions [42].

We therefore tested heterozygous mutants for JNK, encoded by the gene *basket* and Akt/PKB, encoded by *Akt1*, and ERK, encoded by *rolled*, in *Drosophila*. In addition, we tested mutations in the caspase-9 gene, *dronc*, and mutations in the proapoptotic gene, *reaper*. These kinases function in myriad biological processes but are particularly known to respond to various cellular stress. We hypothesized that they should also play key roles in the toxic responses triggered by PQ.

We exposed heterozygous mutants with loss of function alleles of *bsk* and *Akt* to 10 mM PQ alone or in combination with 1 mM MC and observed that both sets of mutants had apparently slightly elevated sensitivity to PQ although not statistically significant (Figure 7(a)). Interestingly, however, MC failed to improve the survival of either mutant, while survival of the control strain was significantly improved. To clarify the effects of mutations in these kinase genes, we tested additional *bsk* and *Akt* alleles, decreasing the PQ concentration (1 mM) to slow the progression of PQ-induced damage as in the *Punch* mutant experiments described above. In this experiment, we expanded our analysis to include a mutant allele of the ERK gene, *rolled*, and mutants for the

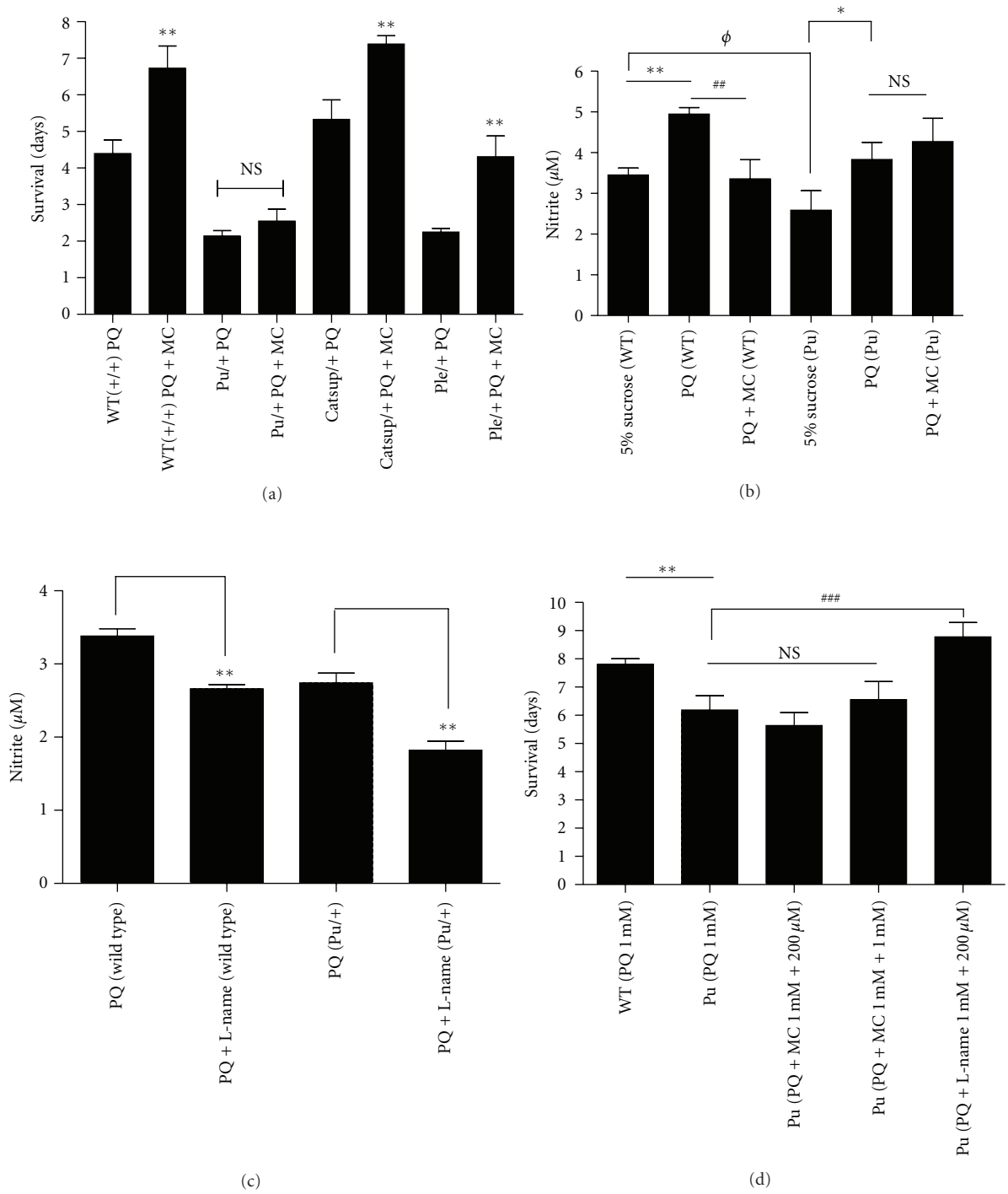

Figure 6: MC fails to rescue *Punch* mutants due to dysregulation of nitric oxide synthase catalytic function. (a) Effect of 1 mM MC co-fed with 10 mM PQ on DA regulatory mutants, $Catsup^{26}$/+, Pu^{Z22}/+ and ple^{2}/+. *Catsup* and *ple* mutant flies showed extension of life span, while *Pu* mutants did not. NS = not significant. ** = $P < 0.005$ and represents significant differences between PQ and PQ with MC. (b) After 24 hr of PQ, or PQ with MC exposure, suppression of NOS was detected in wild type heads but not in *Punch* mutants where NO levels of non-PQ-treated *Pu* mutants assayed are significantly lower than NO levels of non-PQ-treated wild type heads. * or $^{\phi}P =< 0.05$ and ** or $^{\#\#}P =< 0.005$. (c) Co-feeding of L-NAME with 1 mM PQ reduced NO production in wild type and *Pu* mutants. ** = $P < 0.005$. (d) The survival of *Pu* mutants was improved by co-feeding PQ with L-NAME, but not with MC when compared with survival of *Pu* mutants on PQ alone. * represents significant differences between control and PQ-exposed flies, while $^{\#}$ represents significant differences between flies fed PQ only and PQ with MC. ** = $P < 0.005$ and $^{\#\#\#} = P < 0.001$. NS = not significant. Error bars represent standard error of the mean and n = 100–120 fly heads for NOS assays and 50–60 flies for survival where experiments were replicated thrice with the same sample size.

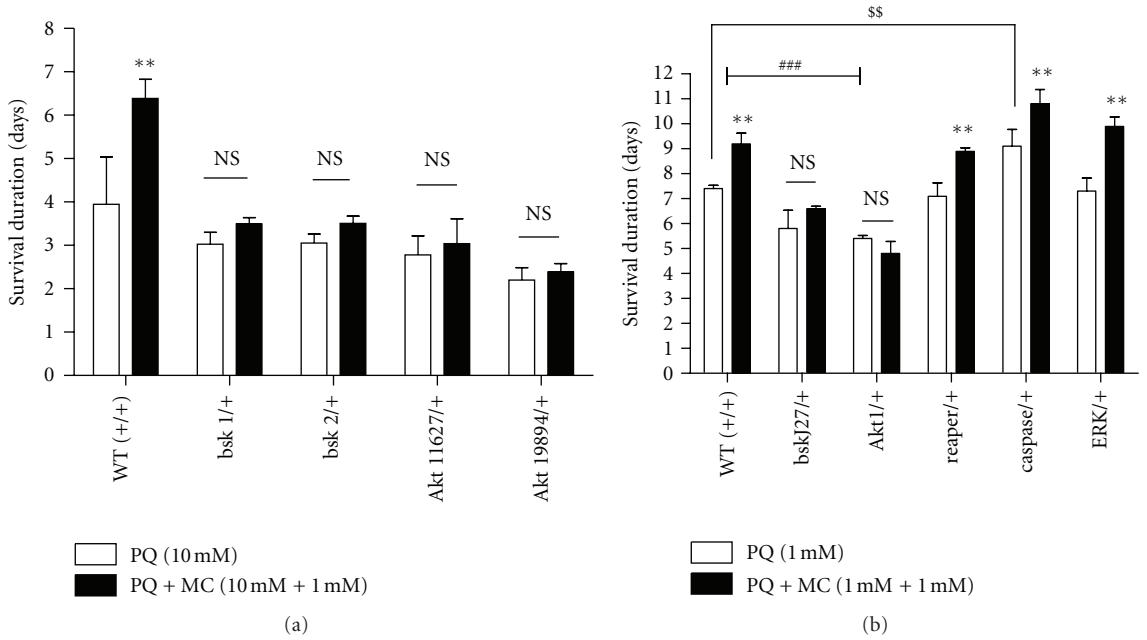

FIGURE 7: PQ and MC effects on viability are modified by components of stress response pathways. (a) Effect of *bsk* and *Akt* loss-of-function mutant alleles on PQ and MQ effects on survival. Treatment with 1 mM MC failed to improve the survival of *bsk* and *Akt* loss-of-function mutants fed 10 mM PQ. $n = 120$ and each data point represents at least three independent replications of 40 flies for each.genotype. (b) Effect of 1 mM PQ and 1 mM MC on loss-of-function mutants of signaling pathways, JNK, Akt, reaper, caspase, and ERK. *rolled* (ERK), *reaper* and *caspase* mutants showed an extension of life span with MC treatment, while the survival of JNK and Akt mutants was unmodified in the presence of MC. ** = $P < 0.005$ represents significant difference between PQ and PQ with MC groups. ## = $P < 0.005$ and shows a significant difference between PQ-fed wild type and PQ-fed *bsk* and *Akt* loss-of-function mutants. NS = not significant. $$ = $P < 0.005$ represents significant difference between PQ-fed wild type and PQ-fed caspase loss-of–function mutant. Error bars represent standard error of the mean. $n = 180$ and each data point represents at least three independent replications of 50–60 flies each.

apoptotic pathway genes *dronc* (Caspase) and *reaper*. Under these conditions, the heterozygous *bsk* and *Akt* mutants showed increased sensitivity to PQ, dying, on average, two days before wild type flies, and again MC was ineffective in rescuing these mutants (Figure 7(b)). These results suggest either that JNK and Akt signaling pathways are important in the protective response of MC in flies or that diminution of their activity heightens the oxidative environment to a point that the beneficial effects of MC are lost. However, the sensitivity of heterozygous *reaper* and *rolled* mutants to PQ and the ability of MC to increase survival were indistinguishable from the wild type controls. In contrast, the heterozygous caspase mutant, *dronc*, survived two days more than the wild type controls on PQ and minocycline improved survival an additional two days (Figure 7(b)).

3.8. Overexpression of JNK and AKT Confers Protection against Paraquat-Induced Toxicity in Dopaminergic Neurons. The observations that *JNK* and *Akt* loss-of-function heterozygous mutants increase the sensitivity to PQ and that normal expression of these genes appears to be important for MC-mediated protective responses against PQ led us to test whether this effect is reversed when JNK and Akt are overexpressed. Since PQ toxicity initially is observed in dopaminergic neurons and DA itself appears to interact in this process, we drove expression of wild type JNK and Akt in DA neurons using the GAL4-UAS system [43]. Even though we employed PQ at the higher concentration of 10 mM for these experiments, the expression of JNK and Akt in dopaminergic neurons resulted in approximately a two-fold increase in the survival duration in both cases (Figure 8(a)). MC improved life span in all strains by 30% compared to 10 mM PQ alone. Importantly the combination of MC plus overexpression of Akt in dopaminergic neurons enhanced survival over three-fold relative to the wild type control. These results demonstrate that both Akt and JNK have prosurvival functions in PQ-induced DA toxicity, with Akt expression having the strongest effect.

We further verified the protective effect of wild type JNK and Akt by examining the survival of at-risk dopaminergic neurons in the adult brain. The transgenic strain, *TH-Gal4; UAS-eGFP* was crossed with *UAS-JNK*^{WT} and *UAS-Akt*^{WT}, expression of GFP in concert with JNK or Akt. We observed that MC was able to protect against neuron loss in subgroups of posterior brain DA neurons expressing GFP, but otherwise wild type, relative to the brains of flies from the same cultures exposed to PQ only (Figure 8(b)). The overexpression of Akt or JNK in dopaminergic neurons prevents PQ-induced DA neuron loss in most subgroups of DA neurons relative to the control brains. Similarly, the transgenic brains, *TH-GAL4; UAS-eGFP/UAS-bsk*^{WT}

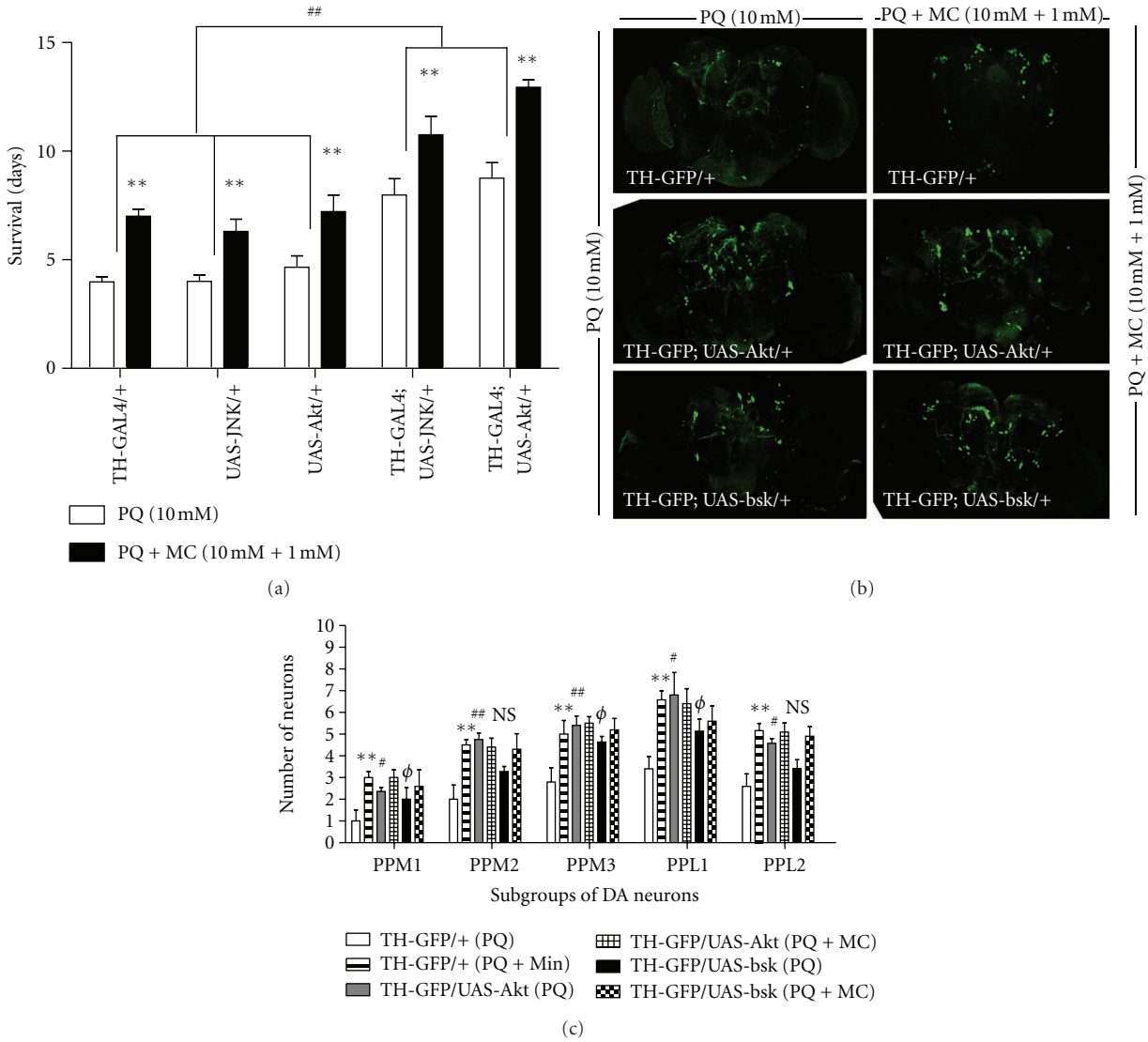

Figure 8: Overexpression of wild type BSK/JNK and Akt provides protection against PQ. (a) Adult males of genotypes *TH-GAL4*/+, *UAS-bsk*^{1}/+, *UAS-Akt*^{1}/+, *TH-GAL4*; *UAS-bsk*^{1}/+, and *TH-GAL4*; *UAS-Akt*^{1}/+ flies were fed, beginning at 48 hr after eclosion, 10 mM PQ or 10 mM PQ and 1 mM MC. The average survival duration for each group was determined. ** = $P < 0.005$ and represents significant differences between the PQ and PQ with MC groups. ## = $P < 0.005$, indicating a significant difference between control and JNK or Akt expressing flies fed only PQ. Error bars represent standard error of the mean. Each data point represents at least three independent replications of 50–60 flies each. (b) The effect of PQ (10 mM) and PQ + MC (10 mM + 1 mM) on brains of transgenic lines shown in the images. The overexpression of wild type Akt and Bsk/JNK in dopaminergic neurons provides protection to DA neurons against PQ, however; addition of MC in fails to provide additional protective to transgenic lines, *TH-Gal4; UAS-eGFP/UAS-Akt*^{WT} and *TH-GAL4; UAS-eGFP/UAS-bsk*^{WT} against PQ. (c) The average number of neurons per subset was determined 24 hr after the initiation of feeding in these transgenic lines. MC ingestion significantly improved the survival of DA neurons against PQ-induced loss of DA neurons in *TH-Gal4; UAS-eGFP*/+ brains.The overexpression of wild type Akt and JNK supports the survival of DA neurons against 10 mM PQ but addition of 1 mM MC failed to provide additional protection against PQ mediated DA neuron loss in these transgenic lines. ** = $P < 0.005$ and represent significant differences between PQ and PQ and MC-treated *TH-Gal4; UAS-eGFP*/+ brains. # represents significant differences between PQ-treated *TH-Gal4; UAS-eGFP*/+ and PQ-treated *TH-Gal4; UAS-eGFP/UAS-Akt*^{WT} and Φ represent significant differences between PQ-treated *TH-Gal4; UAS-eGFP*/+ and PQ-treated *TH-GAL4; UAS-eGFP/UAS-bsk*^{WT} brains, respectively. #/Φ = $P < 0.05$ while ## = $P < 0.005$. n = 8–12 brains for each transgenic lines. NS = not significant.

that were fed PQ (Figure 8(b)) displayed significantly greater DA neuron numbers. However, cofeeding of 1 mM MC with PQ failed to provide neuroprotection above that observed in Akt or JNK overexpression (Figures 8(b) and 8(c)). These results are in line of the survival data where the protective effect of MC on transgenic lines, *TH-GAL4;UAS-JNK* and *TH-GAL4;UAS-Akt*/+, was proportionate to those observed with control flies, rather than further enhancing survival.

4. Discussion

4.1. MC Imparts Antioxidant Effects in a PQ-Induced Drosophila Model for Parkinson's Disease. PQ is considered an oxidative stressor, generating superoxide and hydroxyl radicals [31]. Moreover, epidemiological and experimental studies point to PQ as an etiological agent for PD [44]. We have used PQ ingestion to establish an *in vivo Drosophila* PD model [21] and here employ this model to explore genetic interactions that alter the effects of MC, as a model for analysis of drugs offering therapeutic benefits in PD. As may be seen in the results reported in this study, this system has provided a fruitful avenue for exploring the effects of genetic alterations that may play roles in DA neuron susceptibility to deleterious environmental insult. It is noteworthy that we observe strong effects, both on PQ toxicity and on the protective capacity of MC, despite the fact that in all instances we are working with homozygous lethal mutant alleles, necessitating the use of heterozygotes with a wild type allele also present in each instance. It is increasingly recognized that dopaminergic neurons are at heightened oxidative risk, largely due to the interactive nature of DA itself. It is imperative that DA homeostatic mechanisms and oxidative surveillance are sensitively regulated and balanced to avoid catastrophic neuronal destruction. We note that comparable studies in mammalian models, incorporating a large collection of mutant alleles, are more difficult to implement. However, such studies are straightforward using the *Drosophila* model system, and our results with these heterozygous strains clearly support to prevailing view of the exquisite balance of pathways needed for the well-being of dopaminergic neurons.

MC has been shown to have anti-inflammatory and antioxidant properties in numerous neurodegenerative and injury-induced mammalian models [15, 45]. Although the exact biological targets for MC are still not well known, it has been reported that MC causes the inhibition of the cytochrome c release from mitochondria, the inhibition of caspase-1 and -3 expression, and the suppression of microglial activation [8, 15, 46].

Despite numerous reports supporting the efficacious role of MC in numerous models of neurological disease and injury, other studies have reported the absence of effects or even increased deleterious effects [12, 13]. Diguet et al. [12] reported that the protective or deleterious effects of MC depend on the mode of administration and dose of the drug. Because there is continuing controversy in MC studies, we first conducted a toxicity test employing a range of MC doses. Since we found that concentrations above 5 mM were toxic when fed to wild type adult flies, we employed 1 mM MC, a concentration substantially below toxic levels and yet effective in ameliorating the deleterious effects of 10 mM PQ. In addition, we tested various treatment paradigms and found that both pre-feeding and co-feeding regimens were equally protective. Bonilla et al. [19] also reported the prevention of PQ-induced reduction of survival duration in *Drosophila*, but the mechanism through which MC imparts this effect in *Drosophila* was not investigated in that study. More recently, Faust et al. [20] tested the efficacy of MC in ameliorating dopaminergic neuron loss in *Drosophila* when expression of DJ-1A was blocked by specific expression of *DJ-1A RNAi* in these neurons. In this study of a genetic model for PD, higher concentrations of MC (50–100 mM) were able to rescue the DJ-1RNAi-mediated loss of DA neurons. These investigators also assessed the effect of MC on DA pools and on the survival of DA neurons in the DCM region of the brain. Our study supports and extends this interesting study, demonstrating that this antibiotic is also effective in an environmental toxin model of PD. We also find improvement in survival and DA pools, but also a striking rescue of DA neurons, not only in the specific region investigated by Faust et al. but, interestingly, in all subsets of DA neurons. Mobility also was rescued in our study, as were markers of oxidative stress and inflammation. Thus, the efficacious effects of MC in both a genetic and a toxin model of PD in *Drosophila* produce comparable outcomes despite the fact that the *DJ-1* knockdown effects were observed at approximately 10 to 25 days after eclosion, while this PQ study tested more acute responses. Formally, there is a possibility that MC chemically interacts with and detoxifies PQ. However, the fact that comparable results are observed in both genetic and PQ models of PD in *Drosophila* argues strongly against this selective chemical interaction. Thus, we conclude that *Drosophila* systems present a robust model for investigating mechanisms of therapeutic action.

We have shown previously that PQ induces first a rapid activation of DA synthesis, as well as the BH_4 cofactor pathway required for both DA biosynthesis and NOS activity, followed by rapid oxidative turnover of BH_4 and DA [21]. We therefore expanded our neurochemical analysis to monitor L-DOPA and DOPAC. We detected suppression of each of these neurochemical responses upon MC treatment, confirming a strong antioxidant function for MC in this system from the perspective of DA metabolite responses as well as for the generation of ROS responses, by catalase and lipid peroxidation assays.

Kraus et al. [11] compared the antioxidant property of MC with other known antioxidants. The antioxidant property was assessed on mammalian neuron cell culture via cell-based glutamate-induced oxidative stress assays and cell-free antioxidant activity assays including lipid peroxidation. MC along with other known antioxidants such as (±) tocopherol showed direct radical scavenging activity, proposed to be due to the presence of phenolic ring capable of reacting with free radicals, leading to the formation of relatively stable and unreactive phenol-derived free radicals [15]. Our results, combined with those of Bonilla et al. [19] and Faust et al. [20], strongly support a similar ability of MC in these whole organism studies under a variety of oxidative stress paradigms.

4.2. Failure of MC Protection against PQ in Punch Mutants. Having previously shown that mutants with defects in DA biosynthesis pathways show differential susceptibility to PQ [21], we employed these mutants to test for gene-environment interactions that might modify the efficacy of

MC. Interestingly, MC improved the survival of *pale* and *Catsup* mutants proportionate to those with wild type flies, while it failed to rescue *Pu* mutants. While one possible explanation for this lack of effect is that a deleterious MC effect is revealed in the *Pu* mutant, we have observed no evidence of altered survival when MC alone, at concentrations employed in this study, is ingested by this mutant strain. These results suggested that functions of *Pu* other than its role in DA homeostasis might impact its effect on MC protection. BH_4, the terminal product of the GTPCH pathway, also functions as an essential cofactor for NO production, facilitating the dimerization of NOS and functioning as a single electron donor during the process of NO production [35]. The limiting BH_4 pools, as in heterozygous *Pu* mutants, cause the uncoupling of electron transfer in NOS catalytic function, in consequence, the generation of superoxide and peroxynitrites radicals [35, 47]. In support of this interpretation of our results, we found that *Punch* mutants exhibited lower than normal NOS activity and that *in vivo* inhibition of NOS catalytic function with the inhibitor L-NAME improved the survival of PQ-fed flies. The inability of MC to prevent excessive generation of peroxynitrites in *Punch* mutants presents an example of modified drug-gene interaction and may help to explain the phenomenon of drug failure response in PD and other neurodegenerative diseases. Our data also validates *Drosophila* as an *in vivo* model for screening of drug molecules for possible drug-gene interaction.

4.3. Identification of Signal Transduction Pathways Necessary for MC Protection against PQ-Induced Neurotoxic and Neuroinflammatory Responses. Our investigation of signaling pathways mediating PQ-induced neurotoxic in *Drosophila* seeks insights into signal transduction pathways that can modify PQ-mediated toxicity at the whole organism level. Most of the previous mammalian studies have utilized *in vitro* (i.e., cell culture) approaches to address this question. Moreover, these mammalian studies have used primarily pharmacological inhibitors to block the proposed functions of the signaling pathway, which may lack complete specificity of function. Finally, the variations in the type of inhibitor used, inhibitor concentrations, and time of addition as well as cell lines may affect the outcome of these experiments [48, 49].

We have tested the roles of kinases and proapoptotic genes known to be functionally conserved with mammals. The heterozygous loss-of-function mutants for *JNK/bsk* (bsk^{J27}, bsk^{1} and bsk^{2}) and *Akt* (Akt^{1}, Akt^{11627} and Akt^{19894}) exhibit sensitivity to PQ in the absence of MC and fail to respond to antibiotic treatment. Moreover, overexpression of the wild type form of either kinase results in resistance to PQ. These results indicate crucial roles for these signaling pathways against neuronal stress responses to PQ. In contrast, heterozygous loss-of-function mutants for ERK and reaper mutants were equivalent to wild type flies in their sensitivity to PQ. We note that this lack of effects does not necessarily indicate an absence of roles for these latter genes. Leaky mutations or redundant functions could easily prevent the detection of deleterious effects. Ongoing studies will address these issues more fully.

In mammals, Akt1 plays a crucial role in cell survival and also is regulated by the PI3K-mediated signaling pathway [41]. Deregulation of the Akt1-mediated signaling pathway has been well documented in familial and sporadic forms of PD models [38, 50]. Stimulation of the Akt1 signaling pathway in *in vitro* or *in vivo* models resulted in neurotrophic, antiapoptotic effects [41]. Yang et al. [50] found suppression of ROS and survival of DA neurons in transgenic strains over-expressing *Drosophila* Akt1 in DJ1 RNAi strains, again illustrating that the PQ model parallels genetic PD models in many respects.

In mammalian PD models, JNK, which initiates programmed cell death by inactivating the antiapoptotic protein Bcl-xl, is activated in TH neurons in a PQ-induced mammalian PD model suggesting a role JNK in neurodegeneration [51]. Similarly, activated JNK has been detected in Parkin mutants in *Drosophila* [52]. SP600125, a specific JNK inhibitor cofed with 20 mM PQ increased the survival and locomotory activity when compared with those fed with 20 mM PQ [53]. Moreover, Wang et al. [54] also demonstrated important roles for JNK in longevity and resistance to PQ-induced oxidative stress. Our data suggest a specific role of JNK in the survival response of DA neurons in our PD model. We further confirm the prosurvival role of *Akt1* and *JNK* in DA neurons against PQ with evaluation of delayed DA neuron loss with overexpression of wild type Akt and JNK in DA neurons. However, addition of MC failed to further prevent the DA neuron loss in the Akt over-expressed DA neurons against PQ. These neuron count data parallel the survival data obtained with the flies over-expressed with wild type Akt and JNK against PQ and PQ with MC. MC improved the survival of the flies over-expressed with wild type Akt and JNK in the same proportional as in wild type (control) flies against PQ.

We found that heterozygous loss-of-function mutant ERK/*rolled* lacks any detectable functional involvement in our model, although the result could also infer the lack of sufficient knockdown due to the heterozygosity of the strain. Recently, genetic interaction between *Drosophila* DJ-1 and Ras/ERK but not with PI3K/Akt thereby indicating that the prosurvival effect of DJ-1 is mediated via ERK in DA neurons [55]. While the lack of effect in our examination of an *ERK/rolled* mutant may be explained, as noted above, by insufficient reduction of function, this may also be an instance in which the cellular effects of PQ and mutations in PD genes may diverge. Future studies will address this point.

Finally, we analyzed the role of programmed cell death in PQ neurotoxicity by testing heterozygous mutants for the pro-apoptotic gene, *reaper*, and the programmed cell death initiator, caspase-9 ortholog, *dronc*. We found that a heterozygous loss-of-function *reaper* mutant displayed comparable survival to wild type flies on PQ, while *dronc* mutants showed an increase in lifespan. PQ has been shown to induce apoptosis via activation of caspases 3 and 9 and inhibition of Bcl-2 family members except Bax [56]. Thus, our results for *dronc* suggest a parallel mode of action in flies and mammals.

In conclusion, in addition to our finding of protective mechanisms of MC against PQ in this PD model and novel MC-*Punch* mutant interactions, our results here provide *in vivo* evidence for essential roles for stress-responsive kinases in the response to PQ. In this paper, we present data showing the failure of heterozygous *Akt1* and *JNK* loss-of-function mutants to respond to MC. However, ingestion of 10 mM MC by flies over-expressing wild type Akt1 and JNK in DA neurons does not provide additional levels of protection against PQ. Thus, these pathways may not be directly affected by MC or, alternatively, there may be an upper limit above which these kinases can no longer be effective as damage from continuous PQ exposure in these acute toxin model accumulates. Further exploration of the roles of these pathways in various mutant backgrounds in chronic or sporadic exposure models of the effects of PQ will be productive avenues to follow as will analyses of tissue-specific Akt and JNK responses.

Acknowledgments

This work was supported in part by grants from the American Parkinson Disease Foundation and the National Institutes of Health (R15ND078728) to J. O'Donnell. In addition, the authors gratefully acknowledge additional support from the University of Alabama. They wish to thank Jay Hirsh and Tien Hsu for *Drosophila* strains and other members of the O'Donnell lab for their insights and suggestions for this project. All HPLC analyses were expertly performed by research assistant Janna Brown.

References

[1] R. Betarbet, T. B. Sherer, G. MacKenzie, M. Garcia-Osuna, A. V. Panov, and J. T. Greenamyre, "Chronic systemic pesticide exposure reproduces features of Parkinson's disease," *Nature Neuroscience*, vol. 3, no. 12, pp. 1301–1306, 2000.

[2] A. L. McCormack, J. G. Atienza, L. C. Johnston, J. K. Andersen, S. Vu, and D. A. Di Monte, "Role of oxidative stress in paraquat-induced dopaminergic cell degeneration," *Journal of Neurochemistry*, vol. 93, no. 4, pp. 1030–1037, 2005.

[3] K. Nuytemans, J. Theuns, M. Cruts, and C. van Broeckhoven, "Genetic etiology of Parkinson disease associated with mutations in the *SNCA, PARK2, PINK1, PARK7*, and *LRRK2* genes: a mutation update," *Human Mutation*, vol. 31, no. 7, pp. 763–780, 2010.

[4] S. Hunot, F. Boissière, B. Faucheux et al., "Nitric oxide synthase and neuronal vulnerability in Parkinson's disease," *Neuroscience*, vol. 72, no. 2, pp. 355–363, 1996.

[5] C. K. Glass, K. Saijo, B. Winner, M. C. Marchetto, and F. H. Gage, "Mechanisms underlying inflammation in neurodegeneration," *Cell*, vol. 140, no. 6, pp. 918–934, 2010.

[6] H. Macdonald, R. G. Kelly, E. S. Allen, J. F. Noble, and L. A. Kanegis, "Pharmacokinetic studies on minocycline in man," *Clinical Pharmacology and Therapeutics*, vol. 14, no. 5, pp. 852–861, 1973.

[7] Y. Du, Z. Ma, S. Lin et al., "Minocycline prevents nigrostriatal dopaminergic neurodegeneration in the MPTP model of Parkinson's disease," *Proceedings of the National Academy of Sciences of the United States of America*, vol. 98, no. 25, pp. 14669–14674, 2001.

[8] D. C. Wu, V. Jackson-Lewis, M. Vila et al., "Blockade of microglial activation is neuroprotective in the 1-methyl-4-phenyl-1,2,3,6-tetrahydropyridine mouse model of Parkinson disease," *Journal of Neuroscience*, vol. 22, no. 5, pp. 1763–1771, 2002.

[9] X. Wang, S. Zhu, M. Drozda et al., "Minocycline inhibits caspase-independent and -dependent mitochondrial cell death pathways in models of Huntington's disease," *Proceedings of the National Academy of Sciences of the United States of America*, vol. 100, no. 18, pp. 10483–10487, 2003.

[10] M. G. Purisai, A. L. McCormack, S. Cumine, J. Li, M. Z. Isla, and D. A. Di Monte, "Microglial activation as a priming event leading to paraquat-induced dopaminergic cell degeneration," *Neurobiology of Disease*, vol. 25, no. 2, pp. 392–400, 2007.

[11] R. L. Kraus, R. Pasieczny, K. Lariosa-Willingham, M. S. Turner, A. Jiang, and J. W. Trauger, "Antioxidant properties of minocycline: neuroprotection in an oxidative stress assay and direct radical-scavenging activity," *Journal of Neurochemistry*, vol. 94, no. 3, pp. 819–827, 2005.

[12] E. Diguet, P. O. Fernagut, X. Wei et al., "Deleterious effects of minocycline in animal models of Parkinson's disease and Huntington's disease," *European Journal of Neuroscience*, vol. 19, no. 12, pp. 3266–3276, 2004.

[13] M. Tsuji, M. A. Wilson, M. S. Lange, and M. V. Johnston, "Minocycline worsens hypoxic-ischemic brain injury in a neonatal mouse model," *Experimental Neurology*, vol. 189, no. 1, pp. 58–65, 2004.

[14] K. Kupsch, S. Hertel, P. Kreutzmann et al., "Impairment of mitochondrial function by minocycline," *FEBS Journal*, vol. 276, no. 6, pp. 1729–1738, 2009.

[15] J. M. Plane, Y. Shen, D. E. Pleasure, and W. Deng, "Prospects for minocycline neuroprotection," *Archives of Neurology*, vol. 67, no. 12, pp. 1442–1448, 2010.

[16] D. M. Roden and A. L. George, "The genetic basis of variability in drug responses," *Nature Reviews Drug Discovery*, vol. 1, no. 1, pp. 37–44, 2002.

[17] S. S. Ambegaokar, B. Roy, and G. R. Jackson, "Neurodegenerative models in *Drosophila*: Polyglutamine disorders, Parkinson disease, and amyotrophic lateral sclerosis," *Neurobiology of Disease*, vol. 40, no. 1, pp. 29–39, 2010.

[18] I. S. Pienaar, J. Götz, and M. B. Feany, "Parkinson's disease: insights from non-traditional model organisms," *Progress in Neurobiology*, vol. 92, no. 4, pp. 558–571, 2010.

[19] E. Bonilla, S. Medina-Leendertz, V. Villalobos, L. Molero, and A. Bohórquez, "Paraquat-induced oxidative stress in *Drosophila melanogaster*: effects of melatonin, glutathione, serotonin, minocycline, lipoic acid and ascorbic acid," *Neurochemical Research*, vol. 31, no. 12, pp. 1425–1432, 2006.

[20] K. Faust, S. Gehrke, Y. Yang, L. Yang, M. F. Beal, and B. Lu, "Neuroprotective effects of compounds with antioxidant and anti-inflammatory properties in a *Drosophila* model of Parkinson's disease," *BMC Neuroscience*, vol. 10, article 109, 2009.

[21] A. Chaudhuri, K. Bowling, C. Funderburk et al., "Interaction of genetic and environmental factors in a *Drosophila* parkinsonism model," *Journal of Neuroscience*, vol. 27, no. 10, pp. 2457–2467, 2007.

[22] Z. Wang, F. Ferdousy, H. Lawal et al., "Catecholamines up integrates dopamine synthesis and synaptic trafficking," *Journal of Neurochemistry*, vol. 119, no. 6, pp. 1294–1305, 2011.

[23] F. Friggi-Grelin, H. Coulom, M. Meller, D. Gomez, J. Hirsh, and S. Birman, "Targeted gene expression in *Drosophila* dopaminergic cells using regulatory sequences from tyrosine

hydroxylase," *Journal of Neurobiology*, vol. 54, no. 4, pp. 618–627, 2003.

[24] D. G. Stathakis, D. Y. Burton, W. E. McIvor, S. Krishnakumar, T. R. F. Wright, and J. M. O'Donnell, "The *catecholamines up (Catsup)* protein of *Drosophila melanogaster* functions as a negative regulator of tyrosine hydroxylase activity," *Genetics*, vol. 153, no. 5, pp. 361–382, 1999.

[25] W. S. Neckameyer and K. White, "*Drosophila* tyrosine hydroxylase is encoded by the pale locus," *Journal of Neurogenetics*, vol. 8, no. 4, pp. 189–199, 1993.

[26] W. J. Mackay, E. R. Reynolds, and J. M. O'Donnell, "Tissue-specific and complex complementation patterns in the *Punch* locus of *Drosophila melanogaster*," *Genetics*, vol. 111, no. 4, pp. 885–904, 1985.

[27] C. McClung and J. Hirsh, "The trace amine tyramine is essential for sensitization to cocaine in *Drosophila*," *Current Biology*, vol. 9, no. 16, pp. 853–860, 1999.

[28] G. C. Bewley, J. A. Nahmias, and J. L. Cook, "Developmental and tissue-specific control of catalase expression in *Drosophila melanogaster*: correlations with rates of enzyme synthesis and degradation," *Developmental Genetics*, vol. 4, no. 1, pp. 49–60, 1983.

[29] J. A. Buege and S. D. Aust, "Microsomal lipid peroxidation," *Methods in Enzymology*, vol. 52, pp. 302–310, 1978.

[30] J. Kriz, M. D. Nguyen, and J. P. Julien, "Minocycline slows disease progression in a mouse model of amyotrophic lateral sclerosis," *Neurobiology of Disease*, vol. 10, no. 3, pp. 268–278, 2002.

[31] S. Zhu, I. G. Stavrovskaya, M. Drozda et al., "Minocycline inhibits cytochrome c release and delays progression of amyotrophic lateral sclerosis in mice," *Nature*, vol. 417, no. 6884, pp. 74–78, 2002.

[32] J. S. Bus, S. D. Aust, and J. E. Gibson, "Superoxide and singlet oxygen catalyzed lipid peroxidation as a possible mechanism for paraquat (methyl viologen) toxicity," *Biochemical and Biophysical Research Communications*, vol. 58, no. 3, pp. 749–755, 1974.

[33] S. Krishnakumar, D. Burton, J. Rasco, X. Chen, and J. O'Donnell, "Functional interactions between GTP cyclohydrolase I and tyrosine hydroxylase in *Drosophila*," *Journal of Neurogenetics*, vol. 14, no. 1, pp. 1–23, 2000.

[34] A. Presta, U. Siddhanta, C. Wu et al., "Comparative functioning of dihydro- and tetrahydropterins in supporting electron transfer, catalysis, and subunit dimerization in inducible nitric oxide synthase," *Biochemistry*, vol. 37, no. 1, pp. 298–310, 1998.

[35] R. H. Foxton, J. M. Land, and S. J. R. Heales, "Tetrahydrobiopterin availability in Parkinson's and Alzheimer's disease; potential pathogenic mechanisms," *Neurochemical Research*, vol. 32, no. 4-5, pp. 751–756, 2007.

[36] K. Toska, R. Kleppe, C. G. Armstrong, N. A. Morrice, P. Cohen, and J. Haavik, "Regulation of tyrosine hydroxylase by stress-activated protein kinases," *Journal of Neurochemistry*, vol. 83, no. 4, pp. 775–783, 2002.

[37] W. S. Neckameyer and J. S. Weinstein, "Stress affects dopaminergic signaling pathways in *Drosophila melanogaster*," *Stress*, vol. 8, no. 2, pp. 117–131, 2005.

[38] H. Dudek, S. R. Datta, T. F. Franke et al., "Regulation of neuronal survival by the serine-threonine protein kinase Akt," *Science*, vol. 275, no. 5300, pp. 661–665, 1997.

[39] C. T. Chu, D. J. Levinthal, S. M. Kulich, E. M. Chalovich, and D. B. DeFranco, "Oxidative neuronal injury: the dark side of ERK1/2," *European Journal of Biochemistry*, vol. 271, no. 11, pp. 2060–2066, 2004.

[40] L. Chang and M. Karin, "Mammalian MAP kinase signalling cascades," *Nature*, vol. 410, no. 6824, pp. 37–40, 2001.

[41] R. E. Burke, "Inhibition of mitogen-activated protein kinase and stimulation of Akt kinase signaling pathways: two approaches with therapeutic potential in the treatment of neurodegenerative disease," *Pharmacology and Therapeutics*, vol. 114, no. 3, pp. 261–277, 2007.

[42] S. J. Harper and P. LoGrasso, "Signalling for survival and death in neurones: the role of stress-activated kinases, JNK and p38," *Cellular Signalling*, vol. 13, no. 5, pp. 299–310, 2001.

[43] A. H. Brand and N. Perrimon, "Targeted gene expression as a means of altering cell fates and generating dominant phenotypes," *Development*, vol. 118, no. 2, pp. 401–415, 1993.

[44] R. J. Dinis-Oliveira, F. Remião, H. Carmo et al., "Paraquat exposure as an etiological factor of Parkinson's disease," *NeuroToxicology*, vol. 27, no. 6, pp. 1110–1122, 2006.

[45] H. S. Kim and Y. H. Suh, "Minocycline and neurodegenerative diseases," *Behavioural Brain Research*, vol. 196, no. 2, pp. 168–179, 2009.

[46] M. Chen, V. O. Ona, M. Li et al., "Minocycline inhibits caspase-1 and caspase-3 expression and delays mortality in a transgenic mouse model of Huntington disease," *Nature Medicine*, vol. 6, no. 7, pp. 797–801, 2000.

[47] E. R. Werner, A. C. F. Gorren, R. Heller, G. Werner-Felmayer, and B. Mayer, "Tetrahydrobiopterin and nitric oxide: mechanistic and pharmacological aspects," *Experimental Biology and Medicine*, vol. 228, no. 11, pp. 1291–1302, 2003.

[48] K. Sekiguchi, T. Yokoyama, M. Kurabayashi, F. Okajima, and R. Nagai, "Sphingosylphosphorylcholine induces a hypertrophic growth response through the mitogen-activated protein kinase signaling cascade in rat neonatal cardiac myocytes," *Circulation Research*, vol. 85, no. 11, pp. 1000–1008, 1999.

[49] V. Waetzig and T. Herdegen, "MEKK1 controls neurite regrowth after experimental injury by balancing ERK1/2 and JNK2 signaling," *Molecular and Cellular Neuroscience*, vol. 30, no. 1, pp. 67–78, 2005.

[50] Y. Yang, S. Gehrke, M. E. Haque et al., "Inactivation of *Drosophila* DJ-1 leads to impairments of oxidative stress response and phosphatidylinositol 3-kinase/Akt signaling," *Proceedings of the National Academy of Sciences of the United States of America*, vol. 102, no. 38, pp. 13670–13675, 2005.

[51] J. Peng, X. O. Mao, F. F. Stevenson, M. Hsu, and J. K. Andersen, "The herbicide paraquat induces dopaminergic nigral apoptosis through sustained activation of the JNK pathway," *Journal of Biological Chemistry*, vol. 279, no. 31, pp. 32626–32632, 2004.

[52] G. H. Cha, S. Kim, J. Park et al., "Parkin negatively regulates JNK pathway in the dopaminergic neurons of *Drosophila*," *Proceedings of the National Academy of Sciences of the United States of America*, vol. 102, no. 29, pp. 10345–10350, 2005.

[53] M. Jimenez-Del-Rio, A. Daza-Restrepo, and C. Velez-Pardo, "The cannabinoid CP55,940 prolongs survival and improves locomotor activity in *Drosophila melanogaster* against paraquat: implications in Parkinson's disease," *Neuroscience Research*, vol. 61, no. 4, pp. 404–411, 2008.

[54] M. C. Wang, D. Bohmann, and H. Jasper, "JNK signaling confers tolerance to oxidative stress and extends lifespan in *Drosophila*," *Developmental Cell*, vol. 5, no. 5, pp. 811–816, 2003.

[55] L. Aron, P. Klein, T. T. Pham, E. R. Kramer, W. Wurst, and R. Klein, "Pro-survival role for Parkinson's associated gene DJ-1 revealed in trophically impaired dopaminergic neurons," *PLoS Biology*, vol. 8, no. 4, Article ID e1000349, 2010.

[56] Q. Fei, A. L. McCormack, D. A. Di Monte, and D. W. Ethell, "Paraquat neurotoxicity is mediated by a Bak-dependent mechanism," *Journal of Biological Chemistry*, vol. 283, no. 6, pp. 3357–3364, 2008.

Hindawi Publishing Corporation
Parkinson's Disease
Volume 2012, Article ID 697564, 6 pages
doi:10.1155/2012/697564

Research Article

A Novel, Sensitive Assay for Behavioral Defects in Parkinson's Disease Model *Drosophila*

Ronit Shaltiel-Karyo,[1] Dan Davidi,[1] Yotam Menuchin,[1] Moran Frenkel-Pinter,[1] Mira Marcus-Kalish,[2] John Ringo,[3] Ehud Gazit,[1] and Daniel Segal[1,4]

[1] *Department of Molecular Microbiology and Biotechnology, Tel Aviv University, 69978 Tel Aviv, Israel*
[2] *Interdisciplinary Center for Technology Analysis & Forecasting (ICTAF), Tel Aviv University, 69978 Tel Aviv, Israel*
[3] *School of Biology, The University of Maine, Orono, ME 04469, USA*
[4] *Sagol School of Neurosciences, Tel Aviv University, 69978 Tel Aviv, Israel*

Correspondence should be addressed to Ehud Gazit, euhdga@tauex.tau.ac.il and Daniel Segal, dsegal@post.tau.ac.il

Received 8 December 2011; Revised 25 March 2012; Accepted 23 April 2012

Academic Editor: Katerina Venderova

Parkinson's disease is a common neurodegenerative disorder with the pathology of α-synuclein aggregation in Lewy bodies. Currently, there is no available therapy that arrests the progression of the disease. Therefore, the need of animal models to follow α-synuclein aggregation is crucial. *Drosophila melanogaster* has been researched extensively as a good genetic model for the disease, with a cognitive phenotype of defective climbing ability. The assay for climbing ability has been demonstrated as an effective tool for screening new therapeutic agents for Parkinson's disease. However, due to the assay's many limitations, there is a clear need to develop a better behavioral test. Courtship, a stereotyped, ritualized behavior of *Drosophila*, involves complex motor and sensory functions in both sexes, which are controlled by large number of neurons; hence, behavior observed during courtship should be sensitive to disease processes in the nervous system. We used a series of traits commonly observed in courtship and an additional behavioral trait—nonsexual encounters—and analyzed them using a data mining tool. We found defective behavior of the Parkinson's model male flies that were tested with virgin females, visible at a much younger age than the climbing defects. We conclude that this is an improved behavioral assay for Parkinson's model flies.

1. Introduction

Parkinson's disease (PD) is a common progressive neurodegenerative disorder, characterized by the deposition of amyloid fibrils in Lewy bodies (LBs) in the *substantia nigra* pars compacta, leading to loss of dopaminergic (DA) neurons and to severe motor symptoms [1–4]. α-synuclein (α-syn), a 140-amino-acid protein, is the main component of the LB [5, 6]. Since the aggregation of the protein in the brain has been implicated as a vital step in the development of PD, one path for the current search for drugs is focused on arresting or modifying the pattern of α-syn deposition in the brain [7].

With no currently available drug that arrests or slows down the progression of the disease, therapy treats motor dysfunction, and its effectiveness declines as the disease progresses [8]. Therefore, the development and characterization of animal models may hold promise for screening and testing of new drugs that target the pathogenic process itself rather than the symptoms of PD [9].

The fruit fly *Drosophila melanogaster* is a useful organism for studying mechanisms of human neurodegenerative diseases, including PD [10]. Notwithstanding the conspicuous differences between *Drosophila* and humans, many genes and signaling pathways are conserved between them [11]. Feany and Bender [12] reported a *Drosophila* model for PD that expresses normal human α-syn, as well as strains expressing each of the two mutant proteins (A30P and A53T) associated with familial Parkinson's disease in all *Drosophila* neurons; the *Drosophila* genome does not contain a clear α-syn homolog [12]. Transgenic flies expressing α-syn panneurally display aggregates, suffer loss of DA neurons, and exhibit locomotor defects [12]. They are valuable for drug screening and testing [13] as well for identifying genes and cellular

processes relevant to PD pathogenesis, many of which are evolutionarily conserved [11].

A few phenotypes have been detected in PD fly models [11] but only three common phenotypes in flies expressing α-syn [12]. The first two are (i) accumulation of α-syn aggregates, detected with anti-α-syn antibody, and (ii) loss of DA neurons in the brain, detected with anti-TH antibody, which specifically recognizes these neurons in paraffin sections or whole-mount brains [12, 14–16]. The third phenotype is a behavioral outcome of nervous system dysfunction, age-dependent defects in locomotion. The latter is clearly deduced using a simple assay: while normal flies climb up a vertical tube (geotaxis), α-syn-expressing flies tend to remain at the bottom [12, 13]. Compared to wild-type flies, the transgenic flies with panneural expression of α-syn develop locomotor dysfunction at a relatively early age. This behavioral phenotype has been demonstrated in the past by our group and others as an effective tool for screening of new therapeutics for PD [12, 13, 17, 18].

Courtship in *Drosophila* is a stereotyped, ritualized behavior, which requires males to be athletic and to respond rapidly and appropriately to females. This activity accounts for most interactions between adult individuals and is rich in content, complex in structure, and robust in execution [19]. A male fly can perform the entire courtship ritual immediately upon encountering a virgin female, even if he was raised in complete isolation from egg to adult [20]. In these complex actions, the male and female nervous systems function to generate sexual behavior. Male courtship consists of visual, chemosensory, auditory, and mechanosensory signals [21]. The courtship ritual involves orientation of the male towards the female, serenading the female with a species-specific love song (wing vibration), licking the female's genitalia, and attempting copulation [21, 22].

Since courtship involves many neural and motor elements [23], it might be affected by the expression of α-syn. Here we demonstrate an overall decline in the behavioral responses of male transgenic flies expressing A30P α-syn in the brain [12], when these males are paired with virgin females. This may potentially serve as a novel, more sensitive assay to study locomotor deficits in *Drosophila*.

2. Methods

2.1. Strains and Rearing. We used three strains of *Drosophila*: elav-Gal4, UAS-α-syn A30P, and Oregon-R (wild type). Flies were reared on standard cornmeal-molasses medium at 25°C. Crosses were conducted using virgin females collected no more than eight hours after eclosion at 25°C or 18 hours after eclosion at 18°C. Crosses were performed at 29°C. Adult offspring (F_1) from the crosses were collected up to 9 days after the beginning of their eclosion at 25°C in order to avoid offspring from the next generation (F_2).

2.2. Crosses. Female flies carrying the driver *elav-Gal4* on their X chromosome were crossed to males carrying the *UAS*-regulated α-syn A30P transgene located on chromosome 2 (kindly provided by Professor Mel Feany). All F_1 offspring expressed α-syn A30P in the nervous system, giving us a model for PD.

2.3. Locomotor (Climbing) Assay. 5 vials, each containing 10 flies expressing α-syn A30P or 10 Oregon-R flies were analyzed for locomotor behavior. The vials were tapped gently on the table and left standing for 18 seconds. The number of flies that climbed at least one cm was recorded. Altogether, we used 100 flies, half expressing α-syn A30P and half wild-type Oregon flies.

2.4. Courtship Assay. Flies used for the courtship assay were kept in an opaque box. Taking into account the diel periodicity of *Drosophila* courtship behavior [24], the courtship assay was conducted between 9 : 00 and 15 : 00. A 6-day-old virgin male (Oregon-R or α-syn A30P) was placed with a 6-day-old Oregon-R virgin female in a cylindrical transparent chamber ($r = 1.5$ cm, $h = 0.5$ cm) for 10 minutes or until copulation occurred. The interaction between the flies was recorded via a digital microscope and later analyzed for sexual activity using a newly developed software termed "*Drosophila* Analysis," which allows counting the number of times a fly engages in each element and recording the time it spends in each bout of behavior. We recorded courtship of 56 couples; 28 α-syn A30P males and 28 Oregon-R males. The following essential features of male courtship were measured: (i) orientation, (ii) wing vibration, (iii) licking, and (iv) attempted copulation; we also recorded the occurrence of copulation [25]. In addition, we recorded a novel behavioral parameter, nonsexual encounters (NSEs), encounters between the male and female flies that did not lead to sexual activity. NSE is a measure of general activity. To measure the responsiveness to the female more directly, we computed a "sexual focus index" (SFI): SFI = 1/(NSE + 1).

2.5. Climbing Assay. Currently, the only behavioral assay of PD model flies is the climbing test. Therefore, we performed this test as well. Transgenic flies expressing the mutated *α-syn A30P* in their nervous system were used for the experiment. The climbing ability of the flies was monitored twice, at day 6 (when the flies were six days old) and at day 21.

2.6. Statistical Analysis. Data were categorized as 9 parameters for each fly including "health condition" as a Boolean parameter [26]. We used association rule learning algorithm, which reveals all the "if then" rules that meet the user predetermined thresholds, to determine how the values of the "health condition" field (the dependent variable) are affected by the values of other fields. The analysis was done using a data-mining tool WizWhy [27] to identify the underlying rules that explain the dependent variable—the health condition. WizWhy reveals all positive and negative "if then" rules in the data and a set of necessary and sufficient conditions ("if and only if" rules). Furthermore the algorithm identified, based on the extracted rules, the unexpected cases deviating from the rules and issued predictions for new cases. The rules summary is shown in Table 1.

Table 1: Data mining analysis. An "if and only if" rule, composed of six conditions, was concluded using WizWhy 4.02. Improvement factor of 2.8 (relative to random prediction) was observed.

The following conditions explain when male fly is healthy:
(i) Non-Sexual Encounters occurs 3 to 5 times (average = 4.40)
(ii) Orientation time is 294.00–349.51 (average 320.84)
& Total ritual time is 354.95–407.00 (average = 376.29)
(iii) attempted Copulations occur 3 times
(iv) Licking ig conducted 21 to 56 times (average = 34.50)
& Non-Sexual Encounters occur 6 to 17 times (average = 4.40)
(v) Non-Sexual Encounters occur 1 to 2 times (average = 100.40)
(iv) Vibration of wings last 0 to 77.00 seconds (average = 15.72)
& Non-Sexual Encounters occur 35 to 51 times (average = 43.43)
(iiv) Total ritual times is 516.58 to 519.91 (average = 517.94)
When *at least one* of the conditions holds, the probability that male fly *is* healthy equals *0.821*
(23 out of 28 cases)
When *all* the conditions do not hold, the probability that male fly *is not* healthy equals *0.821* (23 out of 28 cases)
The total number of cases explained by the set of conditions: 46
The total number of cases in the data: 56
Success rate: 0.821 (46/56)
Assuming that the primary probability for a male fly to be healthy equals 0.5 we obtain an
Improvement Factor of 2.800 (0.500/0.179)

3. Results

3.1. Courtship Assay. Sexual activity was normalized to consider Oregon-R flies behavior as ideal (100% sexual activity). Since several couples copulated in less than 10 minutes, we normalized the 4 following measured parameters for each couple, by dividing it in the total time, emphasizing fast copulating males. Orientation time revealed an average of 56.6% in Oregon-R and 41.3% in α-syn A30P presenting a 73% orientation activity of mutant flies relative to Oregon-R (41.3/56.6*100). Similarly, Oregon-R vibration time was 21.5% and α-syn A30P vibrated for 17.2% of the total time with 80% normal activity. Licking and "attempted copulation" (times 100 and divided by total time) values were 3.4 and 0.4 for Oregon-R and mutant flies, respectively. Thus, α-syn A30P flies exhibited a 59% licking activity and 50.7% attempted copulations (ATCs) activity relative to Oregon-R flies. Since copulation is binary, we did not calculate the average copulations per experiment but summed the total copulations that occurred in 28 Oregon-R flies compared to 28 α-syn A30P flies. The sum of copulation was 11 copulations in the Oregon-R flies and 8 copulations in the α-syn A30P, resulting in 27.3% fewer copulations in PD flies. Interestingly, the two groups differed in nonsexual encounters (NSEs). In A30P α-syn flies, mean NSE was 33, and in Oregon-R flies, mean NSE was 21. Here we noticed the occurrence of NSE mainly prior to beginning of any sexual activity; thus we did not divide the measured values by the total time. For the sexual focus index, SFI, Oregon-R-males performed 36% better than A30P α-syn males (Figure 1(a)). As can be seen from the results, α-syn A30P males performed less sexual activity (up to 50% reduction relative to Oregon-R activity) in all sexual parameters (Figure 1(a)).

For further comparison, all parameters of the six traits were summed up and normalized for each group. While each parameter is sufficient to distinguish between the two groups, we find the overall difference as a ratification of the results (Figure 1(b)). Since the six behavioral activities are not strictly independent, the summed score better represents the overall sexual behavior, and the result suggests that the A30P α-syn males were impaired in sexual focus, ability to follow females, and coordination (Figure 1(b)).

3.2. Climbing Assay. The locomotion (climbing) assay, commonly used for assessing behavior of flies expressing amyloidogenic proteins in their brain [28–30], was used to assess the neural dysfunction caused to the flies due to expression of mutant A30P α-syn in the nervous system. We monitored the climbing ability of the flies at the age of 6 days, the age of flies tested in the courtship assay. As can be seen in Figure 2, no difference was detected between Oregon-R flies (control) and A30P α-syn flies as expected in this model. Additional measurement conducted at the age of 21 days revealed significant locomotor dysfunction of PD flies, reflecting 28% reduction in climbing ability (Figure 2). Our results did not indicate a significant difference between the two groups prior to 21 days (data not shown), as was also reported previously [12, 13].

3.3. Statistical Analysis. Based on the results obtained in the courtship assay, we used a data mining software to develop a set of rules ("if then" rules and "if and only if" rules) as a diagnostic tool. As each male fly represented an array of numbers, describing 8 parameters with regards to the 6 sexual activities, we established a two-dimensional matrix. Choosing health condition as the dependent variable, we used WizWhy 4.02 for the analysis as it (i) enables combined data sets analysis, (ii) relates to the whole set of data with no data modification or neglection, (iii) is less sensitive to overfitting (in small data sets), and (iv) is proven to reveal all "if then," and a set of the necessary and sufficient conditions ("if and only if" rules) each with its significance level [31]. The software uses association rule learning algorithm to calculate the correlations that hold between the one independent variable, or combination of several parameters, the target function (the dependent variable), that is, to quantify the contribution of each of the 8 parameters to the decision whether a given fly is A30P α-syn (sick) or WT (healthy). The "if and only if" rule lists seven conditions (see Table 1). Our analysis revealed that if at least one of the seven conditions holds for a given fly, it was healthy with a probability of 82.1%. However, if none of the seven conditions holds, there was 82.1% probability that the fly carries α-syn A30P mutation (Table 1). Thus we were able to predict the health condition of 82.1% (46 out of 56 couples) of the flies. 10 flies (17.9%) did not follow this set of

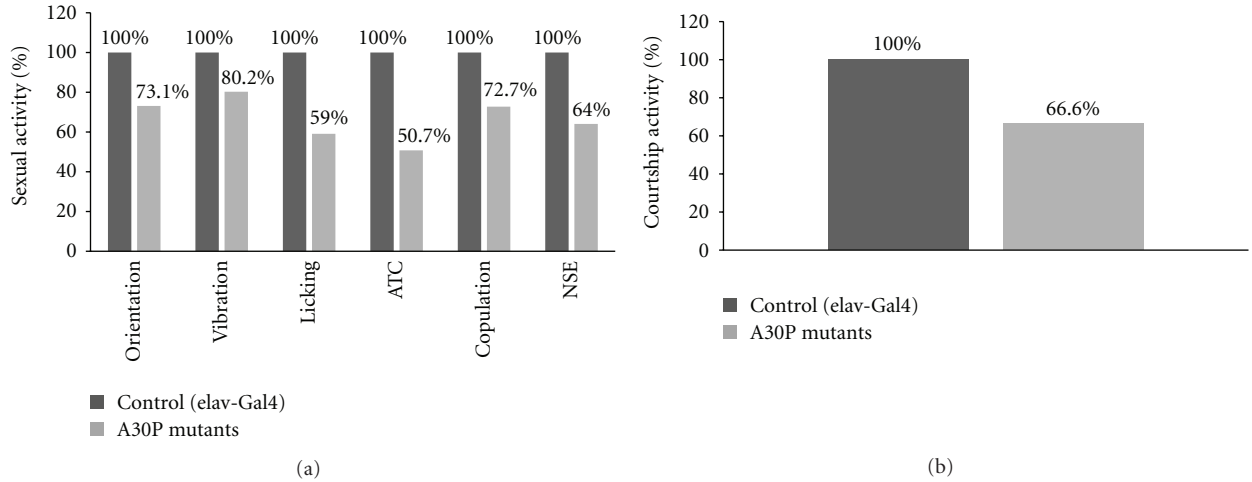

Figure 1: Sexual activity of *Drosophila* flies. Control flies (shown in dark grey) are set as displaying 100% sexual activity. PD model flies are shown in light gray. (a) Courtship behavior was measured using 5 common parameters: orientation, vibration, licking, attempted copulations (ATC), and copulations. In addition, the number of nonsexual encounters (NSEs) was recorded. All parameters were normalized to introduce same scale. (b) Final courtship score, representing the sum of all above 6 parameters.

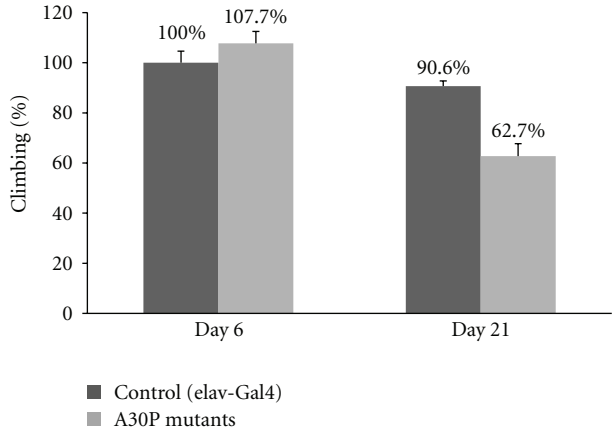

Figure 2: Climbing ability. Two classes of flies, each containing 5 tubes of 10 flies, were analyzed using the climbing assay. Control flies (shown in dark grey) are set as displaying 100% climbing ability. PD fly model presented in light grey. Results show the percent of flies which climbed along the test tube after 18 seconds.

rules, leading to an improvement factor of 2.8 (0.5/0.179) in comparison to random prediction (Table 1).

4. Discussion

Drosophila has been used extensively as a model for human brain diseases, mainly due to the simplicity of the experiments along with the similarity to humans. *Drosophila* has a central nervous system containing orders of magnitude fewer neuronal and glial cells than in vertebrate central nervous systems, yet they share the same types of neurotransmitter systems such as GABA, glutamate, dopamine, serotonin, and acetylcholine, and they are able to perform complex behavior, including sexual displays, social behavior, and learning [32].

In this report, we present an alternative behavioral assay, employing courting pairs, for monitoring behavioral deficits in the α-syn A30P fly model and compare it to the well-established climbing assay. Courtship in *Drosophila* was studied and described in detail [20, 33–36], but to the best of our knowledge, this is the first time that it is characterized in a PD fly model. We examined five essential components of the male's courtship ritual and suggest one new activity, NSE, and its inverse, SFI. In all traits, PD male flies performed worse. Surprisingly, NSE was the most well-represented characteristics in the if-and-only-if rules, composing 4 out of the 7 derived conditions. This suggests that α-syn A30P mutant males are less responsive to females than are Oregon-R males. Further study is needed to explore the relationship between courtship and sexual focus in male PD model flies.

When compared to the well-established climbing assay, thoroughly reported as a convenient behavioral measure to determine neurological damage and aging in *Drosophila* flies [12, 13], courtship is a more complex behavior to assay. In courtship, the male must follow the female closely and engage in several coordinated behaviors, which is physically more demanding than simple climbing and which engages all the senses, as described previosly. Furthermore, the courtship abnormality is apparent at a much earlier age than the climbing deficiency. While at age 5–10 days the PD male flies court maximally, it takes approximately three weeks for the appearance of severe climbing phenotype in them (Figure 2). On the other hand, the climbing assay yields a binary score, pass or fail, whereas courtship must be evaluated quantitatively. Our results immediately suggest a follow-up experiment, evaluating behavior with the courtship assay at various ages post eclosion.

On balance, this behavioral assay provides a better evaluation of PD pathology dysfunction, and may allow

assessment of dopaminergic dysfunction prior to loss of dopaminergic neurons, although the exact neuronal deficits underlying this behavioral phenotype need to be determined in follow-up studies. Interestingly, in the case of Fragile X, another brain disorder modeled in *Drosophila*, McBride et al. [37] demonstrated that lithium or mGluR antagonists could rescue several aspects of behavior including courtship impairments. This was followed by studies in the mouse model and now clinical studies in afflicted patients [38, 39]. Therefore, behavioral deficiencies during courtship in disease model flies can be an important and relevant assay for drug screening.

Authors' Contribution

R. Shaltiel-Karyo and D. Davidi contributed equally to this work.

Acknowledgment

This work was supported in part by a grant from the Parkinson's Disease Foundation.

References

[1] C. M. Dobson, "Getting out of shape," *Nature*, vol. 418, no. 6899, pp. 729–730, 2002.

[2] C. W. Olanow and W. G. Tatton, "Etiology and pathogenesis of Parkinson's disease," *Annual Review of Neuroscience*, vol. 22, pp. 123–144, 1999.

[3] P. Jenner and C. W. Olanow, "The pathogenesis of cell death in Parkinson's disease," *Neurology*, vol. 66, no. 10, pp. S24–S30, 2006.

[4] N. P. Reynolds, A. Soragni, M. Rabe et al., "Mechanism of membrane interaction and disruption by α-synuclein," *Journal of the American Chemical Society*, vol. 133, no. 48, pp. 19366–19375, 2011.

[5] M. G. Spillantini, M. L. Schmidt, V. M. Y. Lee, J. Q. Trojanowski, R. Jakes, and M. Goedert, "α-synuclein in Lewy bodies," *Nature*, vol. 388, no. 6645, pp. 839–840, 1997.

[6] M. R. Cookson, "Synuclein and neuronal cell death," *Molecular Neurodegeneration*, vol. 4, no. 1, 2009.

[7] K. Ono, M. Hirohata, and M. Yamada, "α-synuclein assembly as a therapeutic target of Parkinson's disease and related disorders," *Current Pharmaceutical Design*, vol. 14, no. 30, pp. 3247–3266, 2008.

[8] J. M. Savitt, V. L. Dawson, and T. M. Dawson, "Diagnosis and treatment of Parkinson disease: molecules to medicine," *Journal of Clinical Investigation*, vol. 116, no. 7, pp. 1744–1754, 2006.

[9] T. M. Dawson, H. S. Ko, and V. L. Dawson, "Genetic animal models of Parkinson's disease," *Neuron*, vol. 66, no. 5, pp. 646–661, 2010.

[10] L. T. Reiter, L. Potocki, S. Chien, M. Gribskov, and E. Bier, "A systematic analysis of human disease-associated gene sequences in *Drosophila melanogaster*," *Genome Research*, vol. 11, no. 6, pp. 1114–1125, 2001.

[11] N. Paricio and V. Muñoz-Soriano, "*Drosophila* models of Parkinson's disease: discovering relevant pathways and novel therapeutic strategies," *Parkinson's Disease*, vol. 2011, Article ID 520640, 14 pages, 2011.

[12] M. B. Feany and W. W. Bender, "A *Drosophila* model of Parkinson's disease," *Nature*, vol. 404, no. 6776, pp. 394–398, 2000.

[13] R. Shaltiel-Karyo, M. Frenkel-Pinter, N. Egoz-Matia et al., "Inhibiting α-synuclein oligomerization by stable cell-penetrating β-synuclein fragments recovers phenotype of parkinson's disease model flies," *PLoS One*, vol. 5, no. 11, Article ID e13863, 2010.

[14] A. A. Cooper, A. D. Gitler, A. Cashikar et al., "α-synuclein blocks ER-Golgi traffic and Rab1 rescues neuron loss in Parkinson's models," *Science*, vol. 313, no. 5785, pp. 324–328, 2006.

[15] R. Wassef, R. Haenold, A. Hansel, N. Brot, S. H. Heinemann, and T. Hoshi, "Methionine sulfoxide reductase A and a dietary supplement S-methyl-L-cysteine prevent Parkinson's-like symptoms," *Journal of Neuroscience*, vol. 27, no. 47, pp. 12808–12816, 2007.

[16] K. Trinh, K. Moore, P. D. Wes et al., "Induction of the phase II detoxification pathway suppresses neuron loss in *Drosophila* models of Parkinson's disease," *Journal of Neuroscience*, vol. 28, no. 2, pp. 465–472, 2008.

[17] A. M. Todd and B. E. Staveley, "Pink1 suppresses α-synuclein-induced phenotypes in a *Drosophila* model of Parkinson's disease," *Genome*, vol. 51, no. 12, pp. 1040–1046, 2008.

[18] R. G. Pendleton, F. Parvez, M. Sayed, and R. Hillman, "Effects of pharmacological agents upon a transgenic model of Parkinson's disease in *Drosophila melanogaster*," *Journal of Pharmacology and Experimental Therapeutics*, vol. 300, no. 1, pp. 91–96, 2002.

[19] J. C. Hall, "The mating of a fly," *Science*, vol. 264, no. 5166, pp. 1702–1714, 1994.

[20] R. J. Greenspan and J. F. Ferveur, "Courtship in *Drosophila*," *Annual Review of Genetics*, vol. 34, pp. 205–232, 2000.

[21] H. T. Spieth, "Courtship behavior in *Drosophila*.," *Annual Review of Entomology*, vol. 19, pp. 385–405, 1974.

[22] A. H. Sturtevant, "Castle and wright on crossing over in rats," *Science*, vol. 42, no. 1080, p. 342, 1915.

[23] J. C. Hall, "Complex brain and behavioral functions disrupted by mutations in *Drosophila*," *Developmental Genetics*, vol. 4, no. 4, pp. 355–378, 1984.

[24] T. Sakai and N. Ishida, "Circadian rhythms of female mating activity governed by clock genes in *Drosophila*," *Proceedings of the National Academy of Sciences of the United States of America*, vol. 98, no. 16, pp. 9221–9225, 2001.

[25] C. P. Kyriacou, "Behavioral genetics: sex in fruitflies is *fruitless*," *Nature*, vol. 436, no. 7049, pp. 334–335, 2005.

[26] N. A. Sakhanenko and D. J. Galas, "Probabilistic logic methods and some applications to biology and medicine," *Journal of Computational Biology*, vol. 19, no. 3, pp. 316–336, 2012.

[27] A. Meidan and B. Levin, "Choosing from competing theories in computerised learning," *Minds and Machines*, vol. 12, no. 1, pp. 119–129, 2002.

[28] D. C. Crowther, K. J. Kinghorn, E. Miranda et al., "Intraneuronal Aβ, non-amyloid aggregates and neurodegeneration in a *Drosophila* model of Alzheimer's disease," *Neuroscience*, vol. 132, no. 1, pp. 123–135, 2005.

[29] A. Frydman-Marom, A. Levin, D. Farfara et al., "Orally administrated cinnamon extract reduces β-amyloid oligomerization and corrects cognitive impairment in Alzheimer's disease animal models," *PLoS One*, vol. 6, no. 1, Article ID e16564, 2011.

[30] R. Scherzer-Attali, R. Pellarin, M. Convertino et al., "Complete phenotypic recovery of an Alzheimer's disease model by a

quinone-tryptophan hybrid aggregation inhibitor," *PLoS One*, vol. 5, no. 6, p. e11101, 2010.

[31] I. S. Naftulin and O. Y. Rebrova, "Application of C&RT, CHAID, C4.5 and WizWhy algorithms for stroke type diagnosis," *Artificial Intelligence and Soft Computing*, vol. 6113, no. 1, pp. 651–656, 2010.

[32] J. A. Botella, F. Bayersdorfer, F. Gmeiner, and S. Schneuwly, "Modelling Parkinson's disease in *Drosophila*," *NeuroMolecular Medicine*, vol. 11, no. 4, pp. 268–280, 2009.

[33] D. S. Manoli, M. Foss, A. Villella, B. J. Taylor, J. C. Hall, and B. S. Baker, "Male-specific *fruitless* specifies the neural substrates of *Drosophila* courtship behaviour," *Nature*, vol. 436, no. 7049, pp. 395–400, 2005.

[34] B. S. Baker, B. J. Taylor, and J. C. Hall, "Are complex behaviors specified by dedicated regulatory genes? Reasoning from *Drosophila*," *Cell*, vol. 105, no. 1, pp. 13–24, 2001.

[35] J. C. Billeter, S. F. Goodwin, and K. M. C. O'Dell, "3 Genes mediating sex-specific behaviors in *Drosophila*," *Advances in Genetics*, vol. 47, pp. 87–116, 2002.

[36] D. S. Manoli and B. S. Baker, "Median bundle neurons coordinate behaviours during *Drosophila* male courtship," *Nature*, vol. 430, no. 6999, pp. 564–569, 2004.

[37] S. M. J. McBride, C. H. Choi, Y. Wang et al., "Pharmacological rescue of synaptic plasticity, courtship behavior, and mushroom body defects in a *Drosophila* model of Fragile X syndrome," *Neuron*, vol. 45, no. 5, pp. 753–764, 2005.

[38] E. Berry-Kravis, A. Sumis, O. K. Kim, R. Lara, and J. Wuu, "Characterization of potential outcome measures for future clinical trials in fragile X syndrome," *Journal of Autism and Developmental Disorders*, vol. 38, no. 9, pp. 1751–1757, 2008.

[39] S. Jacquemont, S. Birnbaum, S. Redler, P. Steinbach, and V. Biancalana, "Clinical utility gene card for: fragile X mental retardation syndrome, fragile X-associated tremor/ataxia syndrome and fragile X-associated primary ovarian insufficiency," *European Journal of Human Genetics*, article 19, 2011.

Hindawi Publishing Corporation
Parkinson's Disease
Volume 2012, Article ID 129605, 14 pages
doi:10.1155/2012/129605

Research Article

An NR2B-Dependent Decrease in the Expression of trkB Receptors Precedes the Disappearance of Dopaminergic Cells in Substantia Nigra in a Rat Model of Presymptomatic Parkinson's Disease

Eduardo Riquelme,[1] Jorge Abarca,[1] Jorge M. Campusano,[1] and Gonzalo Bustos[1,2]

[1] *Departamento de Biología Celular y Molecular, Facultad de Ciencias Biológicas, Pontificia Universidad Católica de Chile, Alameda 340, 8331150 Santiago, Chile*
[2] *Programa de Biomedicina, Universidad San Sebastián, Zañartu 1482, Ñuñoa, 7780272 Santiago, Chile*

Correspondence should be addressed to Jorge M. Campusano, jcampusano@bio.puc.cl and Gonzalo Bustos, gbustos@bio.puc.cl

Received 10 January 2012; Revised 19 March 2012; Accepted 2 April 2012

Academic Editor: Kah-Leong Lim

Compensatory changes occurring during presymptomatic stages of Parkinson's disease (PD) would explain that the clinical symptoms of the disease appear late, when the degenerative process is quite advanced. Several data support the proposition that brain-derived neurotrophic factor (BDNF) could play a role in these plastic changes. In the present study, we evaluated the expression of the specific BDNF receptor, trkB, in a rat model of presymptomatic PD generated by intrastriatal injection of the neurotoxin 6-OHDA. Immunohistochemical studies revealed a decrease in trkB expression in SN pars compacta (SNc) seven days after 6-OHDA injection. At this time point, no change in the number of tyrosine hydroxylase (TH) immunoreactive (TH-IR) cells is detected, although a decrease is evident 14 days after neurotoxin injection. The decrease in TH-positive cells and trkB expression in SNc was significantly prevented by systemic administration of Ifenprodil, a specific antagonist of NR2B-containing NMDA receptors. Therefore, an NR2B-NMDA receptor-dependent decrease in trkB expression precedes the disappearance of TH-IR cells in SNc in response to 6-OHDA injection. These results support the idea that a functional coupling between NMDA receptors and BDNF/trkB signalling may be important for the maintenance of the dopaminergic phenotype in SNc during presymptomatic stages of PD.

1. Introduction

Parkinson's disease (PD) a progressive degenerative disorder that is characterized by the disappearance of dopaminergic neurons of the nigrostriatal pathway. The clinical symptoms of PD develop slowly and gradually and are only evident after 50–60% of dopamine (DA) cells loss in substantia nigra (SN) and 70–80% decrease of striatal DA content has occurred [1–4]. Compensating responses and plastic changes in the dopaminergic nigrostriatalsystem during presymptomatic PD would be responsible for the delay in the appearance of the clinical symptoms of the disease [5–10]. Emerging evidence suggests that changes in the expression of brain-derived neurotrophic factor (BDNF) in SN may be one of the molecular signals associated with responses occurring in basal ganglia during presymptomatic PD [11]. In agreement with this, a number of studies have demonstrated transient increases of BDNF mRNA and protein in SN, early after partial lesions of the nigrostriatalDA pathway in a rat presymptomatic model of PD [11–13]. These changes in the expression of BDNF could play an important role during the compensatory changes at early stages of PD. This is consistent with reports indicating that BDNF increases the survival of DA neurons [14–17] and that an augmentation of BDNF levels in basal ganglia may prevent degeneration of these neurons in a rat model of PD [18]. Conversely, inhibiting endogenous BDNF expression by antisense oligonucleotide infusion causes loss of nigral dopaminergic neurons in SN [19].

Interestingly, the disappearance of dopaminergic neurons in SN has been also observed when BDNF levels are normal, but its ability to bind or activate its specific receptor, tropomyosin-related kinase B (trkB), has been impaired [20, 21]. These findings indicate the importance of trkB receptor activation in order to generate a full BDNF-induced response in SN. Along this idea, old mutant mice showing haploinsufficiency for trkB exhibit a greater loss of DA neurons in the SN when compared to old wild-type animals [17], which further suggests a possible participation of this receptor in the development of PD.

TrkB is a tyrosine kinase-type receptor, which belongs to the family of trk receptors that binds neurotrophins, event linked to cell survival and synaptic plasticity [22–24]. TrkB and BDNF are both expressed in dopaminergic neurons located in SN [25–28], which suggests that BDNF exerts autocrine/paracrine functions in this nucleus.

We have recently reported a coupling between increased glutamate release, NMDA receptor activation, and BDNF expression in the adult SN, which represents an important molecular signal triggered in this brain nucleus in response to the early and partial DA loss that occurs in striatal nerve endings during presymptomatic PD [13]. These functional interactions occurring in SN could account in part for adaptive and plastic responses associated with early PD. Conversely, no data are available on the expression of trkB receptors in SN during presymptomatic stages of PD as well as on the possibility that glutamate receptors could modulate trkB expression over the progression of the disease. In the present study, by using immunohistochemistry and in situ hybridization, we evaluated the expression of trkB in SN at different time points in a rat model of presymptomatic PD and compare it to the expression of the DA cell marker, Tyrosine hydroxylase (TH). In addition to this, we also assessed the possibility that glutamate receptors might modulate the expression of trkB receptors in SN. Preliminary version of this data has been previously reported in poster format [29].

2. Materials and Methods

2.1. Animals. Rats weighing 260–300 g were obtained from the Animal Service Unit at the Pontificia Universidad Catolica de Chile and were handled according to the regulations stipulated by the Bioethics and Biosafety Committee of the Faculty of Biological Sciences, Pontificia Universidad Católica de Chile, and by The Animal Care and Use Committee of FONDECYT, Chile.

2.2. 6-Hydroxydopamine (6-OHDA) Lesions. Lesions were carried out as reported [13]. Briefly, adult male Sprague-Dawley rats were anesthetized with chloral hydrate (400 mg/kg, i.p.) and mounted in a stereotaxic apparatus (Stoelting). Twenty micrograms of 6-OHDA in 4 μL of 0.02% ascorbic acid was injected in the right striatum at a rate of 0.5 μL/min. Coordinates for the injection of the neurotoxin were *A*: 1.2 mm, *L*: 2.8 mm, and *V*: 4.5 mm, with respect to Bregma, according to the atlas of Paxinos and Watson [30]. Sham-operated rats were stereotaxically injected with 4 μL of 0.02% ascorbic acid using the same coordinates. The rats were allowed to recover for four, seven, and fourteen days, prior to conducting the experiments described hereinafter.

2.3. Preparation of Brain Tissue for Staining. Procedure has been previously reported [13]. Rats were anesthetized with chloral hydrate (400 mg/kg; i.p.) and transcardially perfused with saline (0.9% NaCl), followed by ice-cold fixative solution (3% paraformaldehyde, 15% picric acid, 0.1% glutaraldehyde, in phosphatebuffered saline solution (PBS) (pH 7.4). Brains were removed from the skull and postfixed for 30 min. Brains were then dehydrated in 25% sucrose solution for 48 hr at 4°C. Afterwards, 20–30 μm thick coronal slices were prepared on a cryostat (CM 1510; Leica, Heidelberg, Germany) at 5.2 to 5.6 mm posterior to Bregma, the brain region where SN is located according to the atlas of Paxinos and Watson [30]. When fluorescence-based double immunohistochemistry and nonisotopic in situ hybridization (ISH) studies were carried out, the procedure used was as described here, except that the fixative solution was ice-cold 4% paraformaldehyde in PBS.

2.4. Immunohistochemical (IHC) Studies. Free-floating coronal midbrain slices were treated with 0.5% H_2O_2, rinsed several times in 0.1 M PBS, and then incubated in blocking solution (3% normal goat serum, 0.02% sodium azide, 0.2% Triton X-100 in PBS) for 60 min. Then, slices were incubated for 72 hours at 4°C with the primary antibodies of interest in blocking solution. The slices were then washed in PBS and reacted with a biotinylated goat anti-rabbit IgG (Vector Laboratories) in PBS containing 0.4% BSA and 0.1% Triton X-100, two hours at room temperature. Afterwards, the slices were rinsed in 0.1 M PBS and the immunoreactivity (IR) was visualized with a standard avidin-biotin-peroxidase reagent (1 : 250 dilution, ABC Elite Kit; Vector Laboratories) for 90 min at room temperature. IHC labelling was revealed with 0.05% diaminobenzidine (in 0.05% NiCl and 0.01% H_2O_2-Tris saline buffer, pH 7.6) and then observed under light microscopy and the number of trkB-immunoreactive (trkB-IR) cells in SN determined by image analysis as described hereinafter. For TrkB staining, slices were incubated with a 1 : 1000 dilution of a polyclonal rabbit anti-trkB (sc-12, Santa Cruz Biotechnology). TrkB-like IR signals were totally blocked when brain tissue coronal slices were incubated with anti-trkB antibody together with an excess amount (100X) of the immunizing peptide (sc-12P, Santa Cruz Biotechnology). In addition, negative controls made by omission of the first antibody did not reveal IR signals. A 1 : 5000 dilution of a polyclonal rabbit anti-TH antibody (Calbiochem) was used for IHC labelling of TH-containing neurons, as reported previously by us [12].

For double immnunofluorescent experiments, free-floating coronal brain slices were rinsed in 0.1 M PBS buffer containing 3% normal goat serum, 0.02% sodium azide, and 0.2% Triton X-100, for 1 hr at room temperature. Then, the slices were incubated for 72 hours at 4°C in presence of a 1 : 1000 dilution of the anti-trkB antibody (Santa Cruz Biotechnology) and a 1 : 2000 dilution of a polyclonal mouse

anti-TH antibody (Calbiochem). Thereafter, the slices were incubated for 1 hour at room temperature with a 1 : 200 dilution of secondary CY3-conjugated anti-rabbit antibody (Jackson ImmunoResearch) and a 1 : 50 dilution of Fluorescein- (FITC-) conjugated anti-mouse antibody (Jackson ImmunoResearch). Finally, the slices were mounted and coverslipped for fluorescence microscopic analysis.

2.5. Nissl Staining. To perform a Nissl staining, coronal brain slices were sequentially immersed in the following solutions: xylene, ethanol (at 100%, 95%, and 70%), water, 0.5% cresyl violet (30 min), water, and ethanol (at 70%, 90%, and 100%). Finally, the tissue slices were mounted on gelatinized glass slides, dried overnight, and observed under light microscopy.

2.6. Nonisotopic In Situ Hybridization (ISH) of TrkB. The procedure used was essentially as reported previously by us, with slight modifications [31].

2.6.1. Labelling of Oligonucleotide Probe. Deoxynucleotide probes (41-mer) synthesized by BIOS-Chile (Santiago, Chile) were used for ISH experiments. TrkB antisense probe 5′-GTG GAG GGG ATC TCA TTA CTT TTG TTT GTA GTA TCC CCG AT-3′ was complementary to nucleotides 1880–1920 of the reported trkB sequence (M-55291). One hundred picomoles of trkB probe were 3′ endlabeled by incubation with 55 units of terminal transferase in 20 μL of tailing buffer, in presence of 9 nmol of dATP and 1 nmol of digoxigenin-labeleled deoxyuridine-triphosphate (DIG-dUTP).

2.6.2. Hybridization Reaction and Immunological Detection. Brain coronal sections were rinsed in PBS and then incubated at 62°C for 30 min in a prehybridization solution containing Denhardt's 1X (Denhardt's 100X composition: 2% Ficoll, 2% polyvinil pyrrolidone, 2% BSA) and SSC 4X (SSC 20x composition: 3 M NaCl, 0.3 M sodium citrate). Thereafter, the tissue slices were incubated in presence of 10 pmol/mL trkB DIG-labeled antisense probes, in a buffer containing 50% formamide, 0.6 M NaCl, 20 mM EDTA, and 0.2% lauryl sarcosine, in Tris-HCl, pH 7.5, for 20 hr at 35°C. After hybridization, the slices were rinsed in SSC and then reacted with an anti-DIG antibody conjugated to alkaline phosphatase (Boehringer-Mannheim Gmbh Biochemica, Germany). Reaction was developed using NBT and BCIP (Gibco, MD) as enzyme substrates. Finally, the slices were mounted on gelatinized glass slides, dried overnight, and coverslipped for light microscopy. As a control, the tissue slices were hybridized as explained previously, in presence of an excess (100X) of unlabeled trkB probe. As a different experimental control, the slices were incubated with a sense oligonucleotide probe labeled with DIG-UTP. These controls generated no positive signals (data not shown).

2.7. Analysis of TrkB and TH Expression in SN. After IHC or ISH procedures, brain sections were examined under a light microscope (Nikon Labophot-2) equipped with a video camera (Sony CCD-Iris) connected to a Macintosh computer. Positive cells for trkB or TH immunostaining and trkB-DIG labelled cells in SN were counted using the NIH image//ppc 1.61 program. For each experimental paradigm, the number of positive cells was evaluated in three different areas per slice, and results shown hereinafter correspond to data obtained from at least four different rats, in which at least three different slices per rat were studied. Only coronal slices corresponding to 5.2 to 5.6 mm posterior to Bregma were used [30].

The number of cells with positive labelling was counted in photomicrographs (20x magnification), with sample areas of 0.042 mm^2 for SNc and 0.065 mm^2 for SN pars reticulata (SNr). Thus, raw results obtained are estimates of cell density in each condition. Results are reported as percentage of cells in the ipsilateral SN compared to the contralateral side (100%) in each experimental condition.

Immunofluorescence results were examined under a Fluoview 100 confocal microscope and an Olympus microscope (Olympus BX51, USA) equipped with a fluorescent system. Positive cells were counted using the Q-Capture Pro software (Q-Imaging, Canada). The number of positive cells for each of the IF was evaluated in each slice as indicated previously, under a 40x magnifications, with sample areas of 0.020 mm^2 for each SNc. Results represent the percentage of cells in SN compacta that exhibit colabelling of TH and trkB over the total number of TH IF-positive cells present in this midbrain subregion.

2.8. Statistical Analysis. All statistical analysis were performed using Prism 4.01 GraphPad software. Data were analyzed by Kruskal-Wallis nonparametric ANOVA, followed by a U-test. Values of $P < 0.05$ were considered statistically significant. All data are reported as means ± S.E.M.

3. Results

3.1. A Decrease in the Expression of TrkB-IR Cells and TrkB mRNA Precedes the Disappearance of TH-IR Cells in SNc of Rats after Unilateral 6-OHDA Intrastriatal Injections. In our laboratory, we have recently used an animal model proposed to imitate the presymptomatic stages of PD [3, 32]. By using this model, which consists of a unilateral intrastriatal injection of the neurotoxin 6-OHDA, we have shown a progressive reduction in rat striatal DA levels 1 to 7 days after neurotoxin injection [13]. We also showed that in SNc, the IR for TH, the key enzyme in the synthesis of DA and a common marker for dopaminergic neurons, is decreased by 14 days after neurotoxin injection [13].

Expanding those studies, we analyzed the number of TH-IR cells in SNc of rats 4, 7, and 14 days after unilateral 6-OHDA intrastriatal injection (Figure 1). We did not visualize changes in the number of TH-IR cells in ipsilateral SNc 4 or 7 days after unilateral 6-OHDA intrastriatal injections, when compared to the contralateral SNc of the respective animal (Figures 1(a) and 1(b) and Figures 1(c) and 1(d), at 4 and 7 days, resp.). However, as shown previously [13], we detected a decrease in the number of TH-IR cells in the ipsilateral SNc 14 days after neurotoxin injection compared to its contralateral side (Figures 1(e) and 1(f)). Quantification of data

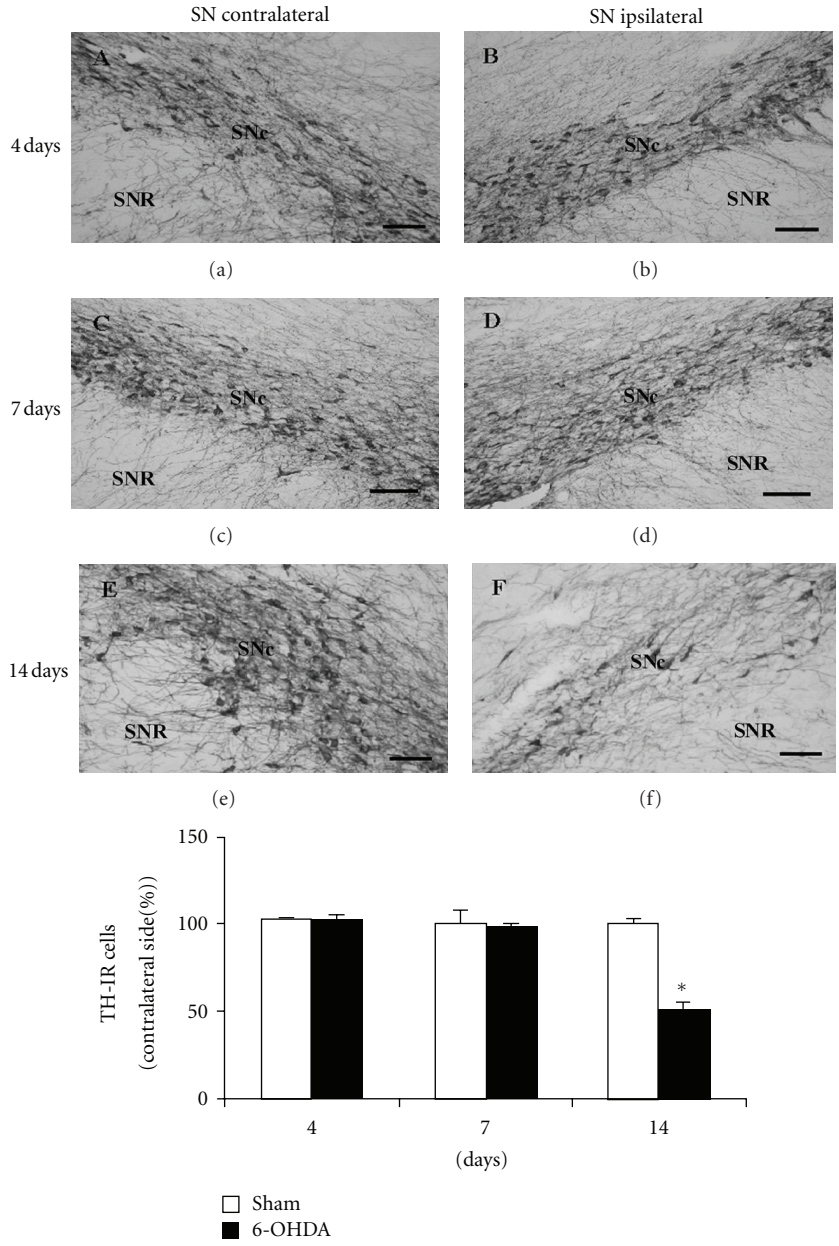

Figure 1: The unilateral intrastriatal injection of 6-OHDA induces a decrease in the number of TH immunoreactive cells in SNc that is only evident 14 days after the neurotoxin injection. Photomicrographs show TH-immunoreactive (IR) cells in the contralateral (a), (c), and (e) and ipsilateral (b), (d), and (f) side of rat SN 4, 7, and 14 days after unilateral 6-OHDA intrastriatal injection, respectively. (a)–(f) scale bar = 100 μm. SNc: substantia nigra pars compacta; SNR: substantia nigra pars reticulata. (g) Percentage of TH-IR cells in the ipsilateral SNc compared to the contralateral side, at 4, 7, and 14 days after unilateral intrastriatal 6-OHDA (black columns) or ascorbic acid (sham, white columns) injections to rats. The number of cells with TH-IR signals per unit area per slice was 507.9 ± 7.8, 484.1 ± 71.4, and 531.7 ± 103.2 cells/mm^2 in contralateral SNc of ascorbate injected rats, at 4, 7, and 14 days after treatment, respectively. In the case of 6-OHDA-treated rats, the number of cells with TH-IR signals in contralateral SNc was 500.0 ± 23.8, 452.4 ± 87.3, and 507.9 ± 111.1 cells/mm^2, at 4, 7, and 14 days after neurotoxin injection, respectively. $n = 6$ rats under each experimental condition. The different experimental groups were compared by a Kruskal-Wallis nonparametric ANOVA, followed by a U-test. $^*P < 0.05$ compared with sham-treated rats.

obtained in several animals after 6-OHDA and sham treatment is shown in Figure 1(g). We only detected a statistically significant reduction in the relative number of TH-IR cells in SNc two weeks after striatal neurotoxin administration (48.6% ± 3.4, $P < 0.01$, 6-OHDA versus sham treatment) and no differences were observed at earlier time points (Figure 1(g)). Interestingly, the number of Nissl-stained cells in ipsilateral SNc remained unaffected 4 to 7 days after

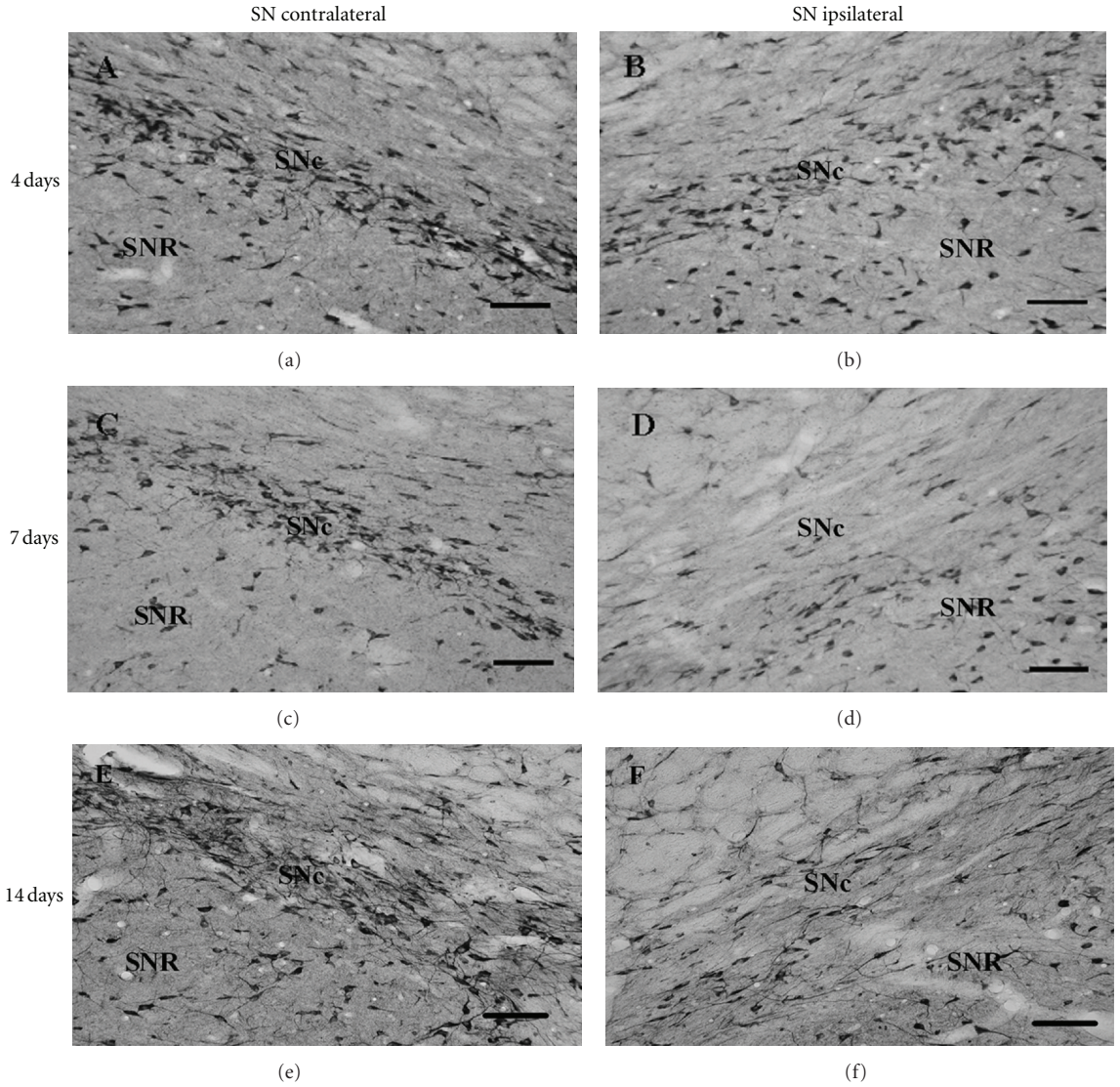

Figure 2: Photomicrographs showing a decrease in the number of trkB-IR cells in ipsilateral SNc at 7 and 14 days, but not at 4 days, after unilateral 6-OHDA intrastriatal injections. Photomicrographs show trkB-immunoreactive (IR) cells in the contralateral (a), (c), and (e) and ipsilateral (b), (d), and (f) sides of rat SN at 4, 7, and 14 days after unilateral intrastriatal injection of 6-OHDA. (a)–(f) scale bar = 100 mm. SNc: substantia nigra pars compacta; SNR: substantia nigra pars reticulata.

unilateral 6-OHDA intrastriatal injection (102 ± 4 and 93 ± 5% of cells in ipsilateral SNc compared to contralateral side at 4 and 7 days after neurotoxin injection, resp.; $P > 0.05$). It was only possible to detect a reduction in the number of Nissl-positive cells 14 days after neurotoxin injection (47 ± 7% of cells in ipsilateral SNc compared to the contralateral side; $P < 0.05$). Altogether, these results demonstrate that the number of TH-IR cells and Nissl-stained cells in SNc is only modified 2 weeks after an intrastriatal injection of 6-OHDA, consistent with a progressive model of PD and with previous results from us and others [12, 33–35].

We have previously shown a transient increase in the genic expression of BDNF in the ipsilateral SN as early as 1 day after a unilateral intrastriatal injection of 6-OHDA and prior to the disappearance of TH-IR cells in SNc [13]. In this work, we decided to evaluate the expression of trkB, the specific BDNF receptor, in SN, using the same experimental paradigm.

Photomicrographs shown in Figures 2(a), 2(c), and 2(e), are representative of the distribution of trkB-IR cells in control SN and are consistent with data in the literature [36, 37]. Immunoreactive cells concentrate densely in SNc while it is also possible to detect a small number of labeled cells scattered over the Substantia Nigra pars reticulata (SNR). This pattern of trkB-IR is dramatically affected in the ipsilateral side of SN at 7 and 14 days after unilateral intrastriatal 6-OHDA injection. The disappearance of the dense immunoreactivity for trkB in SNc (Figures 2(d) and 2(f)) is especially remarkable. In contrast, these studies exhibited no change in the distribution of trkB-IR cells in ipsilateral SNc

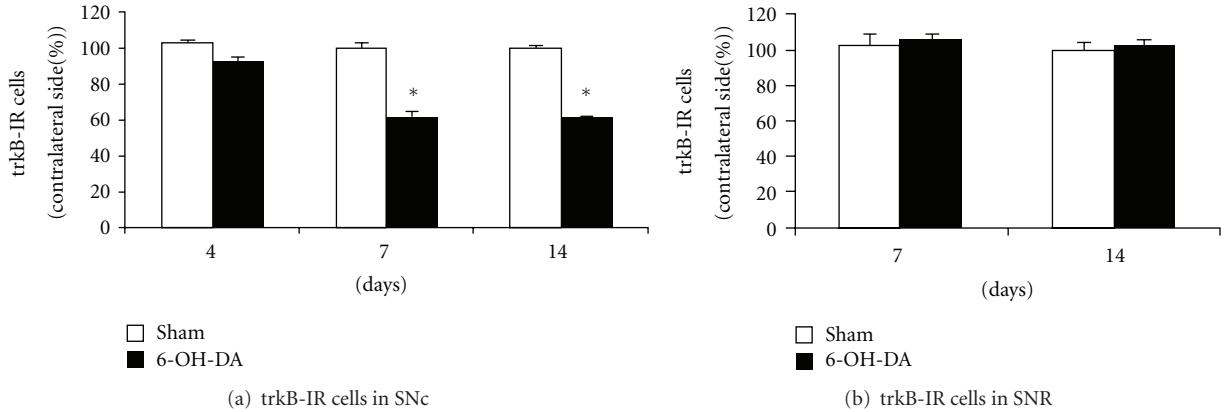

(a) trkB-IR cells in SNc (b) trkB-IR cells in SNR

Figure 3: Unilateral 6-OHDA intrastriatal injection results in a significant decrease in the number of trkB-IR cells in ipsilateral SNc at 7 and 14 days after the injection. (a) Percentage of trkB-IR cells in rat ipsilateral SNc compared to the contralateral side after unilateral 6-OHDA (black columns) or ascorbic acid (sham, white columns) intrastriatal injections. Number of cells with trkB-IR signals in contralateral SNc of ascorbate-injected rats per area unit per slice was 507.9 ± 7.9, 365.1 ± 15.9, and 412.7 ± 10.6 cells/mm^2, at 4, 7, and 14 days after injections, respectively. In the case of 6-OHDA-treated rats, number of cells with trkB-IR signals in contralateral SNc was 484.1 ± 15.9, 381.0 ± 31.7 and 404.7 ± 15.9 cells/mm^2, at 4, 7, and 14 days after 6-OHDA injections, respectively. (b) Percentage of trkB-IR cells in the ipsilateral SNR compared to the contralateral side, at 7 and 14 days after unilateral intrastriatal injections of 6-OHDA (black columns) or ascorbic acid (sham, white columns). Number of cells with trkB-IR signals in contralateral SNR of ascorbate-treated rats was 117.9 ± 5.1 and 143.6 ± 5.1 cells/mm^2, at 7 and 14 days after injections, respectively. In the case of 6-OHDA-treated rats, the number of cells with trkB-IR signals in contralateral SNR amounted to 117.9 ± 5.1 and 148.7 ± 10.3 cells/mm^2, at 7 and 14 days after toxin injections, respectively. $n = 6$ rats under each experimental condition. The different experimental groups were compared by a Kruskal-Wallis nonparametric ANOVA, followed by a U-test. $^*P < 0.05$ compared with sham-treated rats.

as compared to contralateral SNc 4 days after unilateral 6-OHDA injections (Figures 2(a) and 2(b)). Quantification of the number of trkB-IR cells in ipsilateral SN was performed at 4, 7, and 14 days after 6-OHDA or ascorbic acid (sham-treated) unilateral intrastriatal injections (Figure 3). Data are presented as percent change in the number of trkB-IR cells in ipsilateral SNc (Figure 3(a)) or SNR (Figure 3(b)) compared to the respective contralateral side, in both sham- and 6-OHDA-treated animals. A significant $40 \pm 3\%$ and $40 \pm 1.5\%$ reduction in the relative number of trkB-IR cells in ipsilateral SNc was detected in 6-OHDA-treated rats 7 and 14 days after intrastriatal injection of the neurotoxin when compared to sham animals, respectively ($P < 0.05$ in each case) (Figure 3(a)). No differences were observed when comparing the relative number of trkB-IR cells in ipsilateral SNc 4 days after unilateral 6-OHDA or ascorbic acid injections (Figure 3(a)). Interestingly, the reduction in trkB-IR cells observed at 7 and 14 days after 6-OHDA seems to be a subregion specific phenomenon in SN since no change in the relative number of trkB-IR cells was detected in ipsilateral SNR at any time point after neurotoxin injection (Figure 3(b)).

The aforementioned changes in the number of trkB immunoreactive cells in ipsilateral SNc after 6-OHDA injection could be explained by a transcriptional mechanism; that is, the genic expression of trkB could be reduced in this midbrain nucleus after the neurotoxin striatal injection. To provide evidence regarding this proposition, the distribution and number of cells expressing trkB mRNA in SN were evaluated by nonisotopic ISH seven days after the unilateral 6-OHDA intrastriatal injection. Seven days of 6-OHDA treatment was chosen for these ISH studies as no changes in Nissl-stained cells or in TH-IR cells were detected in ipsilateral SNc at this time point after neurotoxin injection compared to sham rats, as indicated previously. The ISH studies revealed a high concentration of cells expressing trkB mRNA in SNc and a more disperse localization of trkB mRNA-expressing cells in SNR, as it is shown in contralateral SN in Figure 4(a). However, this pattern of trkB mRNA expression is quite different in ipsilateral SN at 7 days after unilateral intrastriatal injection of the neurotoxin (Figure 4(b)), since it is possible to observe a diffuse distribution of DIG-labeled cells throughout the SN in conjunction with a relative decrease in the number of these cells in SNc. The evaluation of the number of trkB-DIG labeled cells in ipsilateral SNc at 7 days after unilateral striatal 6-OHDA injection, expressed as percent of change over the contralateral SNc, revealed a $38 \pm 4\%$ decrease compared to sham-treated rats (Figure 4(c), $P < 0.05$). Conversely, no statistical differences were detected when comparing the number of cells expressing the mRNA for trkB in ipsilateral SNR after 6-OHDA or ascorbic acid striatal injections (Figure 4(d)). These results are consistent with those obtained before by IHC and raise the possibility that the specific decrease in the expression of trkB observed in ipsilateral SNc, in response to 6-OHDA injection in the striatum, might be mediated at least in part by a transcriptional mechanism.

3.2. Dopaminergic Neurons of SNc Fail to Express TrkB at Early Stages after 6-OHDA Striatal Administration. The aforementioned results demonstrate that as early as seven days after the unilateral intrastriatal injection of 6-OHDA, it is possible

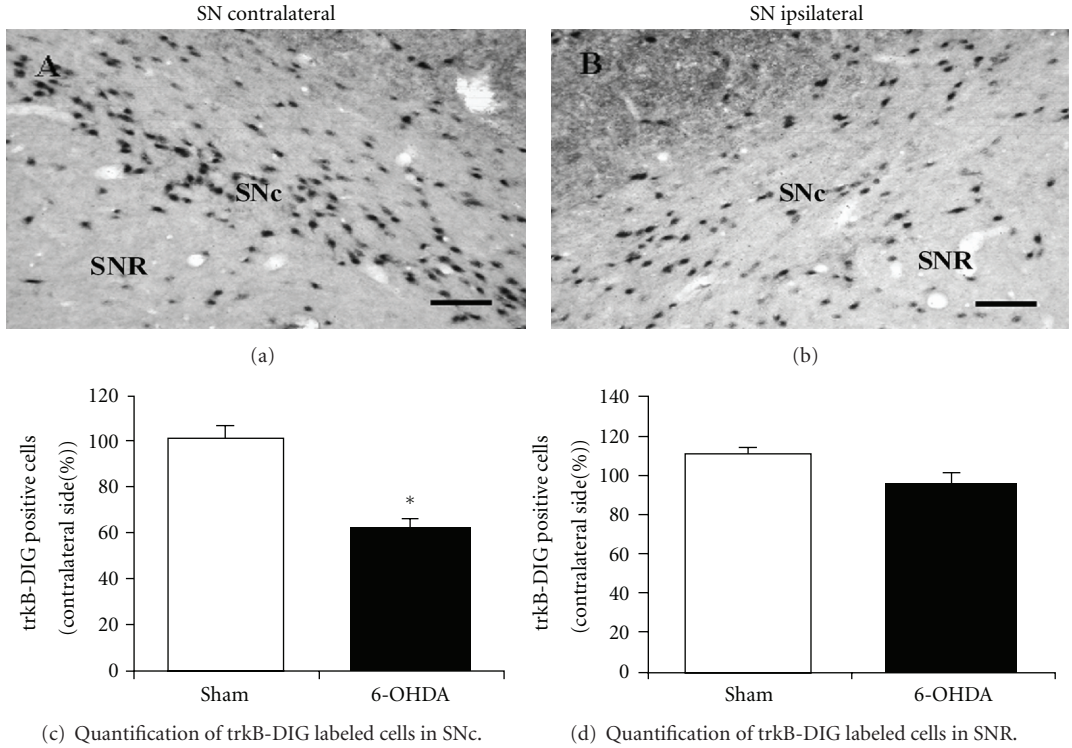

(c) Quantification of trkB-DIG labeled cells in SNc.

(d) Quantification of trkB-DIG labeled cells in SNR.

Figure 4: A specific decrease in the number of positive trkB-mRNA cells is observed in ipsilateral SNc 7 days after unilateral 6-OHDA intrastriatal injections. Photomicrographs from ISH experiments show trkB-DIG positive cells in the contralateral side (a) and ipsilateral side (b) of rat SN 7 days after unilateral 6-OHDA intrastriatal injection, respectively. (a), (b) scale bar = 100 μm. SNc: substantia nigra pars compacta; SNR: substantia nigra pars reticulata. (c) Percentage of trkB-DIG positive cells in the ipsilateral SNc compared with the contralateral side, 7 days after unilateral intrastriatal 6-OHDA (black columns) or ascorbic acid (sham, white columns) injections to rats. Number of cells with trkB-DIG-positive signals in contralateral SNc was 285.7 ± 15.9 and 317.5 ± 31.7 cells/mm^2 in ascorbate and 6-OHDA injected rats, respectively. (d) Percentage of trkB-DIG positive cells in the ipsilateral SNR compared to the contralateral side, 7 days after unilateral intrastriatal 6-OHDA (black columns) or ascorbic acid (sham, white columns) injections to rats. Number of cells with trkB-DIG positive signals in contralateral SNR was 107.7 ± 5.1 and 117.9 ± 5.1 cells/mm^2 in ascorbate and 6-OHDA injected rats, respectively. $n = 4$ rats under each experimental condition. The different experimental groups were compared with a Kruskal-Wallis nonparametric ANOVA, followed by a U-test. $^*P < 0.05$ compared with sham-treated rats.

to detect a decrease in the number of trkB-IR cells in SNc (Figures 2 and 3) without a change in the number of TH-positive cells in this midbrain subarea (Figure 1). On the other hand, the total number of cells detected by Nissl staining remained unchanged in SNc at this time point after 6-OHDA treatment. Therefore the early decrease in trkB-IR cells might be the consequence of a reduced expression of trkB in the population of dopaminergic neurons and not due to the disappearance of these neurons in SNc. We decided to evaluate this proposition.

We first studied the expression of trkB in TH-positive cells by double immunofluorescence (IF), in naïve control animals. As expected, TH-IF positive cell bodies are only observed in SNc (Figure 5(a)). Even though there are no TH-positive cell bodies in SNR, it is possible to observe a significant number of TH-IF labeled neurites projecting from the SNc to the SNR (Figure 5(a)). On the other hand, IF studies exhibited trkB-positive cells in both SNc and SNR (Figure 5(b)), in agreement with the IHC results shown before. When both images are merged, it is possible to observe colocalization of TH-IF and trkB-IF in SNc, while this colocalization does not occur in SNR (Figure 5(c)). Indeed, approximately 80% of the total TH-IF cells in SNc were found to coexpress trkB (see the following).

Immunofluorescence studies conducted 7 days after unilateral intrastriatal injection of 6-OHDA showed results compatible with a reduction in the number of trkB-IF cells in ipsilateral compared to contralateral SNc (Figures 6(c) and 6(d)), while the number of TH-IF cells remained unchanged (Figures 6(a) and 6(b)). In addition, the merge of these pictures indicates a decrease in the number of cells coexpressing TH and trkB in SNc ipsilateral to the striatal injection of 6-OHDA (Figures 6(e) and 6(f)). Indeed, quantification of the results obtained in several animals revealed a statistically significant reduction in the colocalization of TH-IF and trkB-IF cells in ipsilateral SNc compared to its contralateral side after neurotoxin treatment ($39 \pm 8\%$ reduction, $P < 0.05$) (Figure 6(g)). No such change was observed in sham-treated rats (Figure 6(g)). These results indicate that the early decrease in trkB expression observed in ipsilateral SNc after intrastriatal 6-OHDA injection is most likely due to a reduced expression of the neurotrophin receptor in

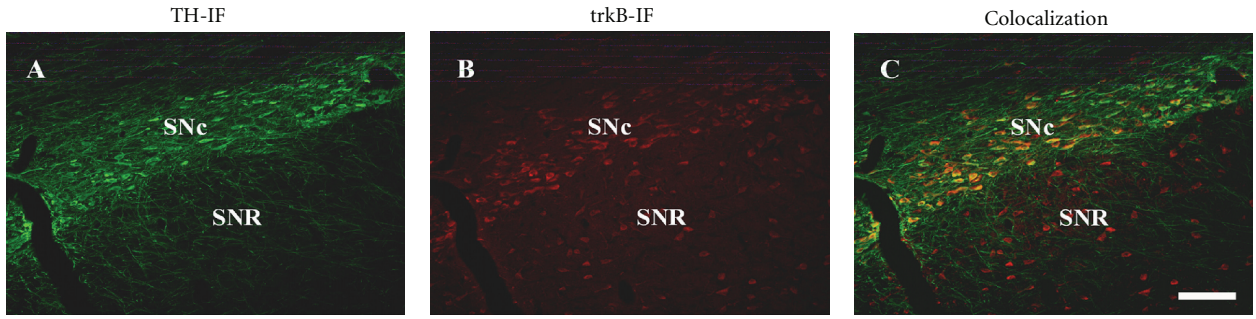

Figure 5: TH and trkB immunoreactivities are highly colocalized in rat SNc. Immunofluorescent detection of TH (a) and trkB (b) in SN in untreated naïve rats. (c) Merge of (a) and (b). (a)–(c) scale bar = 150 μm. SNc: substantia nigra pars compacta; SNR: substantia nigra pars reticulata.

TH-positive cells occurring in SNc and not to the disappearance of these cells in this midbrain subregion.

3.3. Ifenprodil Inhibits Both TrkB Downregulation and TH Decreased Expression in SNc Induced by a Unilateral 6-OHDA Intrastriatal Microinjection. Recent results from us suggest the induction of a coupling between Glutamatergic drive, NMDA receptor activation, and increased BDNF expression in SN at the very early stages of the present rodent model of presymptomatic PD [11, 13]. Therefore, we sought to determine, by means of a Glutamate receptor antagonist, whether NMDA receptors might be involved in the early decrease in trkB expression as well as in the TH-IR cell disappearance that is observed in SNc in response to 6-OHDA intrastriatal injection. The selective NR2B-NMDA receptor antagonist, ifenprodil, was chosen for these studies because of reports indicating that activation of these receptor subtypes might suppress BDNF/trkB receptor complex expression and initiate or facilitate signaling cascades involved in neuronal cell death [38].

In the following experiments, four groups of rats were treated with consecutive i.p. injections of Ifenprodil (5 mg/kg) or saline solution, administered 1 day before and 3, 5, and 7 days after 6-OHDA or ascorbic acid (sham rats) intrastriatal injection. A marked decrease in the relative expression of trkB-IR cells occurs in the ipsilateral SNc of saline pretreated rats after 14 days of 6-OHDA intrastriatal injection compared with the ipsilateral SNc of sham rats (Figure 7(a), first versus second column, $P < 0.05$). Such 6-OHDA-induced decrease of trkB-IR cells in the ipsilateral SNc was significantly prevented in rats pretreated with Ifenprodil (Figure 7(a), second versus fourth column). Ifenprodil pretreatment also totally prevented the decrease of trkB expression observed in the ipsilateral SNc 7 days after neurotoxin intrastriatal injection (41.4 ± 4% reduction versus 3.5 ± 0.4% reduction in the number of trkB-IR cells in the SNc when comparing 6-OHDA injected rats versus 6-OHDA plus Ifenprodil injected rats, $P < 0.01$). On the other hand, saline and Ifenprodil pretreatment produced no effect on trkB-IR cell numbers, as evidenced in the ipsilateral SNc of sham rats (Figure 7(a), first versus third column).

IHC studies with antibodies against TH were also conducted in Ifenprodil- and saline-treated rats after unilateral 6-OHDA or ascorbic acid (sham) intrastriatal administration. The IHC studies illustrated in Figure 7(b) were performed 14 days after neurotoxin or ascorbate injections. As shown in Figure 7(b), decreases in the number of TH-IR cells in the ipsilateral SNc are readily observed after 6-OHDA striatal injections to saline pretreated rats (columns under saline pretreatment, $P < 0.05$). In contrast, Ifenprodil pretreatment blocked the appearance of such 6-OHDA-induced decrease of TH-IR cells observed in SNc (Figure 7(b)). On the other hand, decreases in the number of TH-IR cells in SNc were not detected 7 days after 6-OHDA injection (Figure 1) and the expression of TH observed at this time point was not statistically modified by ifenprodil pretreatment ($P > 0.05$).

Therefore, these studies show that trkB expression in SNc of rats may be decreased after a partial lesion of the nigrostriatal DAergic neuronal pathway induced by 6-OHDA and that this decrease along with that of TH-IR occurring in SNc may be prevented by NR2B-containing NMDA receptors antagonists such as Ifenprodil.

4. Discussion

4.1. The 6-OHDA Presymptomatic Rat Model of Parkinson Disease. One of the main pathological hallmarks of PD is the progressive and selective loss of dopaminergic neurons in SN. The clinical symptoms of PD appear when striatal DA is depleted 70–80% and when 50–60% of DA cell loss has occurred in SNc [1, 2, 4, 39]. In the present work, we have used a rat model that closely mimics the neurochemical characteristics of early PD, producing a slow degeneration of the dopaminergic nigrostriatal pathway over a period of several weeks [32, 34, 40, 41]. In essence, this model of presymptomatic PD is produced by an intrastriatal unilateral injection of 6-OHDA, which initially induces a partial damage (20 to 50%) of DA terminals in the striatum followed by a slow progressive degeneration of dopaminergic cells in the ipsilateral SN [13, 32]. In these conditions, we were only

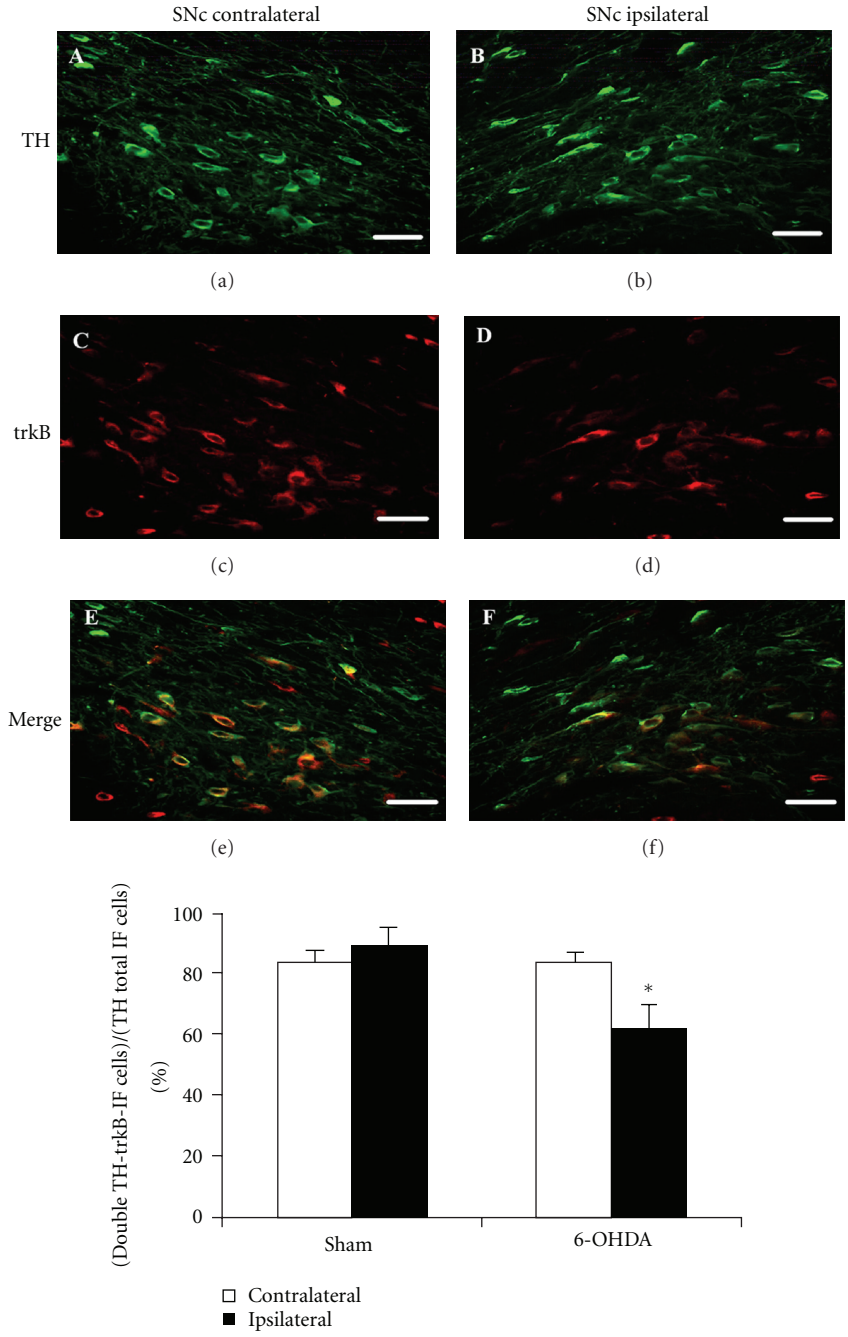

(g) Quantification of double TH-trkB IF cells.

FIGURE 6: A decrease in the percentage of double labeling for TH and trkB in SNc is detected 7 days after unilateral 6-OHDA intrastriatal injections. Photomicrographs show TH-IF cells (a), (b) and trkB-IF cells (c), (d) in rat SNc, 7 days after unilateral 6-OHDA intrastriatal injection. (e) Merge of (a) and (c); (f) merge of (b) and (d). (a), (c), and (d) correspond to contralateral SNc while (b), (d), and (f) to ipsilateral SNc. (a)–(f) scale bar = 50 μm. SNc: substantia nigra pars compacta. (g) Quantification of cells that coexpress TH and trkB in the ipsilateral SNc compared to their contralateral side, 7 days after unilateral 6-OHDA or ascorbic acid (sham) intrastriatal injections to rats. The results were expressed as the percentage of cells that coexpress TH and trkB over the number of total TH-IF cells. Number of cells with TH-IF signals and double TH-trkB-IF signals in contralateral SNc after ascorbate injection was 365.1 ± 39.7 and 309.5 ± 39.7 cells/mm^2, respectively. In the case of 6-OHDA-treated rats, number of cells with TH-IF signals and double TH-trkB-IF signals in contralateral SNc was 333.3 ± 23.8 and 277.7 ± 7.9 cells/mm^2, respectively. $n = 4$ rats for each experimental condition. The different experimental groups were compared by a Kruskal-Wallis nonparametric ANOVA, followed by a U-test. $^*P < 0.05$ compared with sham-treated rats.

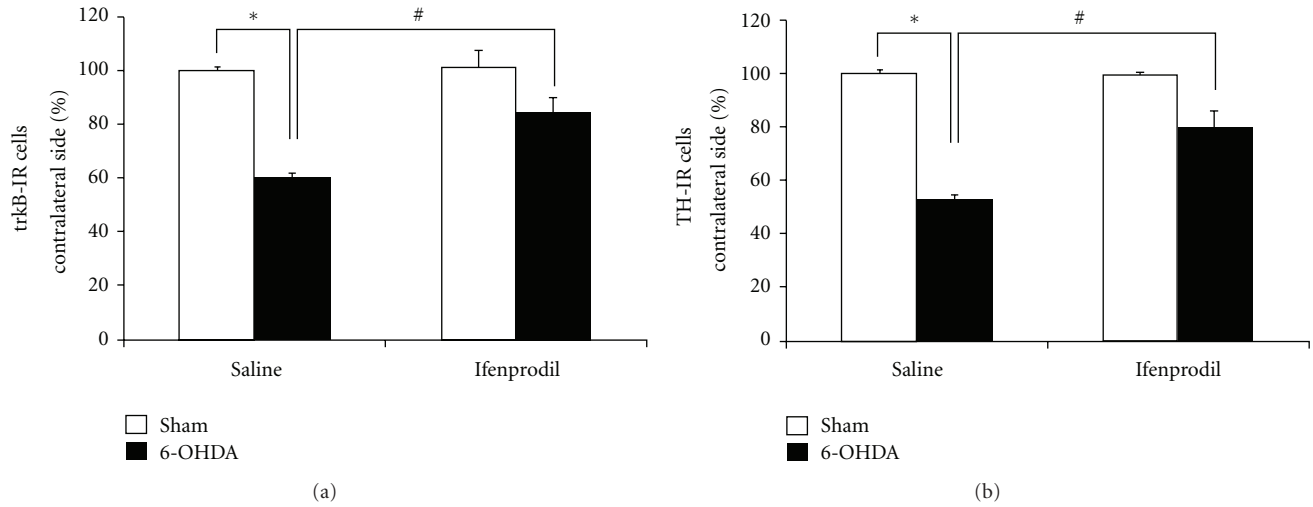

Figure 7: Ifenprodil, an antagonist of NR2B containing NMDA receptors, prevents the decrease in trkB-IR and TH-IR cells occurring in SNc 14 days after 6-OHDA intrastriatal injection. Positive cells for trkB and TH immunostaining in SNc were counted in coronal midbrain slices of treated rats as described in Section 2. Four groups of rats in each case (a) and (b) were pretreated with saline solution or Ifenprodil (5 mg/kg, i.p.), 1 day before and 3, 5, and 7 days after unilateral 6-OHDA (black columns) or ascorbic acid (sham, white columns) intrastriatal administration. The IHC studies were performed 14 days after 6-OHDA or ascorbic acid injections. Results were expressed as a percentage of trkB-IR cells (a) or TH-IR cells (b) in the ipsilateral SNc compared with the contralateral side. (a) Number of cells with trkB-IR signals in sample areas per slice from contralateral SNc was equal to 365.1 ± 15.9, 381.0 ± 31.7, 412.7 ± 10.6, and 404.7 ± 15.9 cells/mm^2 in sham-saline, 6-OHDA-saline, sham-Ifenprodil, and 6-OHDA-Ifenprodil rats, respectively. (b) Number of TH-IR cells in sample areas per slice from contralateral SNc was equal to 404.8 ± 23.8, 357.1 ± 29.8, 386.9 ± 11.9, and 369.0 ± 6.0 cells/mm^2 in sham-saline, 6-OHDA-saline, sham-Ifenprodil, and 6-OHDA-Ifenprodil rats, respectively. The different experimental groups were compared by a Kruskal-Wallis nonparametric ANOVA, followed by a U-test. $^*P < 0.05$, when comparing saline-6-OHDA versus saline-sham rats. $^\#P < 0.05$ when comparing saline-6-OHDA versus Ifenprodil-6OHDA rats. $n = 3$ rats under each experimental condition.

able to observe a significant reduction in the number of TH-IR cells in SN starting fourteen days after 6-OHDA injection, in agreement with previous results from us and others [12, 13, 34, 40]. Indeed, this PD rat model allowed us to study changes in the expression of trkB receptors in SN that might occur prior to any reduction in the number of dopaminergic neurons in this midbrain area.

4.2. Intrastriatal 6-OHDA Injection Induces Changes in the Expression of TrkB in SNc. Recent studies in our laboratory have shown an increased expression of BDNF transcripts in SN as early as one day after 6-OHDA intrastriatal injection [13]. However, nigral BDNF expression returned to basal levels by 7 days after neurotoxin injection. Therefore, a transient upregulation of BDNF expression in SN seems to exist at early stages in this rodent model of PD. We have proposed that these changes in BDNF transcripts may constitute part of compensatory actions triggered to maintain the survival and integrity of DA cells in SN [11, 13]. In this work we decided to expand our knowledge on this model of presymptomatic PD by evaluating the expression of the BDNF receptor, trkB. We detected a decrease in trkB expression in SNc 7 days after 6-OHDA injection. This reduction in the expression of trkB after 6-OHDA treatment does not seem to be accounted by dopaminergic cell death as no change in the number of TH-positive cells or in the total number of cells was detected in SNc at this time point. Indeed, our studies demonstrate that 83% of TH-positive cells in SNc coexpress trkB, which is in agreement with previous results from others [26]. No colocalization was detected in SNR, as no TH-positive cells were observed in this SN subregion [26, 36, 37, 42]. In addition, by seven days after unilateral intrastriatal injection with the neurotoxin it was possible to detect a reduction in the colocalization of trkB and TH in ipsilateral SNc compared to the control contralateral SNc. Since at this time point we did not detect any change in the number of TH-positive cells or in the total number of cells in this brain region, these results suggest that the decrease in trkB receptor expression after 6-OHDA treatment might be due to a reduction in the genic expression of this receptor in TH-positive cells in SNc.

The observation that trkB receptors begin to be downregulated seven days after 6-OHDA injection is intriguing and raises the question whether this might be linked to transient increases of BDNF expression observed in SN at early times after neurotoxin injection [12, 13]. We have reported a substantial increased expression of BDNF transcripts in SN as early as 1–4 days after 6-OHDA intrastriatal injection, an effect that was abolished by MK-801, a nonselective antagonist of NMDA receptors, but not by Ifenprodil, selective antagonist of NR2B-containing NMDA receptors [11–13, 43]. As judged by ISH and IHC studies, such increases in BDNF expression appear to occur preferentially

in SNR [12, 13]. In addition, such increases occur in parallel with mild but significant increases in extracellular levels of glutamate and aspartate in SN [11, 13]. At later stages (7 days) in this presymptomatic PD model, nigral BDNF transcripts expression started to return to basal levels, whereas glutamate and aspartate extracellular levels kept increasing quite dramatically in SN [13]. This last time point after striatal 6-OHDA injection seems to determine the initiation of trkB downregulation in SN as reported in this work. However and in contrast to BDNF upregulation, the changes in trkB expression shown occur predominantly in SNc and are selectively blocked by an antagonist of NR2B-containing NMDA receptor such as Ifenprodil. Therefore, such downregulation of trkB in SNc after neurotoxin injection could be triggered by an increased overflow of excitatory amino acids and a parallel activation of NR2B-NMDA receptors. Despite the previous considerations, it is not possible to disregard that increased endogenous BDNF levels in SN may contribute also to the neurotoxin-induced decrease of trkB observed in this midbrain subregion. Indeed, BDNR-IR cells in SNc and SNr remained significantly elevated at 7 days of this 6-OHDA presymptomatic model, although this coincided with BDNF transcripts expression actually returning to basal levels [13]. Therefore, elevated levels of BDNF protein in SNc might very well induce an internalization process and a later proteolysis of the trkB receptor. Supporting this idea, studies conducted in primary cultures of hippocampal neurons and cerebellar granule neurons demonstrate that exposure of these cultures to the BDNF ligand results in a decrease both in trkB mRNA and protein and that these changes are prevented by inhibitors of proteosomal function [44, 45]. It remains to be established whether such BDNF-dependent trkB internalization occurs in SNc at early times after 6-OHDA intrastriatal injections.

It is interesting that the 6-OHDA intrastriatal administration induces a downregulation of trkB receptor specifically in SNc while no effect is detected in SNR. According to the data presented in this work, trkB shows a lower expression in SNR than in SNc. As discussed before, early after neurotoxin injection an increased expression of BDNF transcripts occurs preferentially in SNR as compared to SNc [12, 13], while no change is detected in trkB expression in any of the SN subregions. Therefore, it would be possible to suggest that early after the 6-OHDA-induced injury there is an increased BDNF/trkB ratio in SNR compared to SNc, which might explain the differential effects induced by the toxin in each SN subregions. Additionally, relative differences in glutamate overflow and subsequent NR2B-NMDA receptors activation could also contribute to the differential trkB regulation shown here in these SN subregions. It is interesting that a subcellular relocation of NR2B-NMDA receptors from synaptic to extrasynaptic sites has been reported to occur in the striatum of rats after an acute injection of 6-OHDA in SN [46]. It remains to be determined whether such phenomenon also happens in SNc following intrastriatal 6-OHDA injection, our experimental condition. Another important consideration is associated with the fact that the decrease in trkB after 6-OHDA treatment occurs only in TH-IR cells located in SNc, positioning the DA cells as the main targets of this downregulation. Conversely, our results show that trkB coexists in SNR mainly with non-DAergic cells and in this SN subregion no change is observed. Therefore, a combination of DAegic cell phenotype, BDNF/trkB ratio, local glutamate overflow and relative predominance of NR2B-NMDA receptors could contribute to the early and specific downregulation of trkB receptors which is observed in SNc in this experimental model of presymptomatic PD.

4.3. NR2B-Containing NMDA Receptors Mediate the Decrease in TrkB in SNc. It has been shown that in both, the presymptomatic and symptomatic phases of PD, there is an increased glutamatergic drive over the SN arising mainly from the Subthalamic Nucleus (STN). This glutamatergic hyperactivity seems to be a response to the misregulation of output motor information from the basal ganglia, due to the progressive loss of dopaminergic inputs arriving to the striatum [32, 47]. In agreement with this proposition, we have previously shown an increase in extracellular glutamate levels in SN in this presymptomatic model of PD [13]. We have also provided evidence that supports the existence of a functional coupling between increased glutamatergic drive, NMDA receptor activation, and BDNF expression in SN in this rodent PD model [13].

In this regard, results presented in this work indicate that ifenprodil, a selective antagonist of NR2B-NMDA receptors, prevents the downregulation of trkB expression in SNc after striatal 6-OHDA injection. At the molecular level, it has been reported that one of the promoters described for trkB is repressed by increases in intracellular calcium levels [48], and therefore, it would be possible to suggest that an increased glutamatergic drive may induce the activation of calcium permeable NMDA receptors in SN, which could in turn mediate an increase in intracellular calcium levels finally leading to a reduction in trkB expression in this midbrain region.

Altogether, previous and current data allow us to suggest that glutamatergic drive and NMDA receptor activation may exert opposing effects on BDNF and trkB expression in SN during early PD. Essentially, they could be mediating a differential biphasic time pattern expression of the BDNF/trkB receptor complex, which precedes DA cell death in SN and the clinical symptoms of this neurological disease. Thus, early after striatal 6-OHDA injections (1 to 4 days in our rodent model of PD), increased synaptic glutamatergic information in SN would mediate the increase in BDNF expression, neurotrophin that may be associated with positive compensatory actions in SN. Later on (by 7 days), overactivity of glutamatergic pathways innervating SN would specifically activate NR2B-containing NMDA receptors causing a downregulation of trkB receptors. This would be consistent with the proposition that the NR2B-NMDA receptors are partly located extrasynaptically and that spillover from overactive synapses might be involved in the activation of these receptors [49–51]. Finally, a deficit in BDNF-mediated signaling may develop in SNc, which in turn might contribute to proapoptotic actions and to nigral dopaminergic neuronal death in this midbrain subregion. This is a proposition we are currently evaluating in our lab.

4.4. Is a Coupling between NR2B-NMDA Receptors and BDNF/TrkB Signaling Involved in the Maintenance of DA Cell Phenotype in SNc after 6-OHDA Intrastriatal Injections? The study we describe here raises the question whether the NMDA receptor-mediated downregulation of trkB receptor in SN after 6-OHDA treatment occurs as part of compensatory events related to the survival and functional integrity of DA cells in SN. The changes reported here on trkB expression occurred mainly in SNc in a cellular localization coincident with that of TH, an important phenotypic marker of DA cells in SN. Therefore, DA cells were functionally deprived as early as 7 days after neurotoxin injection of an important neurotrophin receptor support via a mechanism involving NR2B-NMDA receptor activation. At a later time point (14 days) after 6-OHDA treatment, the number of Nissl-stained and TH-IR cells in SNc started to decrease through a mechanism which also involves NR2B-NMDA receptor, at least in the case of TH-IR. As shown here, most of the TH-IR cells coexist with trkB receptors in SNc, suggesting that an earlier disappearance of this receptor may render these cells more susceptible to 6-OHDA pro-oxidative effects. In view of the previous considerations, it seems no surprising that prior treatments with an NR2B-NMDA receptor antagonist such as Ifenprodil abolishes not only the reduction in the expression of trkB observed in SNc after 6-OHDA treatment but also the change in TH-IR. Both effects would occur most likely in DAergic cells located in this midbrain subregion. It should be mentioned that the existence of a mechanism which is NMDAR-dependent, but trkB-independent, could also account in part for the reduction of TH-IR in SNc after 6-OHDA treatment. However, by means of the present presymptomatic PD model, it was shown that systemic injection of K-252a, an inhibitor of trkB receptors, significantly anticipates the time point at which TH-IR cells start to disappear in rat SNc in response to 6-OHDA striatal injection [52]. In addition, recent observations in experimental models of PD in adult rodents indicate that compounds such as rasagiline and 7, 8-dihydroxyflavone, a trkB agonist, may induce DAergic neuronal protection in SN through trkB receptor activation [53, 54]. All these results support the suggestion that trkB receptors and NR2B-NMDA receptors may be important for the maintenance of the DAergic phenotype during presymptomatic stages of PD. Notwithstanding the previous considerations, further experiments on cell viability in SNc are necessary in this PD model with specific markers of DAergic cells other than TH to strength the proposition that NMDA receptors and BDNF/trkB signaling are necessary to maintain DAergic neuronal survival. In this regard, consistent with this idea it was shown that old mutant mice with haploinsufficiency for trkB showed a greater loss of DAergic neurons when compared to old wild-type animals [17].

5. Conclusions

These results and those previously reported by us [13], conducted in a rat model of PD, suggest that both BDNF and trkB expression and function may be tightly regulated in SN during the presymptomatic stages of PD. Moreover, the results presented here give further support to the idea that a functional coupling between NMDA receptors and BDNF/trkB signaling may be important for the maintenance of the dopaminergic phenotype in SNc during the presymptomatic stages of this neurological disease.

Acknowledgments

The secretarial help of Ms. Lucy Chacoff is greatly appreciated. This work is supported by the Fondo Nacional de Desarrollo Científico y Tecnológico (FONDECYT, Chile), Grant nos. 105–0981 (G. Bustos) and 110–0965 (J. M. Campusano), and Programa CONICYT-CCTE/PFB16 (Chile).

References

[1] H. Bernheimer, W. Birkmayer, and O. Hornykiewicz, "Brain dopamine and the syndromes of Parkinson and Huntington. Clinical, morphological and neurochemical correlations," *Journal of the Neurological Sciences*, vol. 20, no. 4, pp. 415–455, 1973.

[2] E. Bezard, S. Dovero, C. Prunier et al., "Relationship between the appearance of symptoms and the level of nigrostriatal degeneration in a progressive 1-methyl-4-phenyl-1,2,3,6-tetrahydropyridine-lesioned macaque model of Parkinson's disease," *Journal of Neuroscience*, vol. 21, no. 17, pp. 6853–6861, 2001.

[3] D. Kirik, C. Rosenblad, and A. Björklund, "Characterization of behavioral and neurodegenerative changes following partial lesions of the nigrostriatal dopamine system induced by intrastriatal 6-hydroxydopamine in the rat," *Experimental Neurology*, vol. 152, no. 2, pp. 259–277, 1998.

[4] P. K. Morrish, G. V. Sawle, and D. J. Brooks, "Clinical and [(^{18}F)]dopa PET findings in early Parkinson's disease," *Journal of Neurology Neurosurgery and Psychiatry*, vol. 59, no. 6, pp. 597–600, 1995.

[5] A. L. Acheson, M. J. Zigmond, and E. M. Stricker, "Compensatory increase in tyrosine hydroxylase activity in rat brain after intraventricular injections of 6-hydroxydopamine," *Science*, vol. 207, no. 4430, pp. 537–540, 1980.

[6] Y. Agid, F. Javoy, and J. Glowinski, "Hyperactivity of remaining dopaminergic neurones after partial destruction of the nigro striatal dopaminergic system in the rat," *Nature New Biology*, vol. 245, no. 144, pp. 150–151, 1973.

[7] C. A. Altar and M. R. Marien, "Preservation of dopamine release in the denervated striatum," *Neuroscience Letters*, vol. 96, no. 3, pp. 329–334, 1989.

[8] F. Hefti, A. Enz, and E. Melamed, "Partial lesions of the nigrostriatal pathway in the rat. Acceleration of transmitter synthesis and release of surviving dopaminergic neurones by drugs," *Neuropharmacology*, vol. 24, no. 1, pp. 19–23, 1985.

[9] M. J. Zigmond, A. L. Acheson, M. K. Stachowiak, and E. M. Strickerm, "Neurochemical compensation after nigrostriatal bundle injury in an animal model of preclinical Parkinsonism," *Archives of Neurology*, vol. 41, no. 8, pp. 856–861, 1984.

[10] M. J. Zigmond, E. D. Abercrombie, T. W. Berger, A. A. Grace, and E. M. Stricker, "Compensations after lesions of central dopaminergic neurons: some clinical and basic implications," *Trends in Neurosciences*, vol. 13, no. 7, pp. 290–296, 1990.

[11] G. Bustos, J. Abarca, J. Campusano, V. Bustos, V. Noriega, and E. Aliaga, "Functional interactions between somatodendritic dopamine release, glutamate receptors and brain-derived

neurotrophic factor expression in mesencephalic structures of the brain," *Brain Research Reviews*, vol. 47, no. 1-3, pp. 126–144, 2004.

[12] E. Aliaga, C. Cárcamo, J. Abarca, L. Tapia-Arancibia, and G. Bustos, "Transient increase of brain derived neurotrophic factor mRNA expression in substantia nigra reticulata after partial lesion of the nigrostriatal dopaminergic pathway," *Molecular Brain Research*, vol. 79, no. 1-2, pp. 150–155, 2000.

[13] G. Bustos, J. Abarca, V. Bustos et al., "NMDA receptors mediate an early up-regulation of brain-derived neurotrophic factor expression in substantia nigra in a rat model of presymptomatic Parkinson's disease," *Journal of Neuroscience Research*, vol. 87, no. 10, pp. 2308–2318, 2009.

[14] C. A. Altar, C. B. Boylan, M. Fritsche et al., "Efficacy of brain-derived neurotrophic factor and neurotrophin-3 on neurochemical and behavioral deficits associated with partial nigrostriatal dopamine lesions," *Journal of Neurochemistry*, vol. 63, no. 3, pp. 1021–1032, 1994.

[15] C. Hyman, M. Hofer, Y. A. Barde et al., "BDNF is a neurotrophic factor for dopaminergic neurons of the substantia nigra," *Nature*, vol. 350, no. 6315, pp. 230–232, 1991.

[16] T. Tsukahara, M. Takeda, S. Shimohama et al., "Effects of brain-derived neurotrophic factor on 1-methyl-4-phenyl-1,2,3,6-tetrahydropyridine-induced parkinsonism in monkeys," *Neurosurgery*, vol. 37, no. 4, pp. 733–741, 1995.

[17] O. Von Bohlen Und Halbach, L. Minichiello, and K. Unsicker, "Haploin-sufficiency for trkB and trkC receptors induces cell loss and accumulation of α-synuclein in the substantia nigra," *FASEB Journal*, vol. 19, no. 12, pp. 1740–1742, 2005.

[18] M. Levivier, S. Przedborski, C. Bencsics, and U. J. Kang, "Intrastriatal implantation of fibroblasts genetically engineered to produce brain-derived neurotrophic factor prevents degeneration of dopaminergic neurons in a rat model of Parkinson's disease," *Journal of Neuroscience*, vol. 15, no. 12, pp. 7810–7820, 1995.

[19] M. J. Porritt, P. E. Batchelor, and D. W. Howells, "Inhibiting BDNF expression by antisense oligonucleotide infusion causes loss of nigral dopaminergic neurons," *Experimental Neurology*, vol. 192, no. 1, pp. 226–234, 2005.

[20] M. Baydyuk, M. T. Nguyen, and B. Xu, "Chronic deprivation of TrkB signaling leads to selective late-onset nigrostriatal dopaminergic degeneration," *Experimental Neurology*, vol. 228, no. 1, pp. 118–125, 2011.

[21] A. M. Canudas, S. Pezzi, J. M. Canals, M. Pallàs, and J. Alberch, "Endogenous brain-derived neurotrophic factor protects dopaminergic nigral neurons against transneuronal degeneration induced by striatal excitotoxic injury," *Molecular Brain Research*, vol. 134, no. 1, pp. 147–154, 2005.

[22] M. Barbacid, "The Trk family of neurotrophin receptors," *Journal of Neurobiology*, vol. 25, no. 11, pp. 1386–1403, 1994.

[23] G. Dechant, "Molecular interactions between neurotrophin receptors," *Cell and Tissue Research*, vol. 305, no. 2, pp. 229–238, 2001.

[24] B. Lu, P. T. Pang, and N. H. Woo, "The yin and yang of neurotrophin action," *Nature Reviews Neuroscience*, vol. 6, no. 8, pp. 603–614, 2005.

[25] D. W. Howells, M. J. Porritt, J. Y. F. Wong et al., "Reduced BDNF mRNA expression in the Parkinson's disease substantia nigra," *Experimental Neurology*, vol. 166, no. 1, pp. 127–135, 2000.

[26] T. Nishio, S. Furukawa, I. Akiguchi, and N. Sunohara, "Medial nigral dopamine neurons have rich neurotrophin support in humans," *NeuroReport*, vol. 9, no. 12, pp. 2847–2851, 1998.

[27] S. Numan and K. Seroogy, "Expression of trkB and trkC mRNAs by adult midbrain dopamine neurons: a double-label in situ hybridization study," *The Journal of Comparative Neurology*, vol. 403, pp. 295–308, 1999.

[28] K. B. Seroogy, K. H. Lundgren, T. M. D. Tran, K. M. Guthrie, P. J. Isackson, and C. M. Gall, "Dopaminergic neurons in rat ventral midbrain express brain-derived neurotrophic factor and neurotrophin-3 mRNAs," *Journal of Comparative Neurology*, vol. 342, no. 3, pp. 321–334, 1994.

[29] E. Riquelme, J. Abarca, and G. Bustos, "Ifenprodil, antagonist of NMDA-NR2B type glutamate receptors, blocks both the decrease in trkB expression and the disappearance of dopaminergic cells in SNc in a rat model of presymptomatic Parkinson's disease," in *Proceedings of the 18th Meeting of the Latinoamerican Society of Pharmacology*, vol. 1, p. 123, Coquimbo, Chile, 2008.

[30] G. Paxinos and C. Watson, *The Rat Brain in Stereotaxic Coordinates*, Acadenic Press, New York, NY, USA, 1986.

[31] M. E. Andres, K. Gysling, S. Aravena, A. Venegas, and G. Bustos, "NMDA-NR1 receptor subunit mRNA expression in rat brain after 6-OH-dopamine induced lesions: a non-isotopic in situ hybridization study," *Journal of Neuroscience Research*, vol. 46, pp. 375–384, 1996.

[32] C. Marin, M. C. Rodriguez-Oroz, and J. A. Obeso, "Motor complications in Parkinson's disease and the clinical significance of rotational behavior in the rat: have we wasted our time?" *Experimental Neurology*, vol. 197, no. 2, pp. 269–274, 2006.

[33] W. Dauer and S. Przedborski, "Parkinson's disease: mechanisms and models," *Neuron*, vol. 39, no. 6, pp. 889–909, 2003.

[34] H. Sauer and W. H. Oertel, "Progressive degeneration of nigrostriatal dopamine neurons following intrastriatal terminal lesions with 6-hydroxydopamine: a combined retrograde tracing and immunocytochemical study in the rat," *Neuroscience*, vol. 59, no. 2, pp. 401–415, 1994.

[35] S. Shimohama, H. Sawada, Y. Kitamura, and T. Taniguchi, "Disease model: Parkinson's disease," *Trends in Molecular Medicine*, vol. 9, no. 8, pp. 360–365, 2003.

[36] Q. Yan, M. Radeke, C. Matheson, J. Talvenheimo, A. Welcher, and S. Feinstein, "Immunocytochemical localization of trkB in the central nervous system of the adult rat," *The Journal of Comparative Neurology*, vol. 378, pp. 135–157, 1997.

[37] X. F. Zhou, L. F. Parada, D. Soppet, and R. A. Rush, "Distribution of trkB tyrosine kinase immunoreactivity in the rat central nervous system," *Brain Research*, vol. 622, no. 1-2, pp. 63–70, 1993.

[38] M. Arundine and M. Tymianski, "Molecular mechanisms of calcium-dependent neurodegeneration in excitotoxicity," *Cell Calcium*, vol. 34, no. 4-5, pp. 325–337, 2003.

[39] S. J. Kish, K. Shannak, and O. Hornykiewicz, "Uneven pattern of dopamine loss in the striatum of patients with idiopathic Parkinson's disease. Pathophysiologic and clinical implications," *New England Journal of Medicine*, vol. 318, no. 14, pp. 876–880, 1988.

[40] Y. Ichitani, H. Okamura, D. Nakahara, I. Nagatsu, and Y. Ibata, "Biochemical and immunocytochemical changes induced by intrastriatal 6-hydroxydopamine injection in the rat nigrostriatal dopamine neuron system: evidence for cell death in the substantia nigra," *Experimental Neurology*, vol. 130, no. 2, pp. 269–278, 1994.

[41] S. Przedborski, M. Levivier, H. Jiang et al., "Dose-dependent lesions of the dopaminergic nigrostriatal pathway induced by intrastriatal injection of 6-hydroxydopamine," *Neuroscience*, vol. 67, no. 3, pp. 631–647, 1995.

[42] D. C. German and K. F. Manaye, "Midbrain dopaminergic neurons (nuclei A8, A9, and A10): three-dimensional reconstruction in the rat," *Journal of Comparative Neurology*, vol. 331, no. 3, pp. 297–309, 1993.

[43] E. Riquelme, *Expresion en substantia nigra mesencefalica de trkB, receptor de BDNF, y su regulacion por receptores de glutamato tipo NMDA, frente a un daño progresivo de la via dopaminergica nigroestriatal. Posibles implicancias en relacion a la fase premotora y/o presintomatica de la enfermedad de Parkinson*, Ph.D. thesis, Facultad de Ciencias Biologicas, Pontificia Universidad Catolica de Chile, Santiago, Chile, 2011.

[44] L. Frank, "BDNF down-regulates neurotrophin responsiveness, TrkB protein and TrkB mRNA levels in cultured rat hippocampal neurons," *European Journal of Neuroscience*, vol. 8, no. 6, pp. 1220–1230, 1996.

[45] M. T. Sommerfeld, R. Schweigreiter, Y. A. Barde, and E. Hoppe, "Down-regulation of the neurotrophin receptor TrkB following ligand binding. Evidence for an involvement of the proteasome and differential regulation of TrkA and TrkB," *Journal of Biological Chemistry*, vol. 275, no. 12, pp. 8982–8990, 2000.

[46] F. Gardoni, B. Picconi, V. Ghiglieri et al., "A critical interaction between NR2B and MAGUK in L-DOPA induced dyskinesia," *Journal of Neuroscience*, vol. 26, no. 11, pp. 2914–2922, 2006.

[47] F. Blandini, G. Nappi, C. Tassorelli, and E. Martignoni, "Functional changes of the basal ganglia circuitry in Parkinson's disease," *Progress in Neurobiology*, vol. 62, no. 1, pp. 63–88, 2000.

[48] T. J. Kingsbury, P. D. Murray, L. L. Bambrick, and B. K. Krueger, "Ca^{2+}-dependent regulation of TrkB expression in neurons," *Journal of Biological Chemistry*, vol. 278, no. 42, pp. 40744–40748, 2003.

[49] K. R. Gogas, "Glutamate-based therapeutic approaches: NR2B receptor antagonists," *Current Opinion in Pharmacology*, vol. 6, no. 1, pp. 68–74, 2006.

[50] G. E. Hardingham and H. Bading, "Synaptic versus extrasynaptic NMDA receptor signalling: implications for neurodegenerative disorders," *Nature Reviews Neuroscience*, vol. 11, no. 10, pp. 682–696, 2010.

[51] J. M. Loftis and A. Janowsky, "The N-methyl-D-aspartate receptor subunit NR2B: localization, functional properties, regulation, and clinical implications," *Pharmacology and Therapeutics*, vol. 97, no. 1, pp. 55–85, 2003.

[52] C. Leon-Perez, "Efecto de K252A, antagonista del receptor del factor neurotrofico derivado de cerebro (BDNF), sobre la liberacion de glutamato, aspartato, acido gama aminobutırico y dopamina, en cuerpo estriado y substantia nigra de rata: estudios in vivo mediante la tecnica de microdıalisis," Memoria de Investigacion para optar al tıtulo de Bioquımico, Facultad de Ciencias Biologicas, Pontificia Universidad Catolica de Chile, Santiago, Chile, 2006.

[53] S. W. Jang, X. Liu, M. Yepes et al., "A selective TrkB agonist with potent neurotrophic activities by 7,8-dihydroxyflavone," *Proceedings of the National Academy of Sciences of the United States of America*, vol. 107, no. 6, pp. 2687–2692, 2010.

[54] S. A. Mandel, Y. Sagi, and T. Amit, "Rasagiline promotes regeneration of substantia nigra dopaminergic neurons in post-MPTP-induced parkinsonism via activation of tyrosine kinase receptor signaling pathway," *Neurochemical Research*, vol. 32, no. 10, pp. 1694–1699, 2007.

Hindawi Publishing Corporation
Parkinson's Disease
Volume 2012, Article ID 296875, 9 pages
doi:10.1155/2012/296875

Research Article

Patterns of Cell Activity in the Subthalamic Region Associated with the Neuroprotective Action of Near-Infrared Light Treatment in MPTP-Treated Mice

Victoria E. Shaw,[1] Cassandra Peoples,[1] Sharon Spana,[1] Keyoumars Ashkan,[2] Alim-Louis Benabid,[3] Jonathan Stone,[4] Gary E. Baker,[5] and John Mitrofanis[1]

[1] *Discipline of Anatomy and Histology, The University of Sydney, Sydney, NSW 2006, Australia*
[2] *Deptartment of Neurosurgery, King's College Hospital, London SE59RS, UK*
[3] *Clinatec LETI-DTBS, CEA, 38054 Grenoble, France*
[4] *Discipline of Physiology, The University of Sydney, Sydney, NSW 2006, Australia*
[5] *Deptartment of Optometry and Visual Science, City University London, London EC1VOHB, UK*

Correspondence should be addressed to John Mitrofanis, john.mitrofanis@sydney.edu.au

Received 1 January 2012; Revised 4 March 2012; Accepted 8 March 2012

Academic Editor: Yuzuru Imai

We have shown previously that near-infrared light (NIr) treatment or photobiomodulation neuroprotects dopaminergic cells in substantia nigra pars compacta (SNc) from degeneration induced by 1-methyl-4-phenyl-1,2,3,6-tetrahydropyridine (MPTP) in mice. The present study explores whether NIr treatment changes the patterns of Fos expression in the subthalamic region, namely, the subthalamic nucleus (STN) and zona incerta (ZI); both cell groups have abnormally overactive cells in parkinsonian cases. BALB/c mice were treated with MPTP (100–250 mg/kg) or saline either over 30 hours followed by either a two-hour or six-day survival period (acute model) or over five weeks followed by a three-week survival period (chronic model). NIr and MPTP were applied simultaneously. Brains were processed for Fos immunochemistry, and cell number was estimated using stereology. Our major finding was that NIr treatment reduced (30–45%) the increase in Fos^+ cell number evident in the STN and ZI after MPTP insult. This reduction was concurrent with the neuroprotection of dopaminergic SNc cells shown previously and was evident in both MPTP models (except for the 2 hours survival period which showed no changes in cell number). In summary, our results indicated that NIr had long lasting effects on the activity of cells located deep in the brain and had repaired partially the abnormal activity generated by the parkinsonian toxin.

1. Introduction

Exposure to near-infrared light treatment (NIr), also referred to as photobiomodulation, has been shown to protect dopaminergic cells from degeneration induced by 1-methyl-4-phenyl-1,2,3,6-tetrahydropyridine (MPTP) in both *in vitro* [2, 3] and *in vivo* (within substantia nigra pars compacta; SNc) [4, 5] studies. This neuroprotection is presumably due to the NIr limiting the mitochondrial dysfunction and subsequent oxidative stress and free-radical production caused by the MPTP, which induces Parkinson-like pathology [4, 6]. NIr has been shown to improve mitochondrial function and ATP (adenosine-5′-triphosphate) production by increasing the electron transfer in the respiratory chain and activation of photoacceptors, such as cytochrome oxidase [7, 8]. Although these results are from *in vitro* studies [2, 3] and from an animal model of the disease [4, 5], the outcome is potentially exciting; that a noninvasive procedure offers neuroprotection in Parkinson's disease, a feature that most current forms of treatment, including dopamine-replacement drug therapy, does not do [9].

In this study, we have sought to extend our earlier anatomical findings [4, 5] by examining patterns of cell activation associated with the neuroprotective action of NIr in parkinsonian cases. To this end, we examined cell activity

in the subthalamic region, namely, the subthalamic nucleus (STN) and the zona incerta (ZI). We chose this region for two main reasons (i) STN and ZI cells have abnormal overactivity in parkinsonian cases [10–13] and (ii) both cell groups have become a popular targets for surgical intervention, particularly with deep brain stimulation [14–16]. It is well accepted that an increase in Fos expression, after activation of the cFos gene, reflects an increase in cell activity. This method has been used to study global cell activity patterns in many brain regions after various forms of stimulation and disease states, including parkinsonism [17, 18]. In essence, we tested whether NIr treatment was able to influence the activity of cells located deep in the brain and reverse the abnormal activity induced by the parkinsonian insult.

2. Materials and Methods

2.1. Subjects. Male albino BALB/c mice (~20 g; ~8-week old; $n = 96$) were housed on a 12 hours light/dark cycle with unlimited access to food and water. All experiments were approved by the Animal Ethics Committee of The University of Sydney.

2.2. Experimental Design. An acute [4, 19] and a chronic [5] MPTP model were used in this study. There were four experimental groups in each model, where mice received intraperitoneal injections of either MPTP or saline, combined with simultaneous NIr treatments or not. The different groups were (1) *saline* ($n = 24$): saline injections with no NIr, (2) *saline-NIr* ($n = 24$): saline injections with NIr, (3) *MPTP* ($n = 24$): MPTP injections with no NIr, and (4) *MPTP-NIr* ($n = 24$): MPTP injections with NIr.

For the acute model, four (25 mg/kg injections; total of 100 mg/kg per mouse) MPTP or saline injections were made over a 30-hour period. After the last injection, mice were allowed to survive for either two hours ($n = 32$) or six days ($n = 32$). For the chronic model ($n = 32$), mice had ten injections of MPTP (20 mg/kg per injection; total of 200 mg/kg per mouse) or saline combined with probenecid (250 mg/kg; decreases renal excretion of MPTP and hence maintains the effects of toxin during injection intervals) approximately three and a half days apart, over a five-week period. After the last injection, mice were allowed to survive for three weeks. For both models, the dose regimes and survival periods were the same as those used by previous studies [4, 5, 19]. The survival periods were selected as to determine whether there were any immediate or longer lasting changes in Fos expression after MPTP (or NIr) treatment.

For the NIr treatment, mice in the MPTP-NIr and saline-NIr groups of each model (acute and chronic) were treated with 670 nm light from a light-emitting device (LED; Quantum Devices WARP 10) as described previously [4, 5]. Briefly, mice had NIr treatment (one cycle of 90 seconds; estimated at 0.5 Joule/cm^2 to the brain [4]) for ~15 minutes after each MPTP or saline injection. Hence, for each MPTP insult there would be almost immediate potential therapeutic application. For both models, these NIr treatment regimes were similar to that used by previous studies, in particular, those reporting changes after transcranial irradiation [4, 5, 20, 21]. For each exposure to NIr, the mouse was restrained gently by hand, and the LED was held 1-2 cm above the head [4, 5]. The mice tended to relax during exposure, and reliable delivery of the radiation was achieved readily. The LED generated very little heat and it did not cause the mice any visible discomfort. For the saline and MPTP groups, mice were held under the LED as described above for 90 seconds, but the device was not turned on [4, 5].

Our experimental paradigm, of essentially simultaneous administration of parkinsonian insult and therapeutic application, was similar to that of many previous studies on animal models of Parkinsons disease [4, 5, 19, 22]. This paradigm is unlike the clinical reality where considerable dopaminergic cell loss occurs prior to therapeutic intervention. However, in our experimental study—as with the abovementioned previous ones—we hoped to explore the maximum effect of NIr treatment on the number of dopaminergic cells and hence determine more systematically its effects on functional activity (i.e., Fos expression).

2.3. Immunocytochemistry. Following the survival periods, mice were anaesthetised with an intraperitoneal injection of sodium pentobarbital (60 mg/mL). They were then perfused transcardially with 0.1 M phosphate-buffered saline (PBS; pH 7.4), followed by 4% buffered formaldehyde. The brains were removed and postfixed overnight in the same solution. Next, brains were placed in PBS with the addition of 30% sucrose until the block sank. The forebrain was then sectioned coronally and serially using a freezing microtome. All sections were collected in PBS and then immersed in a solution of 1% Triton (Sigma) and 10% normal goat serum (Sigma) at room temperature for 30 minutes each. Sections were then incubated in anti-cFos (SantaCruz; 1 : 4000) for 48 hours (at 4°C), followed by biotinylated anti-rabbit IgG (Bioscientific; 1 : 200) for three hours (at room temperature), and then streptavidin-peroxidase complex (Bioscientific; 1 : 200) for two hours (at room temperature). To visualise the bound antibody, sections were reacted in nickel-Tris-buffered saline (pH 7.4)-3,3′-diaminobenzidine tetrahydrochloride (Sigma) solution. In between incubations, sections were washed in three changes of PBS. Sections were mounted onto gelatinised slides, air dried overnight, dehydrated in ascending alcohols, cleared in Histoclear, and coverslipped using DPX. Most of our immunostained sections were counterstained lightly with neutral red as well. For controls, sections were processed as described above, except that there was no primary antibody used. These control sections were immunonegative.

2.4. Analysis. Following the procedures outlined by previous studies [4, 5, 19], the number of Fos$^+$ cells within the STN and ZI were estimated using the optical fractionator method (StereoInvestigator, MBF Science). Briefly, systematic random sampling of sites within defined boundaries of the STN and ZI was undertaken. All cells that came into focus within the frame were counted.

Figures 4(e) and 5(e) show schematic diagrams of the mouse brain, and the shaded areas indicate the general regions that were analysed. The distribution maps of Fos^+ cells (Figures 4(a)–4(d), 5(a)–5(d)) were constructed using the StereoInvestigator programme also. For comparisons between groups within each model (six-day survival and two-hour survival acute model and chronic model), a one-way ANOVA test (F and P values) was performed, in conjunction with a Tukey-Kramer multiple comparison test (q and P values) (using GraphPad Prism programme). Schematic diagrams and digital images were constructed using Adobe Photoshop and Microsoft PowerPoint programmes.

3. Results

In what follows, the morphology, number, and distribution of Fos^+ cells in the STN and ZI will be considered separately.

3.1. Morphology. In both the STN and ZI, Fos immunoreactivity was limited to the nuclei of cells (Figure 1). The intensity of immunoreactivity was not consistent across both cell groups; cells were immunostained either strongly (arrows, Figure 1) or weakly (arrowheads, Figure 1). These patterns were evident across the STN (Figures 1(a) and 1(b)) and in each of the different sectors of the ZI, namely, rostral (Figure 1(c)), dorsal (Figure 1(d)), ventral (Figure 1(e)), and caudal (Figure 1(f)) and were similar in all the experimental groups of both acute and chronic MPTP models.

3.2. Number. In this study, we counted the number of Fos^+ cells in the STN and ZI that were immunostained strongly (see above), presumably because they had undergone the most activation [17, 23]. The number of cells in the STN and ZI in the acute and chronic MPTP models will be considered separately below.

3.2.1. Subthalamic Nucleus (STN). The graph in Figure 2(b) shows the estimated number of Fos^+ cells in the STN of the four experimental groups in the acute MPTP model. In the two-hour survival period, there were 50–60% more Fos^+ cells in the saline-NIr, MPTP, and MPTP-NIr groups than in the saline group. Overall, using an ANOVA test, these differences were significant ($F = 6.2$; $P < 0.001$). Using the Tukey-Kramer test, significant differences in total number were found between the saline group and the saline-NIr ($q = 4.0$; $P < 0.05$), MPTP ($q = 4.1$; $P < 0.05$), and MPTP-NIr ($q = 5.9$; $P < 0.01$) groups. There were no significant differences between the saline-NIr group and the MPTP ($q = 0.1$; $P > 0.05$) or MPTP-NIr ($q = 1.9$; $P > 0.05$) groups, nor between the MPTP and MPTP-NIr groups ($q = 1.8$; $P > 0.05$). In the six-day survival period, the MPTP group had more Fos^+ cells than the MPTP-NIr (40%), saline-NIr (80%), and saline (85%) groups. Of particular relevance was that the MPTP-NIr group had fewer Fos^+ cells than the MPTP group, indicating that NIr treatment had reduced the Fos expression induced by the MPTP insult. Further, the MPTP-NIr group had more Fos^+ cells than the saline groups (65–75%), indicating that although there was a reduction in number from the MPTP insult, it did not quite reach control levels. Overall, these differences between the groups were significant using an ANOVA test ($F = 65.7$; $P < 0.0001$). Using the Tukey-Kramer test, significant differences in total number were found between the MPTP group and saline ($q = 17.6$; $P < 0.001$), saline-NIr ($q = 16.0$; $P < 0.001$), and, notably, MPTP-NIr ($q = 8.1$; $P < 0.001$) groups. There were also significant differences between the MPTP-NIr group and saline ($q = 9.5$; $P < 0.001$) and saline-NIr ($q = 7.9$; $P < 0.001$) groups. The differences in total number between the saline and saline-NIr groups were not significant ($q = 1.6$; $P > 0.05$).

The graph in Figure 2(b) shows the estimated number of Fos^+ cells in the STN of the four groups in the chronic MPTP model. The patterns of Fos^+ cell number shown for this model were similar to those described above for the six-day survival acute model. The MPTP group had more Fos^+ cells than the MPTP-NIr (45%), saline-NIr (75%), and saline (75%) groups. The MPTP-NIr group had fewer Fos^+ cells than the MPTP group but many more cells than in the saline groups (55%). Overall, these differences between the groups were significant using an ANOVA test ($F = 34.2$; $P < 0.0001$). Using the Tukey-Kramer test, significant differences in total number were found between the MPTP group and saline ($q = 12.4$; $P < 0.001$), saline-NIr ($q = 12.3$; $P < 0.001$), and MPTP-NIr ($q = 7.1$; $P < 0.001$) groups. There were also significant differences between the MPTP-NIr group and the saline ($q = 5.4$; $P < 0.01$) and saline-NIr ($q = 5.2$; $P < 0.01$) groups. The differences in total number between the saline and saline-NIr groups were not significant ($q = 0.2$; $P > 0.05$).

It should be noted that the number of tyrosine hydroxylase $(TH)^+$ cells in the substantia nigra pars compacta (SNc), from the same brains from as those used here for Fos immunocytochemistry, have been analysed also, and full details of the results have been published [4, 5]. Briefly, these studies showed substantial TH^+ cell loss in the SNc in both acute (~60%, six-day survival; no change in TH^+ cell number in two-hour survival period) and chronic (~45%) MPTP models. In addition, there was also fewer TH^+ terminals in the striatum, the major termination zone of the SNc axons, of the MPTP groups compared to the others. Finally, the MPTP-NIr groups of both models had more TH^+ cells than in the MPTP group (30–35%) but not quite as many as in the saline control groups (25–30%).

3.2.2. Zona Incerta (ZI). The graph in Figure 3(a) shows the estimated number of Fos^+ cells in the ZI of the four experimental groups in the acute MPTP model. In the two-hour survival period, there were no significant differences between the number of Fos^+ cells in the different groups using an ANOVA test ($F = 2.4$; $P > 0.05$). Using the Tukey-Kramer test, no significant differences in total number were found between the saline group and saline-NIr ($q = 3.4$; $P > 0.05$), MPTP ($q = 2.6$; $P > 0.05$), and MPTP-NIr ($q = 3.0$; $P > 0.05$) groups, between the saline-NIr group and MPTP ($q = 0.9$; $P > 0.05$), and MPTP-NIr ($q = 0.5$; $P > 0.05$) groups, nor between the MPTP and MPTP-NIr groups ($q = 0.4$; $P > 0.05$). In the six-day survival period, the MPTP

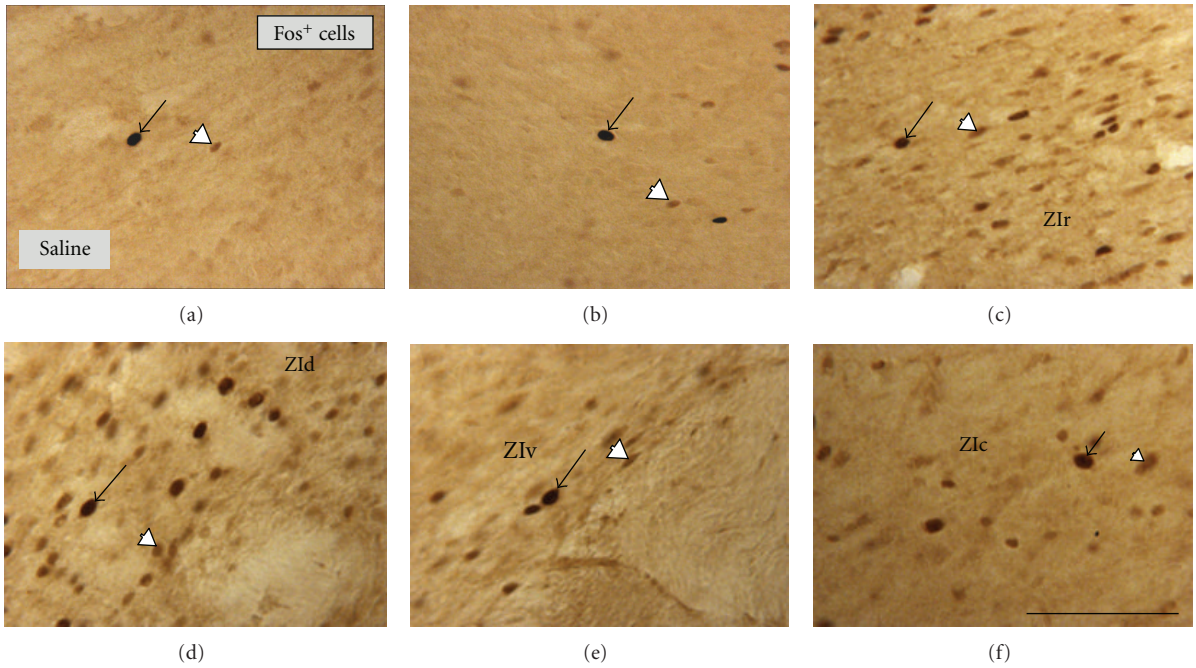

Figure 1: Fos$^+$ cells in the STN (central region) and in the different sectors of the ZI, namely, ZIr (a), ZId (b), ZIv (c), and ZIc (d). Fos immunoreactivity was apparent in cell nuclei; cells were either strongly (black arrows) or weakly immunostained (white arrowheads). All cases are from the saline group; patterns of immunostaining were similar in the other groups of both acute and chronic models. All figures are of coronal sections; dorsal to top and lateral to right. Scale bar = 100 μm.

group had many more Fos$^+$ cells than the MPTP-NIr (35%), saline-NIr (55%), and saline (75%) groups. Of particular relevance was that the MPTP-NIr group had fewer Fos$^+$ cells than the MPTP group but more than the saline (65%) and saline-NIr (35%) groups. Overall, these differences between the groups were significant using an ANOVA test ($F = 43.3$; $P < 0.0001$). Using the Tukey-Kramer test, significant differences in total number were found between the MPTP group and saline ($q = 15.4$; $P < 0.001$), saline-NIr ($q = 11.2$; $P < 0.001$), and, notably, MPTP-NIr ($q = 6.8$; $P < 0.001$) groups. There were also significant differences between the saline group and the saline-NIr ($q = 4.2$; $P < 0.05$) and MPTP-NIr ($q = 8.6$; $P < 0.001$) groups and between the MPTP-NIr and Saline-NIr groups ($q = 4.5$; $P < 0.05$).

The graph in Figure 3(b) shows the estimated number of Fos$^+$ cells in the ZI of the four groups in the chronic MPTP model. The patterns of Fos$^+$ cell number shown for this model were similar to those described above for the six-day survival acute model. The MPTP group had more Fos$^+$ cells than the MPTP-NIr (30%), saline-NIr (60%), and saline (80%) groups. The MPTP-NIr group had fewer Fos$^+$ cells than the MPTP group but many more cells than the saline (70%) and saline-NIr (45%) groups. Overall, these differences between the groups were significant using an ANOVA test ($F = 66.8$; $P < 0.0001$). Using the Tukey-Kramer test, significant differences in total number were found between the MPTP group and saline ($q = 18.5$; $P < 0.001$), saline-NIr ($q = 14.4$; $P < 0.001$), and MPTP-NIr ($q = 7.0$; $P < 0.001$) groups. There were also significant differences between the MPTP-NIr group and the saline ($q = 11.5$; $P < 0.001$) and saline-NIr ($q = 7.4$; $P < 0.001$) groups and between the saline and saline-NIr groups ($q = 4.1$; $P < 0.05$).

In summary, MPTP insult generated a substantial increase in the number of Fos$^+$ cells in both the STN and ZI, and NIr treatment reduced this increase significantly. These changes were concurrent with changes in TH$^+$ cell number in the SNc in the acute model with six-day survival period and chronic model [4, 5]. Unlike in the STN, there was a significant increase in the number of Fos$^+$ cells in the ZI after NIr treatment alone.

4. Distribution

4.1. Subthalamic Nucleus (STN). Figure 4 shows schematic diagrams of the distribution of Fos$^+$ cells in the STN in the acute MPTP model with six-day survival period (distributions were similar in the chronic model; in the two-hour survival period, the distributions in all the groups were similar to the saline group). In all groups, Fos$^+$ cells tended to be scattered across the nucleus, with no clear zone of concentration. There were more Fos$^+$ cells evident in the MPTP-NIr and, in particular, the MPTP group than in the saline controls (see above).

4.2. Zona Incerta (ZI). Figure 5 shows schematic diagrams of the distribution of Fos$^+$ cells in the ZI and its sectors (rostral, dorsal, ventral, and caudal) of the different groups in the acute MPTP model with six-day survival period (as with STN, distributions were similar in other models). In the

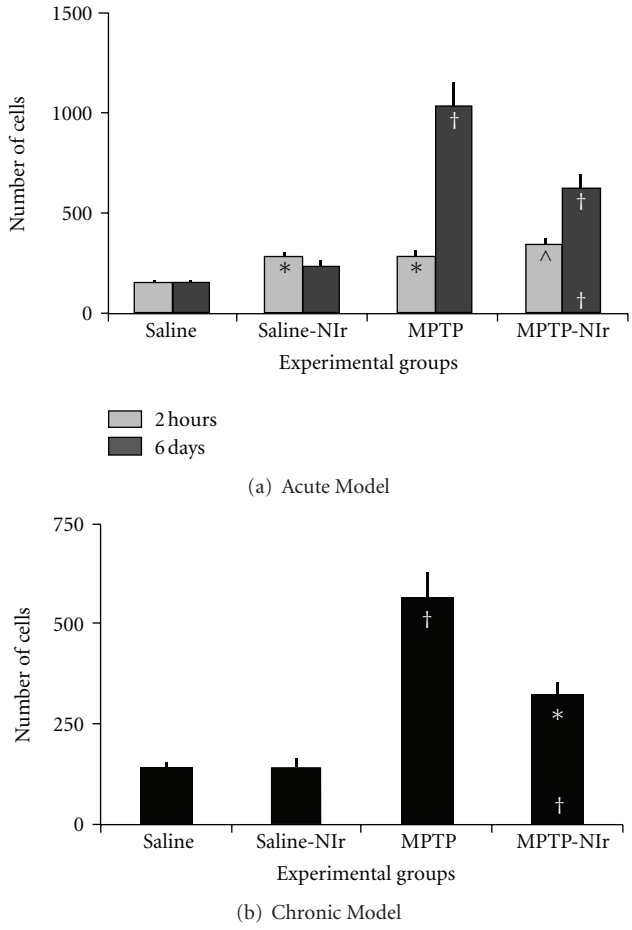

Figure 2: Graphs showing number of Fos$^+$ cells in the STN of the four groups in the acute (a) and chronic (b) MPTP mouse models. Columns show the mean ± standard error of the total number of cells in each group. In (a) and (b), † represents $P < 0.001$ and ^ represent $P < 0.01$ significant difference in cell number between different groups (using Tukey-Kramer multiple comparison test). The symbols at the top of each column represents differences with the saline group, while the symbols at the bottom of MPTP-NIr group column represent differences with the MPTP group.

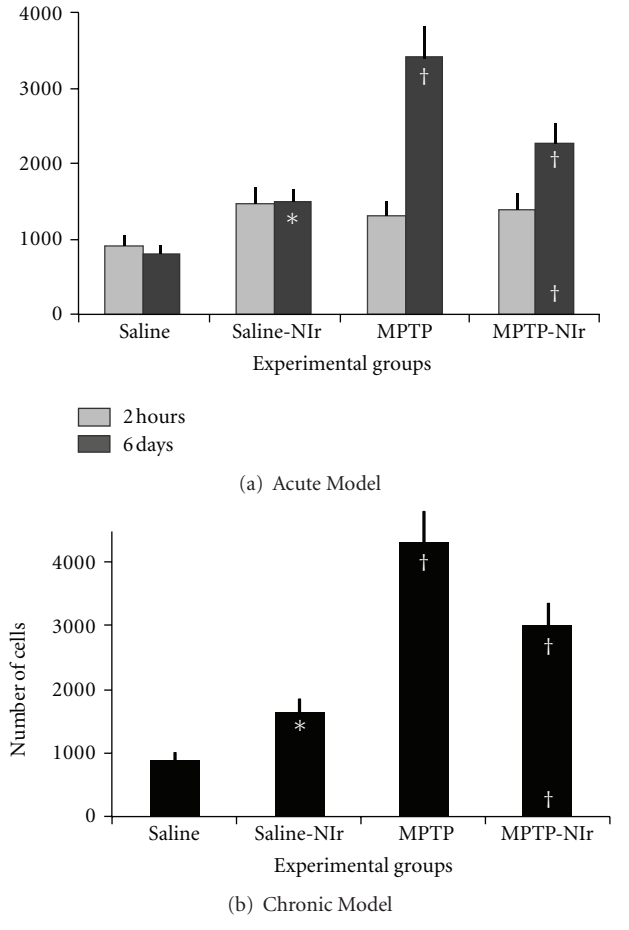

Figure 3: Graphs showing number of Fos$^+$ cells in the ZI of the four groups in the acute (a) and chronic (b) MPTP mouse models. Columns show the mean ± standard error of the total number of cells in each group. In (a) and (b), † represents $P < 0.001$ and ^ represent $P < 0.01$ significant difference in cell number between different groups (using Tukey-Kramer multiple comparison test). The symbols at the top of each column represents differences with the saline group, while the symbols at the bottom of MPTP-NIr group column represent differences with the MPTP group.

saline group, Fos$^+$ cells were scattered sparsely across each incertal sectors but with a tendency to concentrate in the dorsal sector (Figure 5(a)). In the saline-NIr (Figure 5(b)), MPTP (Figure 5(c)), and MPTP-NIr (Figure 5(d)) groups, Fos$^+$ cells were also found somewhat scattered, albeit in higher numbers, across each of the sectors. In these groups, the same concentration in the dorsal sector was evident.

In summary, the Fos$^+$ cells in the STN showed no clear pattern of topography across the nucleus, while in the ZI, most cells were located in the dorsal sector.

5. Discussion

We had three main findings. First, unlike the STN, there were many ZI cells that expressed the Fos protein after NIr treatment. Second, in both the STN and ZI, MPTP insult generated a substantial increase in the number of Fos$^+$ cells. Finally, and most notably, NIr treatment reduced this increase in STN and ZI Fos$^+$ cell number after MPTP insult; this reduction was concurrent with the neuroprotection of TH$^+$ cells in the SNc. These differences in Fos$^+$ cell number were evident in the longer-term survival periods (six days to three weeks) of acute and chronic models, indicating that NIr (and MPTP) treatment had long lasting effects on neuronal function. Each of these issues will be explored below. First, a comparison with previous studies will be considered.

5.1. Comparison with Previous Studies. To the best of our knowledge, there has been no other study that has examined Fos expression in the STN and ZI, nor indeed the brain, after NIr treatment. Several previous studies, using different methods and animal models of Parkinson's disease, have reported on the patterns of cell activity in the STN and ZI. These studies have used either metabolic markers and/or

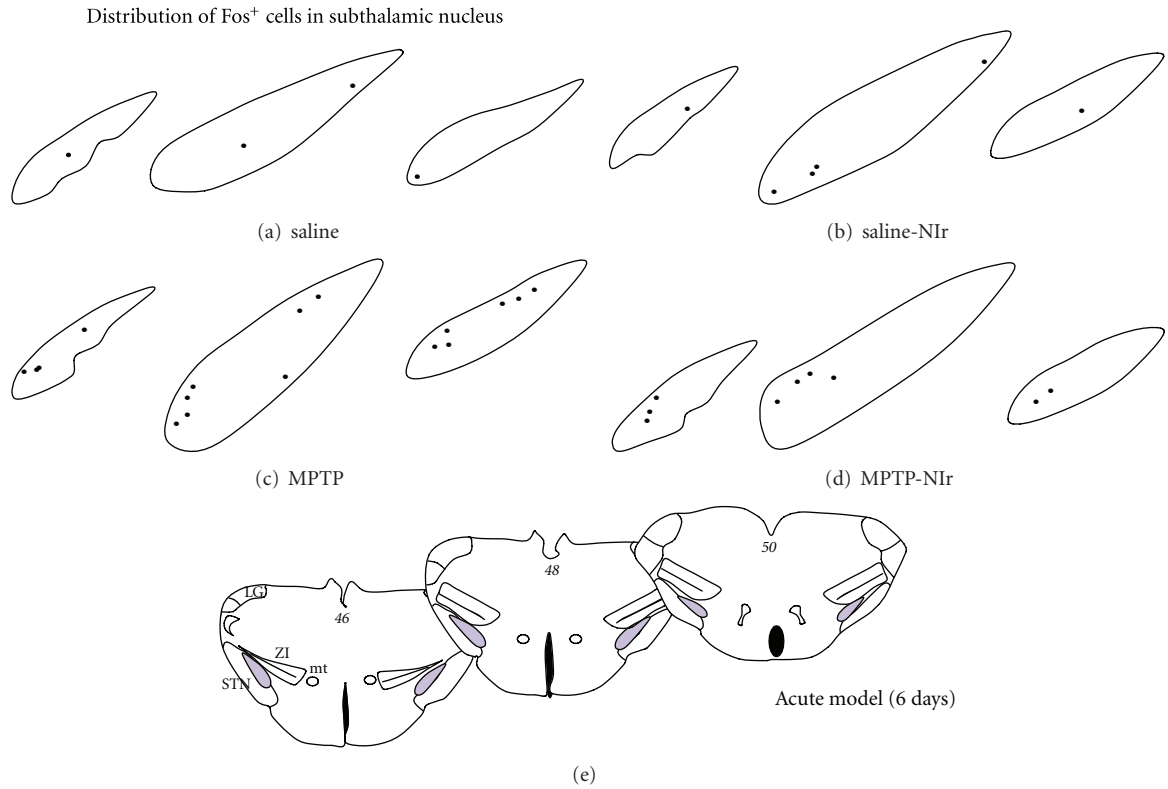

Figure 4: Schematic diagrams of the distribution of Fos+ cells in the different sectors of the STN in the saline (a), saline-NIr (b), MPTP (c) and MPTP-NIr groups. These maps are from the acute model with six-day survival period (similar patterns were evident in the chronic model; in the acute model with two-hour survival period, the distribution of cells was similar to the saline cases shown here). Each black circle represents one cell. These maps were taken from coronal sections similar to the plates of the mouse atlas (numbers in italics [1]) shown in (e).

electrophysiological methods in 6-OHDA-lesioned rats [10, 11, 13] or MPTP-treated monkeys [12]. We confirm these previous reports of an increase in cell activity in STN and ZI by using Fos immunocytochemistry in MPTP-treated mice. It should be noted that somewhat different results have been reported in 6-OHDA-lesioned rats using Fos immunocytochemistry in these nuclei. In these studies, very few Fos+ cells were seen in the STN [24] or ZI [25] after 6-OHDA lesion. The reason for this difference in our studies is not entirely clear, but it may be related to the different animals used (6-OHDA versus MPTP)—and there have been many reports of dissimilar results using the different models [26]—together with the location of the 6-OHDA injection site. In the previous studies, 6-OHDA was injected into the medial forebrain bundle which lies immediately adjacent to the STN and ZI. There could have been some spread of the 6-OHDA toxin from the injection site into the adjacent STN and ZI, and this may have influenced the expression of Fos in these cases. Indeed, in cases where 6ODHA was injected directly into the SNc, a region well away from the STN and ZI, an increase in cellular STN and ZI activity was apparent [10–13]. Perhaps 6-OHDA injections into the SNc or striatum, regions well away from the STN and ZI, may generate results similar to ours seen here in MPTP-treated mice.

5.2. NIr Treatment Induced Fos Expression in Zona Incerta. One of our most striking, and least expected, findings was of an increase in Fos expression within the ZI but not the STN after the application of NIr treatment alone. Two mechanisms for this increase in expression can be suggested. First, NIr could have activated an excitatory afferent pathway, one that terminates in the ZI and not the STN, triggering Fos expression. Such a pathway was likely to originate from the superior colliculus, which has a very heavy projection to the ZI (in particular to its dorsal sector), but not the STN [27–29]. The superior colliculus receives a large and direct input from the retina, whose cells may have been activated directly by NIr. Further, the retina has a direct, albeit very small, input to the ZI but not to the STN [27, 29]. This small input, through an extensive network of inter-ZI connections [29], may have contributed to the Fos expression in the ZI as well. Second, NIr could have activated directly the mitochondria within the ZI cells themselves, inducing Fos expression. The ZI cells may have been more susceptible to photoacceptor (cytochrome oxidase) activation than the cells in the STN. It remains to be determined which other cell groups in the central nervous system are activated by NIr treatment alone, and how they may relate to the activated ZI cells described here.

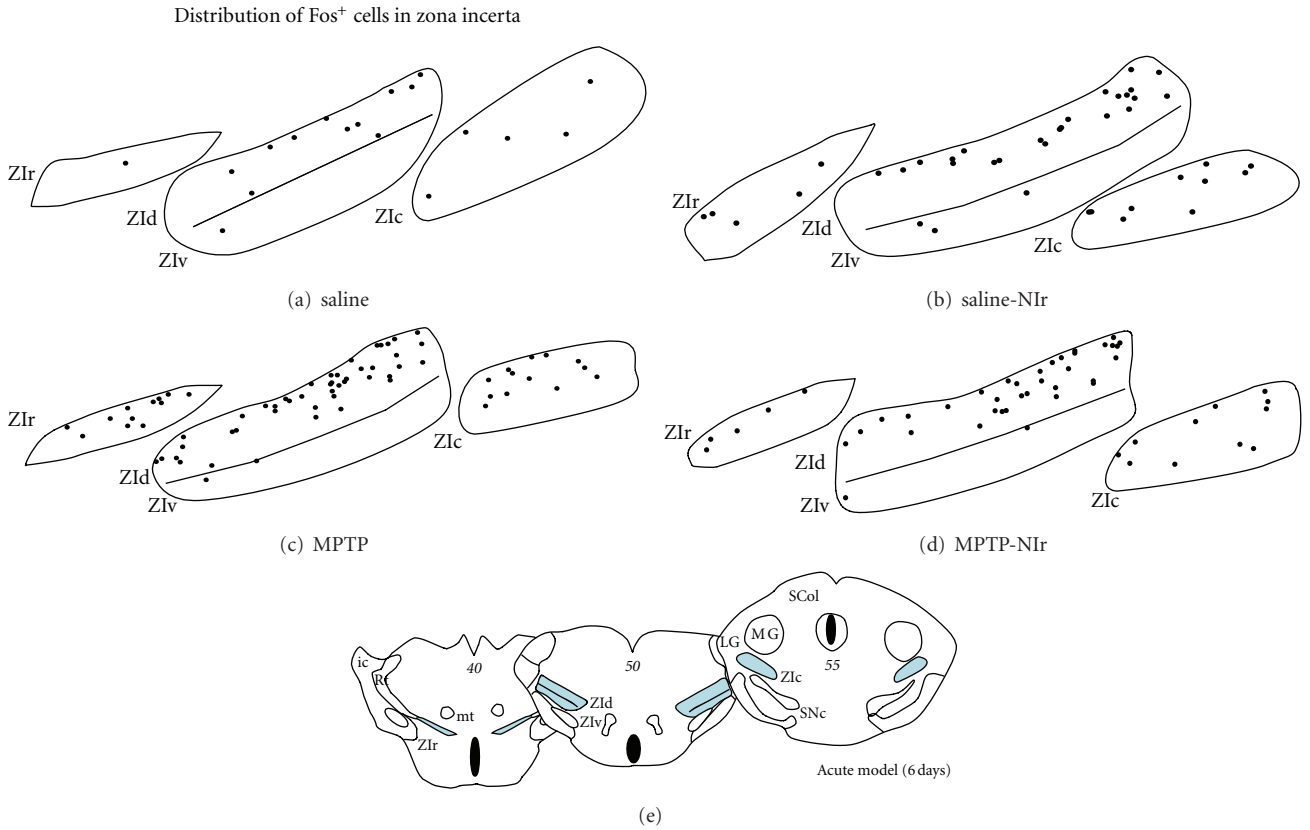

Figure 5: Schematic diagrams of the distribution of Fos+ cells in the different sectors of the STN in the saline (a), saline-NIr (b), MPTP (c) and MPTP-NIr groups. These maps are from the acute model with six-day survival period (similar patterns were evident in the chronic model; in the acute model with two-hour survival period, the distribution of cells was similar to the saline cases shown here). Each black circle represents one cell. These maps were taken from coronal sections similar to the plates of the mouse atlas (numbers in italics [1]) shown in (e).

5.3. Fos Expression after MPTP Treatment. We report that MPTP insult induced Fos expression in the STN and ZI. In fact, the MPTP group had more Fos+ cells in both nuclei than any one of the other groups. This activation was likely to manifest after the loss of SNc dopaminergic cells caused by the MPTP [10–13]. For the ZI, it receives a very weak direct projection from the SNc, hence the activation was likely to occur indirectly via, for example, the PpT, which is overactive in parkinsonian cases and has heavy projections to the ZI [29]. For the STN, it receives a more substantial SNc projection, together with heavy projections from the PpT [27, 28], and hence these projections may have both contributed to the Fos expression in this nucleus.

Hence, there appear to be two very different triggers or mechanisms that generated the Fos expression. In the MPTP group, Fos expression in both the STN and ZI was likely to be induced after a loss of dopaminergic cells from the SNc (and overactive PpT projections), while in the saline-NIr group, a group that had no loss of SNc cells, Fos expression in the ZI may have been induced by pathways stimulated by retinal afferents (via the superior colliculus) after the NIr treatment.

5.4. NIr Treatment Reduced Abnormal Fos Expression Induced by MPTP Insult: A Long-Lasting Effect. Our results showed that neuroprotection or saving of dopaminergic cells in the SNc from MPTP toxicity by NIr treatment [4, 5] resulted in a reduction of the abnormal overactivity (increase in Fos expression) in the STN and ZI. There were fewer Fos+ cells in the MPTP-NIr compared to the MPTP group. The number of cells in the MPTP-NIr group was, however, still higher than in the saline-NIr (30–45%) and saline (60%) control groups, indicating that the NIr treatment did not reduce entirely the abnormal activity generated by the MPTP toxin; if it did, then the MPTP-NIr and saline-NIr groups would have had very similar cell numbers. Nevertheless, the reduction was clear and significant in the MPTP-NIr group and it may represent a reversal, at least in part, of the abnormal circuits generated by MPTP. It remains to be determined whether these changes in neuronal activity by NIr treatment are evident in behavioural and clinical studies.

In the MPTP and MPTP-NIr groups in both the STN and ZI, and saline-NIr group in the ZI, there were many Fos+ cells in the acute model with six-day survival and chronic model (three weeks survival). Previous studies have indicated that although the peak of Fos expression occurs about two hours after some forms of stimulation (e.g., peripheral noxious [17, 23]), it may still be present weeks or months after others (e.g., 6-OHDA lesion [25]). We show here that MPTP

treatment had a long-term (six days to three weeks) impact on Fos expression, presumably due to the triggering and maintenance of abnormal basal ganglia circuitry (see above). Further, we show that even after minimal exposure, NIr treatment generated longer-term effects (six days to three weeks) on cell activity also. This finding is most encouraging when considering therapeutic use. In this context, it has been shown recently that patients suffering from depressive illness show improved depression and anxiety rating scales up to a month after a single dose of NIr treatment [20].

Abbreviations

6-OHDA:	6-hydroxydopamine
ATP:	Adenosine-5′-triphosphate
ic:	Internal capsule
LG:	Lateral geniculate nucleus
MG:	Medial geniculate nucleus
MPTP:	1-methyl-4-phenyl-1,2,3,6-tetrahydropyridine
mt:	Mammillothalamic tract
NIr:	Near-infrared light treatment
PBS:	Phosphate buffered saline
PpT:	Pedunculopontine tegmental nucleus
Rt:	Thalamic reticular nucleus
SCol:	Superior colliculus
SNc:	Substantia nigra pars compacta
SNr:	Substantia nigra pars reticulate
STN:	Subthalamic nucleus
TH:	Tyrosine hydroxylase
ZI:	Zona incerta
ZIc:	Caudal sector zona incerta
ZId:	Dorsal sector zona incerta
ZIr:	Rostral sector zona incerta
ZIv:	Ventral sector zona incerta.

Grant Sponsors

Tenix Corp and Salteri Family.

Acknowledgments

The authors are forever grateful to Tenix Corp and Salteri family for their generous funding of the laboratory. The authors dedicate this work to our friend and colleague, Gary Baker, who passed away during the final stages of the paper preparation.

References

[1] G. Paxinos and K. B. J. Franklin, *The Mouse Brain in Stereotaxic Coordinates*, Academic Press, New York, NY, USA, 2nd edition, 2001.

[2] H. L. Liang, H. T. Whelan, J. T. Eells, and M. T. T. Wong-Riley, "Near-infrared light via light-emitting diode treatment is therapeutic against rotenone- and 1-methyl-4-phenylpyridinium ion-induced neurotoxicity," *Neuroscience*, vol. 153, no. 4, pp. 963–974, 2008.

[3] R. Ying, H. L. Liang, H. T. Whelan, J. T. Eells, and M. T. Wong-Riley, "Pretreatment with near-infrared light via light-emitting diode provides added benefit against rotenone- and MPP+-induced neurotoxicity," *Brain Research*, vol. 1243, pp. 167–173, 2008.

[4] V. E. Shaw, S. Spana, K. Ashkan et al., "Neuroprotection of midbrain dopaminergic cells in MPTP-treated mice after near-infrared light treatment," *Journal of Comparative Neurology*, vol. 518, no. 1, pp. 25–40, 2010.

[5] C. Peoples, S. Spana, K. Ashkan et al., "Photobiomodulation enhances nigral dopaminergic cell survival in a chronic MPTP mouse model of Parkinson disease," *Parkinsonism & Related Disorders*. In press.

[6] J. W. Langston, "The etiology of Parkinson's disease with emphasis on the MPTP story," *Neurology*, vol. 47, no. 6, pp. S153–S160, 1996.

[7] S. Passarella, E. Casamassima, S. Molinari et al., "Increase of proton electrochemical potential and ATP synthesis in rat liver mitochondria irradiated in vitro by helium-neon laser," *FEBS Letters*, vol. 175, no. 1, pp. 95–99, 1984.

[8] B. Beauvoit, T. Kitai, and B. Chance, "Contribution of the mitochondrial compartment to the optical properties of the rat liver: a theoretical and practical approach," *Biophysical Journal*, vol. 67, no. 6, pp. 2501–2510, 1994.

[9] J. Jankovic, "Motor fluctuations and dyskinesias in Parkinson's disease: clinical manifestations," *Movement Disorders*, vol. 20, no. 11, pp. S11–S16, 2005.

[10] E. C. Hirsch, C. Périer, G. Orieux et al., "Metabolic effects of nigrostriatal denervation in basal ganglia," *Trends in Neurosciences*, vol. 23, no. 10, pp. S78–S85, 2000.

[11] C. Périer, M. Vila, J. Féger, Y. Agid, and E. C. Hirsch, "Functional activity of zona incerta neurons is altered after nigrostriatal denervation in hemiparkinsonian rats," *Experimental Neurology*, vol. 162, no. 1, pp. 215–224, 2000.

[12] I. J. Mitchell, C. E. Clarke, S. Boyce et al., "Neural mechanisms underlying Parkinsonian symptoms based upon regional uptake of 2-deoxyglucose in monkeys exposed to 1-methyl-4-phenyl-1,2,3,6-tetrahydropyridine," *Neuroscience*, vol. 32, no. 1, pp. 213–226, 1989.

[13] R. H. P. Porter, J. G. Greene, D. S. Higgins, and J. T. Greenamyre, "Polysynaptic regulation of glutamate receptors and mitochondrial enzyme activities in the basal ganglia of rats with unilateral dopamine depletion," *Journal of Neuroscience*, vol. 14, no. 11, pp. 7192–7199, 1994.

[14] D. Nandi, M. Chir, X. Liu et al., "Electrophysiological confirmation of the zona incerta as a target for surgical treatment of disabling involuntary arm movements in multiple sclerosis: Use of local field potentials," *Journal of Clinical Neuroscience*, vol. 9, no. 1, pp. 64–68, 2002.

[15] P. Plaha, S. Khan, and S. S. Gill, "Bilateral stimulation of the caudal zona incerta nucleus for tremor control," *Journal of Neurology, Neurosurgery and Psychiatry*, vol. 79, no. 5, pp. 504–513, 2008.

[16] A. L. Benabid, S. Chabardes, J. Mitrofanis, and P. Pollak, "Deep brain stimulation of the subthalamic nucleus for the treatment of Parkinson's disease," *The Lancet Neurology*, vol. 8, no. 1, pp. 67–81, 2009.

[17] S. Reyes and J. Mitrofanis, "Patterns of Fos expression in the spinal cord and periaqueductal grey matter of 6OHDA-lesioned rats," *International Journal of Neuroscience*, vol. 118, no. 8, pp. 1053–1079, 2008.

[18] M. S. Turner, T. S. Gray, A. L. Mickiewicz, and T. C. Napier, "Fos expression following activation of the ventral pallidum in normal rats and in a model of Parkinson's Disease: implications for limbic system and basal ganglia interactions," *Brain Structure and Function*, vol. 213, no. 1-2, pp. 197–213, 2008.

[19] J. Ma, V. E. Shaw, and J. Mitrofanis, "Does melatonin help save dopaminergic cells in MPTP-treated mice?" *Parkinsonism and Related Disorders*, vol. 15, no. 4, pp. 307–314, 2009.

[20] F. Schiffer, A. L. Johnston, C. Ravichandran et al., "Psychological benefits 2 and 4 weeks after a single treatment with near infrared light to the forehead: a pilot study of 10 patients with major depression and anxiety," *Behavioral and Brain Functions*, vol. 5: 46, 2009.

[21] M. A. Naeser, A. Saltmarche, M. H. Krengel, M. R. Hamblin, and J. A. Knight, "Improved cognitive function after transcranial, light-emitting diode treatments in chronic, traumatic brain injury: two case reports," *Photomedicine and Laser Surgery*, vol. 29, no. 5, pp. 351–358, 2011.

[22] B. Piallat, A. Benazzouz, and A. L. Benabid, "Subthalamic nucleus lesion in rats prevents dopaminergic nigral neuron degeneration after striatal 6-OHDA injection: behavioural and immunohistochemical studies," *European Journal of Neuroscience*, vol. 8, no. 7, pp. 1408–1414, 1996.

[23] E. Bullitt, C. L. Lee, A. R. Light, and H. Willcockson, "The effect of stimulus duration on noxious-stimulus induced c-fos expression in the rodent spinal cord," *Brain Research*, vol. 580, no. 1-2, pp. 172–179, 1992.

[24] C. E. Heise, S. Reyes, and J. Mitrofanis, "Sensory (nociceptive) stimulation evokes Fos expression in the subthalamus of hemiparkinsonian rats," *Neurological Research*, vol. 30, no. 3, pp. 277–284, 2008.

[25] C. E. Heise and J. Mitrofanis, "Fos immunoreactivity in some locomotor neural centres of 6OHDA-lesioned rats," *Anatomy and Embryology*, vol. 211, no. 6, pp. 659–671, 2006.

[26] A. Schober, "Classic toxin-induced animal models of Parkinson's disease: 6-OHDA and MPTP," *Cell and Tissue Research*, vol. 318, no. 1, pp. 215–224, 2004.

[27] A. Parent and L. N. Hazrati, "Functional anatomy of the basal ganglia. II. The place of subthalamic nucleus and external pallidum in basal ganglia circuitry," *Brain Research Reviews*, vol. 20, no. 1, pp. 128–154, 1995.

[28] A. M. Taylor, G. Jeffery, and A. R. Lieberman, "Subcortical afferent and efferent connections of the superior colliculus in the rat and comparisons between albino and pigmented strains," *Experimental Brain Research*, vol. 62, no. 1, pp. 131–142, 1986.

[29] J. Mitrofanis, "Some certainty for the "zone of uncertainty"? Exploring the function of the zona incerta," *Neuroscience*, vol. 130, no. 1, pp. 1–15, 2005.

Hindawi Publishing Corporation
Parkinson's Disease
Volume 2012, Article ID 128356, 6 pages
doi:10.1155/2012/128356

Review Article

Genetic Rat Models of Parkinson's Disease

Ryan M. Welchko,[1] Xavier T. Lévêque,[2] and Gary L. Dunbar[3,4]

[1] *Field Neurosciences Institute, Laboratory for Restorative Neurology, Department of Psychology, Central Michigan University, Mt. Pleasant, MI 48859, USA*
[2] *Field Neurosciences Institute, Laboratory for Restorative Neurology, Program in Neuroscience, Central Michigan University, Mt. Pleasant, MI 48859, USA*
[3] *Field Neurosciences Institute, Laboratory for Restorative Neurology, Department of Psychology and Program in Neuroscience, College of Medicine, Central Michigan University, Mt. Pleasant, MI 48859, USA*
[4] *Field Neurosciences Institute, St. Mary's of Michigan, Saginaw MI 48604, USA*

Correspondence should be addressed to Gary L. Dunbar, dunba1g@cmich.edu

Received 10 December 2011; Accepted 20 January 2012

Academic Editor: Kah-Leong LIM

Parkinson's disease (PD) is a neurodegenerative disease characterized by a specific loss of dopaminergic neurons. Although the vast majority of PD cases are idiopathic in nature, there is a subset that contains genetic links. Of the genes that have been linked to PD, α-synuclein and leucine-rich repeat kinase 2 have been used to develop transgenic rat models of the disease. In this paper we focused on the various transgenic rat models of PD in terms of their ability to mimic key symptoms of PD in a progressive manner. In general, we found that most of these models provided useful tools for the early stages of PD, but the development of new transgenic rats that present significant neuropathologic and motoric deficits in a progressive manner that more accurately mimics PD is needed.

1. Introduction

Parkinson's disease (PD) is the second most common neurodegenerative disorder. It is hypothesized that PD is caused by a combination of genetic and environmental factors. A specific loss of dopaminergic (DA) neurons in the substantia nigra (SN) in PD results in the significant loss of DA innervation of the neostriatum via the nigrostriatal pathway. The progressive loss of this DA innervation, in turn, is responsible for the characteristic motor symptoms of PD, which include akinesia, resting tremors, and postural instability.

A hallmark histopathological marker for PD is the presence of cytoplasmic inclusions, known as Lewy bodies (LBs), which are found throughout the mesencephalon of the PD brain, including the substantia nigra [1]. The major component of LBs is the presynaptic protein called α-synuclein (α-syn) [2]. To date, it is not known whether the mechanisms underlying the formation of LBs are the cause or a consequence of the disease. Some familial forms of PD have been linked to mutations in genes that code for α-syn, as well as genes that code for leucine-rich repeat kinase 2 (LRRK2), DJ-1, and Parkin [3, 4]. These mutations have formed the basis of developing transgenic rodent models of PD.

Presently, the only treatments for PD are palliative in nature and usually utilize dopamine agonists, such as levodopa (L-DOPA). Surgical techniques, such as pallidotomies and deep-brain stimulation, have also proved to be successful in reducing some of the major motor symptoms of PD. To date, the most promising avenue of research aimed at restoring lost function in PD appears to be cell therapies, and much of the recent research efforts in this domain have focused on use of stem cells.

However, significant advances in developing effective therapies for PD have been limited by the lack of a valid animal model that closely mimic the progressive neuropathology and behavioral deficits of PD. Most research on PD has utilized rodents that are given specific neurotoxins, including 6-hydroxydopamine (6-OHDA), 1-methyl-4-phenyl-1,2,3,6-tetrahydropyridine (MPTP), paraquat, and

Table 1: Summary of studies using genetic rat models of PD. Note that % cell loss SNpc is percentage of cell loss in the substantia nigra, pars compacta, relative to number of cells in the intact, untreated controls; "n.a." indicates data for percentage loss of SNpc cells was not available; plus sign (+) indicates significant differences and "n.s." indicates non-significant differences between genetically altered rats and wild-type controls on measures of protein aggregation or behavioral deficits (i.e., stimulant-induced rotational activity, paw placement in cylinder task, and/or spontaneous motor activity in open-field).

Gene	Method	Percentage of cell loss SNpc	Protein aggregation	Behavior deficit	Author year
hα-syn, α-syn A53T	rAAV	30%–80%	+	+ (in 25% of animals)	Kirik et al. 2002 [12]
hα-syn A30P	rAAV	53%	+	n.s.	Klein et al. 2002 [13]
hα-syn A30P	HIV-1 Lentivirus	33%	+	None performed	Lo Bianco et al. 2002 [14]
hα-syn A53T	HIV-1 Lentivirus	24%	+	None performed	Lo Bianco et al. 2002 [14]
hα-syn	rAAV	50%	+	n.s.	Yamada et al. 2004 [15]
hα-syn	rAAV2/5	40–60%	+	None performed	Gorbatyuk etal. 2008 [16]
hα-syn S129A	rAAV2/5	66–70%	+	None performed	Gorbatyuk etal. 2008 [16]
hα-syn S129D	rAAV2/5	n.a.	+	None Performed	Gorbatyuk et al. 2008 [16]
hα-syn	rAAV2/6	11–22%	+	None Performed	da Silveira et al. 2009 [17]
hα-syn A30P	rAAV2/6	11–22%	+	None Performed	da Silveira et al. 2009 [17]
hα-syn WT S129A	rAAV2/6	over 70%	+	None Performed	da Silveira et al. 2009 [17]
hα-syn WT S129D	rAAV2/6	n.a.	+	None Performed	da Silveira et al. 2009 [17]
hα-syn A30P S129A	rAAV2/6	over 70%	+	None Performed	da Silveira et al. 2009 [17]
hα-syn A30P S129D	rAAV2/6	n.s.	+	None Performed	da Silveira et al. 2009 [17]
hα-syn A30P	TAT	21.3–31.3%	n.s.	+	Recchia et al. 2008 [18]
hα-syn A30P A53T	Microinjection	n.a.	n.s.	+	Lelan et al. 2011 [19]
LRRK2 G2019S	Rad	21.4%	n.s.	None Performed	Dusonchet et al. 2011 [20]
LRRK2 G2019S	TRE-tTA	0%	n.s.	+	Zhou et al. 2011 [21]

rotenone, that are administrated into the substantia nigra pars compacta (SNpc) or nigrostriatal pathway. Although these models have yielded valuable insights into potentially useful therapies for PD, they do not accurately mimic the full constellation of neuropathological and behavioral deficits associated with PD. Recently, transgenic animal models of PD have been developed by inserting the mutated human gene in rodents. Although most of these transgenic models have been developed in mice, more recent efforts have focused on developing transgenic rat models of PD.

The purpose of this paper is to provide an update on the newly developed genetic rat models of PD and to provide some assessment of their usefulness in therapeutic research. We will attempt to compare each of the newly developed models in terms of their ability to mimic both the neuropathological and behavioral features of the disease (see Table 1). We will also describe some of the early therapeutic research using these models. Although none of these models provide the optimal tool for testing potential treatments for PD, we think that some of these models have the potential to provide an improvement over the more commonly used neurotoxic rat models.

2. α-Synuclein Rat Models

The most thoroughly studied transgenic rat model of PD is the α-synuclein rat model. As indicated previously, some familial forms of PD have been linked to α-syn, a small neuronal 140 amino acid protein (14.4 kDa) [5], that is located in presynaptic terminals. In humans, the gene for α-syn is located on chromosome 4q21-q23 [6] and this protein is highly expressed in the brain. Missense autosomal dominant mutations at A53T [7], E46K [8], and A30P [9] of the gene-coding region of α-syn have been linked to LB aggregates and Lewy neurites in patients with rare, early onset PD. The presynaptic presence of α-syn suggests a role in synaptic vesicle trafficking. It has been shown that α-syn is a dose-dependent inhibitor of tyrosine hydroxylase (TH) [10]. On the other hand, α-syn could be a link in the dopamine transporter and, in this way, increase dopamine reuptake [11]. As such, it appears that an optimal level of α-syn may be critical for proper functioning of DA neurons.

Transgenic α-syn models have been created in adult rats utilizing adenoassociated virus (rAAV) or HIV-1-derived lenti-virus to transduce mutated human α-syn genes into the nigrostriatal pathway. Also, HIV TAT-mediated protein transduction has been used to transduce mutated human α-syn protein. Although there has been some success with achieving expression of α-syn in DA neurons within the SN, the amount of DA neuronal degeneration varied greatly between studies assessed by TH immunohistochemistry (IHC). Some of this variation could be due to differing forms of the α-syn gene used, the method of delivery utilized, or the gene promoter used. For example, Klein et al. [13] found a 53% reduction of TH-positive DA neurons when they injected rAAV expressing the mutant human α-syn A30P into the SN, while Kirik et al. [12] reported a 30–80% reduction when they injected rAAV expressing the mutant

human α-syn A53T in the SN. Klein et al. [13] and Kirik et al. utilized a hybrid cytomegalovirus (CMV)/chicken β-actin (CBA) promoter to drive expression of the differing mutant α-syn genes. This specific promoter is the CBA promoter with enhancer elements from the CMV promoter added. In addition, Kirik et al. [12] found a 50% reduction in TH positive DA striatal innervation at eight weeks after injection. In term of behavior, Kirik et al. [12] reported that 25% of the α-syn-injected rats were impaired during apomorphine-induced rotation assessments and on a paw-reaching (i.e., cylinder) task, an impairment that is compatible to a loss of more than 60% of DA SN neurons. However, Klein et al. [13] did not find a significant behavioral impairment in amphetamine-induced rotations. Both Kirik and Klein groups of investigators reported progressive pattern of neurodegeneration that included α-syn aggregates that resembled LBs in PD patients. As such, these transgenic rat models of PD more closely mimicked the progressive loss of dopaminergic neurons in PD than do the neurotoxic rat models of this disease.

Yamada et. al [15] created an α-syn model using rAAV, but utilized a cytomegalovirus (CMV) promoter which differed from the CMV/CBA promoter used by the Kirik and Klein groups [12, 13]. Yamada et al. reported a 50% decrease in the number of DA neurons in the injected SN, but this decrease was insufficient to produce significant differences between the injected rats and controls when these animals were assessed on measures of apomorphine-induced rotation.

Recchia et al. [18] created an α-syn model of PD by administering intranigral injections of the A30P mutated form of α-syn, fused to a TAT fusion protein. Their study compared unilateral injections of TAT-α-syn A30P protein, α-syn A30P protein, 6-OHDA, and sham controls into the SN at various time points. Neurodegeneration and genetic expression were assessed via IHC, western blot, HPLC analysis, and behavioral assessment. They found that the α-syn A30P protein, without the TAT fusion protein, did not integrate within neurons of the SN, whereas 80% of TH-positive cells were found to express α-syn A30P following TAT-α-syn A30P injection. No formations of LBs or Lewy neurites were found in these animals. The TAT-α-syn A30P distribution, assessed by western blot, was found within the SN, striatum, and contralateral cortex at 24 hours after injection. At 15 and 30 days post-injection, the TAT-α-syn A30P produced a 26.3 $\pm$ 5.0% loss in TH positive neurons, compared to the 81.2 $\pm$ 2.1% loss in TH positive neurons following the 6-OHDA injections. At 7 days post-injection, the TAT-α-syn A30P animals showed a 20.8 $\pm$ 3.6% reduction in DA and 16.6 $\pm$ 2.5% reduction in 3,4-dihydroxyphenylacetic acid (DOPAC) within the ipsilateral, compared to the contralateral, striatum. In comparison, the animals receiving 6-OHDA injections showed a 60.6 $\pm$ 3.6% reduction in DA and a 59.7% $\pm$ 4.5 reduction in DOPAC within the ipsilateral, compared to the contralateral, striatum. Administration of apomorphine did not produce a significant number of ipsilateral rotations in animals receiving TAT-α-syn A30P injections. However, rats receiving TAT-α-syn A30P injections showed increasing motor impairment at day 30 and day 90 when motor function was accessed via rotorod and footprint analysis.

More recently, Sanchez-Guajardo et al. [22] studied the temporal profile of microglia activation in an α-syn rat model of PD. They injected rAAV2/5 expressing human wild type (hWT) α-syn directly into the right SN. Rats were divided into two groups based upon the concentration of rAAV2/5 hWT α-syn. The α-syn neurodegeneration group received a lower concentration of rAAV2/5 hWT α-syn, while the α-syn cell-death group received a greater concentration. The α-syn neurodegeneration rats did not exhibit a significant reduction in TH-positive neurons within the SN. However, a decrease in TH-positive fiber density within the striatum and pathological formations were observed in these animals. The α-syn cell-death group exhibited a significant reduction in TH-positive neurons within the SN and a reduction of TH-positive fiber density within the striatum. An increase in microglia was seen in both groups at four weeks after injection. The activated microglia was significantly higher in the neurodegeneration group at 4 weeks, and the levels of microglia returned to control levels at 8–15 weeks. Within the cell-death group, microglia levels peaked at 8 weeks and returned to control levels at 15 weeks.

Lelan et al. [19] created a transgenic α syn rat utilizing microinjection to transfer the construct pUTHTV expressing the A30P and A53T double-mutated human α syn under the control of the rat TH promoter. These investigators observed the expression of mutated human α-syn in olfactory bulbs and within SN. They also observed an olfactory impairment in mutated human α syn transgenic rats, when compared to wild type rats. No impairment in motor behavior was observed.

Gorbatyuk et al. [16] created three α-syn models with the hWT α-syn or mutated α-syn with S129A, or S129D mutations. Unilateral injections of rAVV2/5 vectors expressing the transgenes were done in the SN. Histological examinations were carried out at 4, 8, or 26 weeks after injection. At 4 weeks, a 70% loss in TH-positive neurons was observed in the rats receiving S129A, whereas all other groups did not show a significant TH-positive neuronal loss, when compared to controls. At 8 weeks, rats receiving an injection of WT α-syn rats exhibited a 40% loss of TH-positive neurons and S129A α-syn rats exhibited a 66% loss of TH neurons. However, rats receiving hWT α-syn exhibited a 60% loss of TH positive neurons at 27 weeks, which was similar to the S129A α-syn rats at that time point. Rats receiving the S129D injections did not exhibit significant neurodegeneration at any of the time points. Striatal DA levels were assessed by HPLC. The HPLC analysis showed that there was a depletion of DA levels, consistent with SN cell loss.

Azeredo da Silveira et al. [17] created an α-syn model to observe a prevention of the phosphorylation of human mutated α-syn which is involved in numerous neurodegenerative diseases. The study utilized the rAAV2/6 vector with the CMV promoter. The site-directed mutations of human A30P α-syn and hWT α-syn were at the serine residue at position 129. The serine residue was converted to alanine (S129A) to abolish phosphorylation or converted to aspartate (S129D) to reproduce effects of phosphorylation.

The two site-directed mutations of the mutated human A30P α-syn and hWT α-syn were compared to hWT α-syn and mutated human A30P α-syn. Rats received two injections within the SN. They observed a dose-dependent loss from 11 to 22% in TH-positive neurons when rats received injections of hWT α-syn. Injection of the S129A-Mutated A30P α-syn and hWT α-syn resulted in a dose-dependent loss of over 70%. Whereas the S129D-mutated A30P α-syn and human WT α-syn resulted in less neurodegeneration in the SN then WT α-syn, rats receiving injections of hWT α-syn with the mutated human A30P α-syn tended to display less neurodegeneration than the WT α-syn rats.

Finally, a series of α-syn models of PD were produced by Lo Bianco et al. [14], using an HIV-1-derived lentivirus, expressing a range of α-syn genes, including wild-type human α-syn, mutated-human A30P α-syn, mutated-human A53T α-syn, and rat wild-type α-syn. The largest reduction of TH-positive neurons within the SN was observed in animals treated with the lenti-WT human α-syn, which exhibited a 35% reduction. Rats treated with A30P α-syn and A53T α-syn also exhibited a 33% and 24% reduction in TH-positive neurons, respectively. Some α-syn inclusions were found in the cytoplasm of neurites and cell bodies of surviving nigral neurons.

Subsequent studies using genes that overexpressed glial derived neurotrophic factor (GDNF), a protein associated with neuroprotection of dopaminergic neurons, were unsuccessful in reducing the cell loss in several of these α-syn rat models of PD. For example, Lo Bianco et al. [23] found that injections of a lenti-GDNF just dorsal to the SN, given two weeks prior to bilateral injections of lenti-A30P-α-syn, failed to reduce the loss of DA neurons as assessed by TH immunohistochemistry. Similarly, Decressac et al. [24] injected lenti-GDNF into the striatum two weeks prior to an intranigral injection of rAAV2-A30P-α-syn and, in a second study, injected rAAV2-GDNF in the striatum and just dorsal to the SN at three weeks prior to an intranigral injection of rAAV2-A30P-α-syn and found that these GDNF injections failed to protect against α-syn-induced neurotoxicity in both studies.

Lo Bianco et al. also tested the potential efficacy of using lenti-viral delivery of parkin in an α-syn rat model of PD [25]. Parkin is a 465-amino-acid protein responsible for protein degradation, and mutated forms of parkin are found in about 50% of the cases of juvenile PD, an autosomal recessive form of this disease [26]. Lo Bianco et al. gave two groups of rats bilateral injections into the right SN of either lenti-A30P-α-syn/lenti-YFP, or lenti-A30P-α-syn/lenti-Parkin (with the Parkin gene being derived from a wild-type rat). Control animals received injections of either lenti-Parkin or lenti-YFP. A 31% reduction of TH-positive neurons in the SN was observed in animals receiving lenti-A30P-α-syn, whereas a 9% reduction in TH positive neurons was observed in the SN of animals receiving lenti-A30P-α-syn with lenti-Parkin. There was a 16% reduction in TH-positive neurites within the striatum of the lenti-A30P-α-syn rats. The animals receiving lenti-A30P-α-syn with lenti-Parkin exhibited a 4% reduction in TH-positive neurites within the striatum. In addition, animals receiving lenti-A30P-α-syn with lenti-Parkin, as evidenced by silver staining, did not show an α-syn-induced neurodegeneration, whereas the lenti-A30P-α-syn group did. Animals receiving lenti-A30P-α-syn with lenti-Parkin exhibited a 45% increase in hyperphosphorylated α-syn inclusion, and lenti-A30P- α-syn animals showed a 43% increase in hyperphosphorylated α-syn inclusions. Similarly, Yamada et al. [4] examined the effects of Parkin on the rAAV α-syn model of PD. They injected rAAV expressing α-syn and rAAV parkin at the same time directly into SN and observed a decrease of cell death of DA neurons within the SN and the number of apomorphine-induced rotations, compared to rat injected with rAAV α-syn alone. Clearly, the α-syn rat models of PD provide many of the features that resemble symptoms of PD. However, most of the models produce a relatively limited cell loss, which provides a useful model of early PD but lacks the extensive cell loss and behavioral deficits to accurately mimic the later stages of this disease. Early therapeutic trials in these rat models have suggested that overexpression of the gene for parkin, but not GDNF, may reduce TH-positive cell loss in this model of PD.

3. 4-Leucine-Rich Repeat Kinase 2 (LRRK2)

A second type of transgenic rat model involves the use of LRRK2, which is a member of the ROCO protein family and the RAS-GTPase super family. The LRRK2 gene contains both a GTPase-like domain and a kinase-like domain. An important number of mutations in the gene have been identified and associated with PD. Of these mutations, G2019S has been found to be the most common [27, 28] and is a point mutation located within the kinase domain. Another common mutation is R1441C, in which a mutation occurs within the GTPase domain.

Zhou et al. [21] utilized LRRK2 transgenic rats possessing the G2019S mutation. Transgenic rats were created by crossing TRE-LRRK2 G2019S transgenic rats with CAG-tTA transgenic rats. These investigators examined the effects of temporal expression of the human LRRK2 mutation, using a promoter that is activated by the absence of doxycycline. They measured the total distance and stereotypical movements the rats made in an open-field maze during a 20-minute assessment period, followed by an addition 20-minute period, which was given 5 minutes after an injection of amphetamine or 20 minutes after an injection of nomifensine (an inhibitor of DA reuptake). They found that the temporal expression of the human LRRK2 G2019S increased the distance traveled as well as the amount of stereotypical behavior. When given nomifensine or amphetamine, the temporal expression of LRRK2 G2019S significantly reduced the amount of evoked responses, compared to controls. In addition to the open-field assessments, these investigators measured intrastriatal DA via microdialysis and found an increase in extracellular DA in the striatum of rats receiving temporal expression of LRRK2. However, there were no increase in the level of DA when amphetamine and nomifensine was administered

to these rats. The researchers attributed these results to an impairment of the DA transporter (DAT) due to preservation of in TH-positive neurons within the SNpc, nor were there any changes observed in the number of axon terminals in the striatum.

Dusonchet et al. [20] produced a transgenic LRRK2 model in adult rats utilizing recombinant human serotype 5 adenovirus (RAd). These investigators compared the overexpression of human wild-type LRRK2 to the LRRK2 G2019S human mutation. They found no loss of TH-positive cells in the human wild-type LRRK2 animals. However, there was a progressive TH-positive cell loss, observed between 10 and 42 days (with a total loss of 21.4%), and a 10% decrease in striatal TH-positive fibers in G2019S LRRK2 animals.

As with the α-syn models, the LRRK2 transgenic rat models of PD appear to provide only a modest loss of TH-positive cells. However, there is evidence of motor deficits, as measured in the open-field maze, when the LRRK2 G2019S gene is activated in this transgenic rat model of PD. As such, this model may also provide a useful tool for evaluating potential treatments during the early stages of PD.

4. Conclusion

In this paper, we have provided an update on the various genetic rat models of PD. Although there is considerable variability among the studies reviewed in terms of the types of genes and techniques used, most of these models revealed a progressive and significant, albeit modest, loss of TH-positive neurons in the SNpc. As can be ascertained from Table 1, the α-syn models show progressive cell loss, with protein aggregation, but little evidence for consistent motoric deficits. The use of the α-syn A53T rat model did produce significant TH-positive cell loss (at about 60%) and concomitant motor deficits, but this occurred in only 25% of the rats receiving this mutated gene. The LRRK2 model produced both a level of cell loss comparable to early-stage PD and motor deficits in the open-field maze, but there is no evidence of protein aggregation in these animals. In terms of treatments, studies using transgenic PD rats have indicated that parkin can provide a significant level of protection against dopaminergic neuronal loss. Collectively, these studies indicate that the currently used transgenic rat models of PD can provide a useful tool for the early stages of PD, but more work is needed in developing a model that mimics the progressive neuropathology and behavioral deficits that are observed throughout the time span of this disease.

Acknowledgments

The authors gratefully acknowledge the generous support from the John G. Kulhavi Professorship (to GLD), the Field Neurosciences Institute, and the College of Humanities and Social and Behavioral Sciences at Central Michigan University.

References

[1] T. M. Dawson, "New animal models for Parkinson's disease," *Cell*, vol. 101, no. 2, pp. 115–118, 2000.

[2] M. G. Spillantini, M. L. Schmidt, V. M. Y. Lee, J. Q. Trojanowski, R. Jakes, and M. Goedert, "α-synuclein in Lewy bodies," *Nature*, vol. 388, no. 6645, pp. 839–840, 1997.

[3] O. Cooper, P. Hallett, and O. Isacson, "Using stem cells and iPS cells to discover new treatments for Parkinson's disease," *Parkinsonism & Related Disorders*, vol. 18, supplement 1, pp. S14–S16, 2012.

[4] M. Yamada, Y. Mizuno, and H. Mochizuki, "Parkin gene therapy for α-synucleinopathy: a rat model of Parkinson's disease," *Human Gene Therapy*, vol. 16, no. 2, pp. 262–270, 2005.

[5] R. Jakes, M. G. Spillantini, and M. Goedert, "Identification of two distinct synucleins from human brain," *FEBS Letters*, vol. 345, no. 1, pp. 27–32, 1994.

[6] M. H. Polymeropoulos, J. J. Higgins, L. I. Golbe et al., "Mapping of a gene for Parkinson's disease to chromosome 4q21-q23," *Science*, vol. 274, no. 5290, pp. 1197–1199, 1996.

[7] M. H. Polymeropoulos, C. Lavedan, E. Leroy et al., "Mutation in the α-synuclein gene identified in families with Parkinson's disease," *Science*, vol. 276, no. 5321, pp. 2045–2047, 1997.

[8] J. J. Zarranz, J. Alegre, J. C. Gómez-Esteban et al., "The new mutation, E46K, of α-synuclein causes Parkinson and Lewy body dementia," *Annals of Neurology*, vol. 55, no. 2, pp. 164–173, 2004.

[9] R. Krüger, W. Kuhn, T. Müller et al., "Ala30Pro mutation in the gene encoding α-synuclein in Parkinson's disease," *Nature Genetics*, vol. 18, no. 2, pp. 106–108, 1998.

[10] R. G. Perez, J. C. Waymire, E. Lin, J. J. Liu, F. Guo, and M. J. Zigmond, "A role for α-synuclein in the regulation of dopamine biosynthesis," *Journal of Neuroscience*, vol. 22, no. 8, pp. 3090–3099, 2002.

[11] F. J. S. Lee, F. Liu, Z. B. Pristupa, and H. B. Niznik, "Direct binding and functional coupling of α-synuclein to the dopamine transporters accelerate dopamine-induced apoptosis," *FASEB Journal*, vol. 15, no. 6, pp. 916–926, 2001.

[12] D. Kirik, C. Rosenblad, C. Burger et al., "Parkinson-like neurodegeneration induced by targeted overexpression of α-synuclein in the nigrostriatal system," *Journal of Neuroscience*, vol. 22, no. 7, pp. 2780–2791, 2002.

[13] R. L. Klein, M. A. King, M. E. Hamby, and E. M. Meyer, "Dopaminergic cell loss induced by human A30P α-synuclein gene transfer to the rat substantia nigra," *Human Gene Therapy*, vol. 13, no. 5, pp. 605–612, 2002.

[14] C. Lo Bianco, J. L. Ridet, B. L. Schneider, N. Déglon, and P. Aebischer, "α-synucleinopathy and selective dopaminergic neuron loss in a rat lentiviral-based model of Parkinson's disease," *Proceedings of the National Academy of Sciences of the United States of America*, vol. 99, no. 16, pp. 10813–10818, 2002.

[15] M. Yamada, T. Iwatsubo, Y. Mizuno, and H. Mochizuki, "Overexpression of α-synuclein in rat substantia nigra results in loss of dopaminergic neurons, phosphorylation of α-synuclein and activation of caspase-9: Resemblance to pathogenetic changes in Parkinson's disease," *Journal of Neurochemistry*, vol. 91, no. 2, pp. 451–461, 2004.

[16] O. S. Gorbatyuk, S. Li, L. F. Sullivan et al., "The phosphorylation state of Ser-129 in human α-synuclein determines neurodegeneration in a rat model of Parkinson disease," *Proceedings of the National Academy of Sciences of the United States of America*, vol. 105, no. 2, pp. 763–768, 2008.

[17] S. A. da Silveira, B. L. Schneider, C. Cifuentes-Diaz et al., "Phosphorylation does not prompt, nor prevent, the formation of α-synuclein toxic species in a rat model of Parkinson's disease," *Human Molecular Genetics*, vol. 18, no. 5, pp. 872–887, 2009.

[18] A. Recchia, D. Rota, P. Debetto et al., "Generation of a α-synuclein-based rat model of Parkinson's disease," *Neurobiology of Disease*, vol. 30, no. 1, pp. 8–18, 2008.

[19] F. Lelan, L. Lescaudron, C. Boyer et al., "Effects of human alpha-synuclein A53T-A30P mutations on SVZ and local olfactory bulb cell proliferation in a transgenic rat model of Parkinson disease," *Parkinson's Disease*, vol. 2011, Article ID 987084, 11 pages, 2011.

[20] J. Dusonchet, O. Kochubey, K. Stafa et al., "A rat model of progressive nigral neurodegeneration induced by the Parkinson's disease-associated G2019S mutation in LRRK2," *Journal of Neuroscience*, vol. 31, no. 3, pp. 907–912, 2011.

[21] H. Zhou, C. Huang, J. Tong, W. C. Hong, Y. -J. Liu, and X. -G. Xia, "Temporal expression of mutant LRRK2 in adult rats impairs dopamine reuptake," *International Journal of Biological Sciences*, vol. 7, no. 6, pp. 753–761, 2011.

[22] V. Sanchez-Guajardo, F. Febbraro, D. Kirik, and M. Romero-Ramos, "Microglia acquire distinct activation profiles depending on the degree of α-synuclein neuropathology in a rAAV based model of Parkinson's disease," *PLoS One*, vol. 5, no. 1, Article ID e8784, 2010.

[23] C. Lo Bianco, N. Déglon, W. Pralong, and P. Aebischer, "Lentiviral nigral delivery of GDNF does not prevent neurodegeneration in a genetic rat model of Parkinson's disease," *Neurobiology of Disease*, vol. 17, no. 2, pp. 283–289, 2004.

[24] M. Decressac, A. Ulusoy, B. Mattsson et al., "GDNF fails to exert neuroprotection in a rat α-synuclein model of Parkinson's disease," *Brain*, vol. 134, no. 8, pp. 2302–2311, 2011.

[25] C. Lo Bianco, B. L. Schneider, M. Bauer et al., "Lentiviral vector delivery of parkin prevents dopaminergic degeneration in an α-synuclein rat model of Parkinson's disease," *Proceedings of the National Academy of Sciences of the United States of America*, vol. 101, no. 50, pp. 17510–17515, 2004.

[26] T. Kitada, S. Asakawa, N. Hattori et al., "Mutations in the parkin gene cause autosomal recessive juvenile parkinsonism," *Nature*, vol. 392, no. 6676, pp. 605–608, 1998.

[27] J. P. Taylor, I. F. Mata, and M. J. Farrer, "LRRK2: a common pathway for parkinsonism, pathogenesis and prevention?" *Trends in Molecular Medicine*, vol. 12, no. 2, pp. 76–82, 2006.

[28] I. F. Mata, O. A. Ross, J. Kachergus et al., "LRRK2 mutations are a common cause of Parkinson's disease in Spain," *European Journal of Neurology*, vol. 13, no. 4, pp. 391–394, 2006.